



Swansea University
Prifysgol Abertawe



Swansea University E-Theses

Some exact singularities of Burgers and heat equations.

Reynolds, Brett T

How to cite:

Reynolds, Brett T (2002) *Some exact singularities of Burgers and heat equations..* thesis, Swansea University.
<http://cronfa.swan.ac.uk/Record/cronfa43017>

Use policy:

This item is brought to you by Swansea University. Any person downloading material is agreeing to abide by the terms of the repository licence: copies of full text items may be used or reproduced in any format or medium, without prior permission for personal research or study, educational or non-commercial purposes only. The copyright for any work remains with the original author unless otherwise specified. The full-text must not be sold in any format or medium without the formal permission of the copyright holder. Permission for multiple reproductions should be obtained from the original author.

Authors are personally responsible for adhering to copyright and publisher restrictions when uploading content to the repository.

Please link to the metadata record in the Swansea University repository, Cronfa (link given in the citation reference above.)

<http://www.swansea.ac.uk/library/researchsupport/ris-support/>

Some Exact Singularities of Burgers and Heat Equations

Thesis submitted to the University of Wales Swansea
by

Brett T Reynolds
mabtr@swansea.ac.uk
brettreynolds_uk@yahoo.co.uk

in candidature for the degree of
Doctor of Philosophy

Department of Mathematics
University of Wales Swansea
Singleton Park
Swansea SA2 8PP
United Kingdom

July 31, 2002

ProQuest Number: 10821407

All rights reserved

INFORMATION TO ALL USERS

The quality of this reproduction is dependent upon the quality of the copy submitted.

In the unlikely event that the author did not send a complete manuscript and there are missing pages, these will be noted. Also, if material had to be removed, a note will indicate the deletion.



ProQuest 10821407

Published by ProQuest LLC (2018). Copyright of the Dissertation is held by the Author.

All rights reserved.

This work is protected against unauthorized copying under Title 17, United States Code
Microform Edition © ProQuest LLC.

ProQuest LLC.
789 East Eisenhower Parkway
P.O. Box 1346
Ann Arbor, MI 48106 – 1346



Declaration

This work has not previously been accepted in substance for any degree and is not being concurrently submitted in candidature for any degree.

Signed (candidate)

Date 31 July 2002

Statement 1

This thesis is the result of my own investigations, except where otherwise stated. Other sources are acknowledged by explicit references. A bibliography is appended.

Signed (candidate)

Date 31 July 2002

Statement 2

I hereby give consent for my thesis, if accepted, to be available for photocopying and for inter-library loan, and for the title and summary to be made available to outside organisations.

Signed (candidate)

Date 31 July 2002

Summary

Our main aim in this work is to study explicit examples of shock waves for Burgers' equation and the corresponding level surfaces for the heat equation. This thesis is in two parts:

In Part I (Chapters 1 and 2) we introduce many of the concepts required for our study. Particularly we give a brief introduction to the heat equation, hydrodynamics and the underlying dynamical theory. Towards the end of Chapter 1 we discuss the stochastic Hamilton-Jacobi theory and begin formulating the notion of caustics and wavefronts in both the classical and stochastic cases. Chapter 2 contains an account of the results presented in [1] and [2] in which the exact Greens functions are calculated for the zero, linear and harmonic oscillator potentials, for both the classical and stochastic cases. We employ these results in the derivation of exact formulae for the corresponding caustics and wavefronts.

In Part II (Chapters 3 and 4) the results obtained from Chapter 2 are applied for several explicit chosen examples. We consider the initial conditions that lead us to the Thom catastrophes of the Cusp and the Butterfly, see [3], and their corresponding wavefronts, the Tricorn and Fish. Some time is taken to consider the meeting points of the caustics and wavefronts and the connection with meeting points of the pre-curves. In several instances we provide conditions for the existence of the pre-wavefronts with respect to the time. A large portion of the work in these chapters relied heavily on *Mathematica* and required an enhanced understanding of the handling of graphics within the package. In examples where we have been unable to calculate the wavefronts directly we have developed numerical methods within *Mathematica* to provide graphical images of them.

Acknowledgements

It is with much appreciation that I would like to thank Prof. A Truman for his guidance and encouragement during the completion of this work. I would also like to thank Dr. I. Davies for the technical expertise and assistance he has provided me with throughout the past few years. I also thank all at U.W. Swansea Mathematics Department for their support in what has been the most trying of times.

I am also grateful to the Engineering and Physical Sciences Research Council (E.P.S.R.C.) for providing all the financial support for my postgraduate studies at Swansea.

Contents

I	Stochastic Heat and Burgers Equations	6
1	Introduction	7
1.1	The Heat Equation	7
1.1.1	The Schrödinger Equation	9
1.2	Hydro-dynamics	10
1.2.1	The Convected Derivative	10
1.2.2	Burgers Equation	11
1.2.3	Hopf-Cole Transformation	11
1.3	Analytical Dynamics	13
1.3.1	Lagrangian Mechanics	13
1.3.2	Hamiltonian Mechanics	15
1.3.3	The Hamilton-Jacobi Theory	16
1.3.4	A Unified Approach Including Viscosity	18
1.4	Classical Laplace Expansions	19
1.5	Wavefronts and Caustics	20
1.5.1	Other Cases	23
1.6	Adding Noise	24
1.6.1	Stochastic Heat and Burgers' Equations and the Hopf-Cole Transformation	24
1.6.2	Stochastic Hamilton-Jacobi Theory	26
1.6.3	Noisy Wavefronts and Caustics	26
2	Stochastic Mehler Kernel Formulae	27
2.1	On Some Recent Papers	27
2.1.1	Stochastic Mehler Kernels and Path Integrals	27
2.2	Classical Green Functions	28
2.2.1	Zero Potential Case	29
2.2.2	Linear Potential Case	32
2.2.3	Harmonic Oscillator Potential Case	34
2.3	Noisy Green Function	37
2.3.1	Zero Potential Case	37
2.3.2	Linear Potential Case	42

<i>CONTENTS</i>	5
2.3.3 Harmonic Oscillator Potential Case	46
II Explicit Examples Using <i>Mathematica</i>	50
3 Cusp and Tricorn	51
3.1 Classical Case	51
3.1.1 Zero Potential	51
3.1.2 Linear Potential	60
3.1.3 Harmonic Oscillator Potential	66
3.2 The Noisy Case	76
3.2.1 Zero Potential	76
3.2.2 Linear Potential	82
3.2.3 Harmonic Oscillator Potential	87
4 Butterfly and Fish	91
4.1 Classical Case	91
4.1.1 Zero Potential	91
4.1.2 Linear Potential	101
4.1.3 Harmonic Oscillator Potential	108
4.2 Noisy Case	117
4.2.1 Zero Potential	117
4.2.2 Linear Potential	124
4.2.3 Harmonic Oscillator Potential	131
III Appendix	137
A On Mechanics	138
A.1 Hopf-Cole Transformation in \mathbb{R}^n	138
B On Stochastics	143
B.1 Itô and Stratonovich Integrals	143
B.1.1 Examples	143
B.2 Evaluating the $\zeta(t)$ Integral in the Zero Potential Case	145
B.3 Approximating Randomness	146
List of Figures	148
Bibliography	153

Part I

**Stochastic Heat and Burgers
Equations**

Chapter 1

Introduction

1.1 The Heat Equation

The heat equation, also known as the diffusion equation, is a mathematical model for the flow of heat through a medium such as a volume of fluid, a gaseous nebula, or a solid object. We shall be considering the heat equation as the following parabolic partial differential equation

$$\frac{\partial u}{\partial t} = \frac{\mu^2}{2} \Delta u + \frac{1}{\mu^2} V(\underline{x}) u, \quad (1.1)$$

where $u = u(\underline{x}, t)$ represents the temperature at the point $\underline{x} \in \mathbb{R}^3$ at time $t \geq 0$. The function $V(\underline{x}) : \mathbb{R}^3 \rightarrow \mathbb{R}$ is the scalar potential at the point \underline{x} , which represents some form of heat generation or loss at the point \underline{x} . Here μ is a parameter whose physical significance we shall make clear later. We shall now consider a physical derivation of the heat equation in 3 dimensions.

Consider a fixed volume \mathcal{V} of a medium bounded by a closed surface S , then assuming that there is no radiative or convective heat transfer, we can make the following argument for the behaviour of heat in our volume:

$$\begin{aligned} \text{rate of increase of heat in } \mathcal{V} &= \text{rate of conduction into } \mathcal{V} \text{ through } S & (1.2) \\ &+ \text{rate of heat generation within } \mathcal{V}. \end{aligned}$$

Now, the rate of increase of heat in \mathcal{V} is given by

$$\int_{\mathcal{V}} \rho \frac{\partial \kappa}{\partial t} d\mathcal{V},$$

where $\rho = \rho(\underline{x}, t)$ is the density of the medium at the point \underline{x} at time t , and κ is the specific internal energy¹ of the volume \mathcal{V} . The specific heat capacity² of the medium

¹The energy per unit volume.

²The heat required to produce a unit temperature rise of a unit mass.

is given by

$$C = \frac{\partial \kappa}{\partial u},$$

where $u = u(\underline{x}, t)$ is the temperature of \underline{x} at time t . This then gives the rate of increase of heat in \mathcal{V} as

$$\int_{\mathcal{V}} \rho C \frac{\partial u}{\partial t} d\mathcal{V},$$

where we are considering the products of partial derivatives in the sense of thermodynamics.

Now, for a surface S with unit normal \hat{n} , the rate at which heat is conducted across the surface S per unit area, in the direction of \hat{n} is given by

$$q = -\mathcal{K} \nabla u \cdot \hat{n},$$

where \mathcal{K} is the thermal conductivity³ and q is the flux of heat in the direction of \hat{n} . Therefore, the rate of heat conduction is given by

$$-\int_S q dS = \int_S \mathcal{K} \nabla u \cdot \hat{n} dS,$$

and, by Stokes' theorem, or the divergence theorem if preferred, this gives the rate of heat conduction into \mathcal{V} through S as

$$\int_{\mathcal{V}} \nabla \cdot (\mathcal{K} \nabla u) d\mathcal{V}.$$

Finally, assuming that the heat generation within the body is occurring at a rate Q per unit volume, we have the rate of heat generation within \mathcal{V} given by

$$\int_{\mathcal{V}} Q d\mathcal{V}.$$

Then equation (1.2), which governs heat transfer in our medium, can now be formulated mathematically as

$$\int_{\mathcal{V}} \rho C \frac{\partial u}{\partial t} d\mathcal{V} = \int_{\mathcal{V}} \nabla \cdot (\mathcal{K} \nabla u) d\mathcal{V} + \int_{\mathcal{V}} Q d\mathcal{V},$$

i.e.

$$\int_{\mathcal{V}} \left(\rho C \frac{\partial u}{\partial t} - \nabla \cdot (\mathcal{K} \nabla u) - Q \right) d\mathcal{V} = 0. \quad (1.3)$$

Hence, since \mathcal{V} is any fixed volume, we have

$$\rho C \frac{\partial u}{\partial t} = \nabla \cdot (\mathcal{K} \nabla u) + Q,$$

³The rate of flow of heat per unit area per unit temperature gradient.

and for a constant \mathcal{K} we have

$$\rho\mathcal{C}\frac{\partial u}{\partial t} = \mathcal{K}\Delta u + Q. \quad (1.4)$$

This is then our heat equation, but we shall deal with this in the form of the parabolic differential equation (1.1). In the study of the partial differential equations we often transform more sophisticated equations into the form of a heat equation so that we may find a solution. Details of how this is done may be found in [4], but we discuss next how the fundamental partial differential equation of quantum mechanics can be formally transformed into the heat equation.

1.1.1 The Schrödinger Equation

In quantum mechanics we examine the behaviour of the energy of a particle with the Schrödinger equation:

$$i\hbar\frac{\partial}{\partial t}\psi(\underline{x}, t) = -\frac{\hbar^2}{2}\Delta\psi(\underline{x}, t) + V(\underline{x})\psi(\underline{x}, t), \quad (1.5)$$

where $\psi : \mathbb{R}^3 \times [0, \infty) \rightarrow \mathbb{C}$ is the wave function that describes the motion of our particle of unit mass with position vector \underline{x} at time t , with $V : \mathbb{R}^3 \rightarrow \mathbb{C}$ being a potential energy function, and $\hbar = \frac{h}{2\pi}$ for Planck's constant h .

This is easily reducible to our heat equation (1.1) by using the transformation of $\tau = it$ which gives $t(\tau) = -i\tau$ and

$$\begin{aligned} \frac{\partial}{\partial \tau}\psi(\underline{x}, t(\tau)) &= \frac{\partial}{\partial t}\psi(\underline{x}, t(\tau))\frac{dt}{d\tau} \\ &= -i\frac{\partial}{\partial t}\psi(\underline{x}, t(\tau)). \end{aligned}$$

This then gives equation (1.5) as

$$\hbar\frac{\partial}{\partial \tau}\psi(\underline{x}, t(\tau)) = \frac{\hbar^2}{2}\Delta\psi(\underline{x}, t(\tau)) - V(\underline{x})\psi(\underline{x}, t(\tau)).$$

Dividing through by \hbar , letting $\mu^2 = \hbar$ and $\psi(\underline{x}, t(\tau)) = u(\underline{x}, \tau)$, then setting $\tau \rightarrow t$ gives us the heat equation (1.1),

$$\frac{\partial u}{\partial t} = \frac{\mu^2}{2}\Delta u + \frac{1}{\mu^2}V(\underline{x})u.$$

This is very useful as it allows us to use the Green functions for the Schrödinger equation, obtained for certain specific potentials $V(\underline{x})$ in [1, 5, 2], to be transformed into results that we can use for the heat equation.

1.2 Hydro-dynamics

The primary purpose of the science of hydro-dynamics is to study the motion of fluids, the cause of the motion, and the effects which the motion produces. Using the Eulerian flow representation of a fluid, one selects a point of space \underline{x} occupied by the fluid and observations are made of the changes in the so-called observables such as velocity, density, temperature, etc, at \underline{x} . This is essentially a field approach and the most important observable in the Eulerian representation is the velocity field $\underline{v} = \underline{v}(\underline{x}, t)$. For a more thorough grounding in Hydro-dynamics, I would suggest Wilson [6].

1.2.1 The Convected Derivative

If we consider $f = f(\underline{x}, t)$ as being the Eulerian representation of some physical observable, either vector or scalar, associated with the element at position \underline{x} at time t , then the time rate of change of $f(\underline{x}, t)$ is given by,

$$\lim_{\delta t \rightarrow 0} \left[\frac{f(\underline{x} + \underline{v}\delta t, t + \delta t) - f(\underline{x}, t)}{\delta t} \right] = \frac{\partial f}{\partial t} + (\underline{v} \cdot \nabla) f,$$

where ∇ is the gradient differential operator with respect to a Cartesian coordinate system. This is the time derivative as measured by an observer moving with the fluid and is defined as the convected derivative of $f(\underline{x}, t)$, written as

$$\frac{Df}{Dt} = \frac{\partial f}{\partial t} + (\underline{v} \cdot \nabla) f. \quad (1.6)$$

Note that if $f(\underline{x}, t)$ is a scalar quantity, then the right hand side is a true scalar, but if $f(\underline{x}, t)$ is a vector quantity then $(\underline{v} \cdot \nabla) f$ is not a true vector. In general, $(\underline{v} \cdot \nabla) f$ should be interpreted as a Cartesian operator with respect to the coordinate directions \underline{i} , \underline{j} and \underline{k} .

It is often necessary to write down equations of motion for the element in position \underline{x} at time t and in doing so we require the Eulerian representation of acceleration, as

$$\underline{a}(\underline{x}, t) = \frac{D\underline{v}}{Dt} = \frac{\partial \underline{v}}{\partial t} + (\underline{v} \cdot \nabla) \underline{v}. \quad (1.7)$$

Now using the vector identity of

$$\nabla(\underline{A} \cdot \underline{B}) = \underline{A} \times (\nabla \wedge \underline{B}) + \underline{B} \times (\nabla \wedge \underline{A}) + (\underline{A} \cdot \nabla) \underline{B} + (\underline{B} \cdot \nabla) \underline{A},$$

where $\nabla \wedge$ is the curl differential operator, and writing $\underline{A} = \underline{B} = \underline{v}$, we obtain

$$(\underline{v} \cdot \nabla) \underline{v} = \frac{1}{2} \nabla v^2 - \underline{v} \times (\nabla \wedge \underline{v}). \quad (1.8)$$

Hence then, in true vector form, we have the Eulerian representation of acceleration of an element in position \underline{x} at time t , given by

$$\underline{a}(\underline{x}, t) = \frac{\partial \underline{v}}{\partial t} + \frac{1}{2} \nabla \underline{v}^2 - \underline{v} \times (\nabla \wedge \underline{v}). \quad (1.9)$$

The important rule here is that when working in a Cartesian coordinate framework, as we shall be throughout this text, it is easier to use (1.7), and when working in some curvilinear coordinate system we must use (1.9), or if possible, we could translate to a Cartesian system.

1.2.2 Burgers Equation

Consider a hydro-dynamical equation of motion, with the Eulerian representation of flow, of an element at position \underline{x} at time t , that is

$$\frac{D\underline{v}}{Dt} = \text{sum of forces}, \quad (1.10)$$

where we consider the element to be under the action of a restoring force $\frac{\mu^2}{2} \Delta \underline{v}$ whose purpose is to smooth out the motion, μ^2 being the coefficient of viscosity. Assume that there also exists a scalar potential of the form $V(\underline{x})$ such that the force acting is due to this potential (i.e. gravity, harmonic oscillator, etc) given by $-\nabla V(\underline{x})$. Thus, this gives an equation of motion as

$$\frac{D\underline{v}}{Dt} = \frac{\mu^2}{2} \Delta \underline{v} - \nabla V(\underline{x}), \quad (1.11)$$

which gives us the Burgers equation,

$$\frac{\partial \underline{v}}{\partial t} + (\underline{v} \cdot \nabla) \underline{v} = \frac{\mu^2}{2} \Delta \underline{v} - \nabla V(\underline{x}). \quad (1.12)$$

As we shall see, the Burgers equation can be explicitly solved and we are primarily interested in the case of vanishing viscosity, i.e. where $\mu \rightarrow 0$. In this case the solution can develop shock waves, depending on the initial conditions. The particle dynamics then correspond to a situation where, if two volumes of fluid collide, they merely pass through each other conserving mass and momentum. A good description of the effects of the restoring force $\frac{\mu^2}{2} \Delta \underline{v}$ in Burgers' equation may be found in [2].

1.2.3 Hopf-Cole Transformation

There is a nice link between the Burgers equation and the heat equation which was first documented by Hopf in [7] and Cole in [8]. If we consider the heat equation (1.1) with a scalar potential $V(\underline{x})$, namely

$$\frac{\partial u}{\partial t} = \frac{\mu^2}{2} \Delta u + \frac{1}{\mu^2} V(\underline{x}) u,$$

then the so-called Hopf-Cole transformation

$$\underline{v} = -\mu^2 \nabla \ln u = -\frac{\mu^2}{u} \nabla u, \quad (1.13)$$

will give us the Burgers' equation (1.12)

$$\frac{\partial \underline{v}}{\partial t} + (\underline{v} \cdot \nabla) \underline{v} = \frac{\mu^2}{2} \Delta \underline{v} - \nabla V(\underline{x}).$$

This can be proved in \mathbb{R}^n but the method is rather clumsy due to the complications involved with the term $(\underline{v} \cdot \nabla) \underline{v}$. The proof in \mathbb{R}^n is not very informative, so here I present a proof in one dimension only and refer the reader to Appendix A.1 for the \mathbb{R}^n approach. Note that the positivity of the solution to the heat equation, i.e. that $u(\underline{x}, t) > 0$, is guaranteed by considering $u(\underline{x}, t)$ in its Feynman-Kac representation.

Theorem 1.2.1.

Consider the heat equation in one dimension with a potential $V(x)$,

$$\frac{\partial u}{\partial t} = \frac{\mu^2}{2} \frac{\partial^2 u}{\partial x^2} + \frac{V}{\mu^2} u, \quad (1.14)$$

where $u = u(x, t)$ with initial condition $u(x, 0) = e^{-\frac{S_0(x)}{\mu^2}}$. Then the Hopf-Cole transformation for $v = v(x, t)$,

$$v = -\mu^2 \frac{\partial}{\partial x} \ln u,$$

satisfies the Burgers equation in one dimension

$$\frac{\partial v}{\partial t} + (v \cdot \nabla) v = \frac{\mu^2}{2} \Delta v - \nabla V, \quad (1.15)$$

with initial condition $v(x, 0) = \nabla S_0(x)$.

Proof.

The Hopf-Cole transformation simplifies a little here to become

$$v = -\mu^2 \frac{\partial}{\partial x} \ln u = -\frac{\mu^2}{u} \frac{\partial u}{\partial x}, \quad (1.16)$$

and looking at the first derivative of v with respect to time t we have, by applying the Hopf-Cole transformation (1.16),

$$\frac{\partial v}{\partial t} = -\frac{v}{u} \frac{\partial u}{\partial t} - \frac{\mu^2}{u} \frac{\partial^2 u}{\partial t \partial x}. \quad (1.17)$$

Now looking at the first derivative of v with respect to position x we have

$$\frac{\partial v}{\partial x} = \frac{v^2}{\mu^2} - \frac{\mu^2}{u} \frac{\partial^2 u}{\partial x^2},$$

but from our heat equation (1.14), we have

$$\frac{\partial v}{\partial x} = \frac{v^2}{\mu^2} - \frac{2}{u} \frac{\partial u}{\partial t} + \frac{2}{\mu^2} V. \quad (1.18)$$

On taking the second derivative of v with respect to position x , we obtain

$$\frac{\partial^2 v}{\partial x^2} = \frac{2}{\mu^2} v \frac{\partial v}{\partial x} + \frac{2}{\mu^2} \left(-\frac{v}{u} \frac{\partial u}{\partial t} - \frac{\mu^2}{u} \frac{\partial^2 u}{\partial x \partial t} \right) + \frac{2}{\mu^2} \frac{\partial V}{\partial x}.$$

Now, assuming that we have a nice continuous solution $u = u(x, t)$ to the heat equation (1.14), we can assume that the second derivatives are also continuous such that

$$\frac{\partial^2 u}{\partial t \partial x} = \frac{\partial^2 u}{\partial x \partial t}.$$

This then lets us use the result for $\frac{\partial v}{\partial t}$, equation (1.17), to obtain

$$\frac{\partial^2 v}{\partial x^2} = \frac{2}{\mu^2} v \frac{\partial v}{\partial x} + \frac{2}{\mu^2} \frac{\partial v}{\partial t} + \frac{2}{\mu^2} \frac{\partial V}{\partial x}. \quad (1.19)$$

This is just the Burgers' equation in one dimension with a potential $V(x)$, i.e.

$$\frac{\partial v}{\partial t} + v \frac{\partial v}{\partial x} = \frac{\mu^2}{2} \frac{\partial^2 v}{\partial x^2} - \frac{\partial V}{\partial x}.$$

□

1.3 Analytical Dynamics

In the study of classical mechanics, one often begins with an understanding of Newton's laws of motion and studies several dynamical systems. Such a process involves constructing, and solving, a system of ordinary differential equations, the Newtonian equations of motion, obtained by examining the forces acting upon a particle. This can be quite difficult to solve, so Lagrange has showed us a way of approaching dynamical systems that involves constructing a system of ordinary differential equations from a knowledge of the kinetic and potential energies of the system.

This is then the beginning of analytical dynamics, whose purpose is to give a procedure to solve all traditional problems of classical mechanics, leading to a geometrical approach of classical mechanics and a connection with quantum mechanics.

1.3.1 Lagrangian Mechanics

In Lagrangian mechanics, the important variables are the n independent generalised co-ordinates $q_\sigma = q_\sigma(t)$, whose specification at time t uniquely fixes the configuration

of a dynamical system. The space of all possible values of the generalised co-ordinates is called the configuration space, and the position of a particle in a dynamical system may be defined by

$$\underline{r} = \underline{r}(q, t), \quad \text{for } q = (q_1, q_2, \dots, q_n).$$

The rate of change of \underline{r} with respect to time t , given by

$$\frac{d\underline{r}}{dt} = \frac{dq_\sigma}{dt} \frac{\partial \underline{r}}{\partial q_\sigma} + \frac{\partial \underline{r}}{\partial t},$$

leads to some interesting results, namely:-

$$\begin{array}{l} \text{Cancellation of the Dot} \\ \text{Commutativity} \end{array} \quad \begin{array}{l} \frac{\partial \dot{\underline{r}}}{\partial \dot{q}_\sigma} = \frac{\partial \underline{r}}{\partial q_\sigma}, \\ \frac{\partial}{\partial q_\tau} \left(\frac{d\underline{r}}{dt} \right) = \frac{d}{dt} \left(\frac{\partial \underline{r}}{\partial q_\tau} \right), \end{array}$$

where we use the convention that a repeated Greek index represents a summation. If we consider a particle of mass m with position vector \underline{r} in a conservative dynamical system where it is subject to a force $-\nabla V(\underline{r})$, then we have kinetic energy given by

$$T(q, \dot{q}) = \frac{m}{2} \dot{\underline{r}}^2,$$

and the so-called Lagrangian \mathcal{L} , the fundamental object of the dynamical system, is given by

$$\mathcal{L}(q, \dot{q}) = T(q, \dot{q}) - V(q). \quad (1.20)$$

We have the Euler-Lagrange equations of motion as

$$\frac{d}{dt} \left(\frac{\partial \mathcal{L}}{\partial \dot{q}_\sigma} \right) - \frac{\partial \mathcal{L}}{\partial q_\sigma} = 0. \quad (1.21)$$

The solution for q of these n coupled ordinary differential equations, is the solution of our dynamical system. It can also be shown that the Euler-Lagrange equations (1.21) are invariant under the set of point transformations $Q = Q(q, t)$ if the inverse transformation $q = q(Q, t)$ exists. This is important when it comes to finding integral solutions of the Euler-Lagrange equations.

Here there is an important connection with the action principle. For a fixed time t , the classical mechanical path $q(s)$ with $s \in [0, t]$ and fixed end points $q(0) = \alpha$, $q(t) = \beta$, has a classical action defined by

$$A[q] = \int_0^t \mathcal{L}(q(s), \dot{q}(s)) ds. \quad (1.22)$$

Then for $u \in C^1$ with $u(0) = u(t) = 0$ and some regularity conditions, we have

$$\frac{d}{d\varepsilon} A[q + \varepsilon u] \Big|_{\varepsilon=0} = \int_0^t \left[\frac{\partial \mathcal{L}}{\partial q} - \frac{d}{ds} \left(\frac{\partial \mathcal{L}}{\partial \dot{q}} \right) \right] u(s) ds. \quad (1.23)$$

Thus the classical mechanical path q extremizes the classical action. This principle is sometimes called (erroneously) the principle of least action. Historically it was the origin of the calculus of variations.

1.3.2 Hamiltonian Mechanics

The Lagrange formulation gives a configuration space description of the time evolution of a dynamical system, i.e. a q space description. The Lagrangian equations are second order in time differentials. The main variables considered in Lagrangian mechanics are the generalised co-ordinates q_σ and their rates of change with respect to time, \dot{q}_σ .

Hamiltonian mechanics takes this a step further by extending to the so-called phase space description, where the main variables are the generalised co-ordinates q_σ and the conjugate momentum p_σ , given by

$$p_\sigma = \frac{\partial \mathcal{L}}{\partial \dot{q}_\sigma}.$$

The Hamilton equations turn out to be $2n$ first order differential equations in time t . For a conservative system with a Lagrangian \mathcal{L} , the Hamiltonian H is given by

$$H = p_\sigma \dot{q}_\sigma - \mathcal{L}(q, \dot{q}, t), \quad (1.24)$$

and we think of $\dot{q} = \dot{q}(q, p, t)$ such that $H = H(q, p, t)$. Then the Euler-Lagrange equations of motion can be transformed into the Hamilton equations of motion, namely

$$\dot{q}_\sigma = \frac{\partial H}{\partial p_\sigma}, \quad \dot{p}_\sigma = -\frac{\partial H}{\partial q_\sigma}, \quad \text{and} \quad \frac{\partial H}{\partial t} = -\frac{\partial \mathcal{L}}{\partial t}. \quad (1.25)$$

Just as Lagrange's equations have a corresponding variational principle, Hamilton's equations have a variational principle for paths in phase space, namely defining the phase-space action for the path $(q(s), p(s))$ for some $s \in [0, t]$ by

$$A[q, p] = \int_0^t \left(p_\sigma \frac{dq_\sigma}{ds} - H(q, p) \right) ds.$$

Then for $\xi(t) = \xi(0) = 0$ where $\xi, \eta \in C^1$, we have

$$\frac{d}{d\varepsilon} A[q + \varepsilon \xi, p + \varepsilon \eta] \Big|_{\varepsilon=0} = \int_0^t \left[\left(-\frac{dp_\sigma}{ds} - \frac{\partial H}{\partial q_\sigma} \right) \xi_\sigma(s) + \left(\frac{dq_\sigma}{ds} - \frac{\partial H}{\partial p_\sigma} \right) \eta_\sigma(s) \right] ds.$$

Hence the solution of Hamilton's equations extremizes the phase-space action. This gives an important way of characterising the solutions of Hamilton's equations. Since the Euler-Lagrange equations (1.21) and Hamilton equations (1.25) are equivalent, we call the class of transformations that leave the Hamilton equations invariant, the contact transformations. Obviously, all the point transformations that leave the Lagrange equations invariant are contact transformations, but clearly the reverse is not always true. For example, if we take $P = -q$ and $Q = p$ then this preserves Hamilton's equations, but is not a point transformation.

1.3.3 The Hamilton-Jacobi Theory

Suppose that (q, p) are the set of generalised co-ordinates and their conjugate momentum variables for which we have the Hamilton equations of motion. Now consider the contact transformation of co-ordinates $Q_\sigma = Q_\sigma(q, p, t)$ and $P_\sigma = P_\sigma(q, p, t)$ such that we have Hamilton equations in the new variables

$$\dot{Q}_\sigma = \frac{\partial \mathcal{H}}{\partial Q_\sigma}, \quad \dot{P}_\sigma = -\frac{\partial \mathcal{H}}{\partial Q_\sigma}, \quad (1.26)$$

for a new Hamiltonian $\mathcal{H}(Q, P, t)$. Since the new Hamilton equations of motion must be invariant for the new co-ordinates (Q, P) , we have, from Hamilton's variational principle, the equation

$$p_\sigma dq_\sigma - H dt = P_\sigma dQ_\sigma - \mathcal{H} dt + dS, \quad (1.27)$$

where S is the generating function of the contact transformation. If we choose a $S = S(q, Q, t)$ then it obviously satisfies

$$dS = \frac{\partial S}{\partial q_\sigma} dq_\sigma + \frac{\partial S}{\partial Q_\sigma} dQ_\sigma + \frac{\partial S}{\partial t} dt. \quad (1.28)$$

For equation (1.27) to be satisfied, we must have

$$p_\sigma = \frac{\partial S}{\partial q_\sigma}, \quad P_\sigma = -\frac{\partial S}{\partial Q_\sigma}, \quad \mathcal{H} = H + \frac{\partial S}{\partial t}.$$

By being more restrictive, we shall consider a generating function S reducing \mathcal{H} to zero so that we have

$$\frac{\partial S}{\partial t} + H(q, p, t) = 0, \quad p = \nabla_q S(q, Q, t),$$

i.e.

$$\frac{\partial S}{\partial t} + H(q, \nabla S, t) = 0,$$

and we also have

$$\dot{Q}_\sigma = \frac{\partial \mathcal{H}}{\partial Q_\sigma} = 0, \quad \dot{P}_\sigma = -\frac{\partial \mathcal{H}}{\partial Q_\sigma} = 0,$$

such that P and Q are constant. S is the generating function of a continuous unfolding of infinitesimal contact transformations, reducing the Hamiltonian instantaneously to zero. The Hamilton-Jacobi equation of motion can thus be computed as

$$\frac{\partial S}{\partial t} + H(q, \nabla S(q), t) = 0, \quad (1.29)$$

i.e.

$$\frac{1}{2m} |\nabla S|^2 + V(q) + \frac{\partial S}{\partial t} = 0. \quad (1.30)$$

The Hamilton-Jacobi equation (1.30) plays an important part in the connection between classical and quantum mechanics. We shall now show an alternate description of obtaining the Hamiltonian-Jacobi equations of motion which we have learned from [9]. Consider the Hamilton characteristic function defined as

$$S(q, t) = \int_0^t \mathcal{L}(q(s), \dot{q}(s), s) ds,$$

where $q(s)$ is the unique classical mechanical path at time $s \in [0, t]$ with end points $q(0) = q_0$ and $q(t) = q$. Begin by taking some fixed momentum $p = \frac{\partial \mathcal{L}}{\partial \dot{q}}$ at time $t = 0$ and continuing along the classical mechanical path $q(s)$ until time t such that in (s, q, p) space we move from $(0, q_0, p = \frac{\partial \mathcal{L}}{\partial \dot{q}})$ to $(t, q, p = \frac{\partial \mathcal{L}}{\partial \dot{q}})$. Now consider an infinitesimal displacement in time Δt giving rise to an infinitesimal change in the generalised coordinates of Δq , then we arrive at the point $(t + \Delta t, q + \Delta q, p = \frac{\partial \mathcal{L}}{\partial \dot{q}})$, see Figure 1.1. By considering the line integral of $\mathcal{L}(q, \dot{q}, s)$ around the closed curve γ in (s, q, p) space, as depicted in Figure 1.1, we have

$$\oint_\gamma \mathcal{L}(q, \dot{q}, s) ds = \oint_\gamma (p\dot{q} - H) ds = \oint_\gamma (p dq - H ds).$$

Now in our coordinate system (s, q, p) , we have

$$\nabla \wedge (-H, p, 0) = \left\| \begin{array}{ccc} \frac{\partial}{\partial s} & \frac{\partial}{\partial q} & \frac{\partial}{\partial p} \\ -H & p & 0 \end{array} \right\| = \left(-1, -\frac{\partial H}{\partial p}, \frac{\partial H}{\partial q} \right),$$

but by the Hamilton equations, we have

$$\text{r.h.s.} = -(1, \dot{q}, \dot{p}) = -\frac{d}{ds}(s, q(s), p(s)),$$

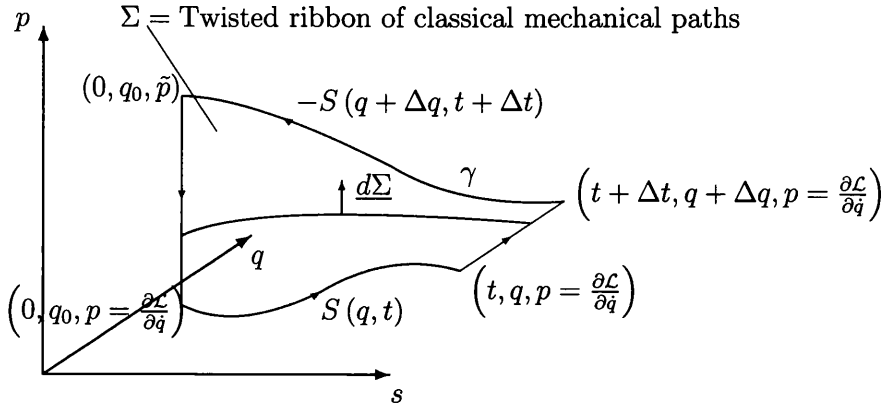


Figure 1.1: Phase Space Diagram

and since $(1, \dot{q}, \dot{p})$ is perpendicular to $d\Sigma$, the unit normal of the surface Σ , we have, by Stoke's Theorem,

$$\oint_{\gamma} (p dq - H ds) = 0.$$

On the vertical section of the path γ , i.e. the section from $(0, q_0, \tilde{p})$ to $(0, q_0, p)$, we have $dq = 0$ and $ds = 0$, which gives the integral around the path γ as

$$S(q + \Delta q, t + \Delta t) - S(q, t) = p\Delta q - H\Delta t = \frac{\partial S}{\partial q}\Delta q + \frac{\partial S}{\partial t}\Delta t,$$

since

$$S(q, t) + \frac{\partial S}{\partial q}\Delta q + \frac{\partial S}{\partial t}\Delta t - S(q + \Delta q, t + \Delta t) = 0.$$

This yields the Hamilton-Jacobi equations,

$$\frac{\partial S}{\partial q} = p \quad \text{and} \quad \frac{\partial S}{\partial t} = -H\left(q, \frac{\partial S}{\partial q}, t\right).$$

S is called the Hamilton principal (characteristic) function of the path q . We show next how this links with our previous approach to the heat equation, Burgers equation and the Hopf-Cole transformation.

1.3.4 A Unified Approach Including Viscosity

If we consider the Hamilton Jacobi equations for a particle of unit mass moving under a potential of the form $V(\underline{x})$ together with a viscosity term $-\frac{\mu^2}{2}\Delta S$, then we have the Hamilton-Jacobi equation with viscosity μ^2 as

$$\frac{\partial S}{\partial t} + \frac{1}{2}|\nabla S|^2 + V = \frac{\mu^2}{2}\Delta S, \quad (1.31)$$

where for a detailed analysis we direct the reader to [10]. We want to look at an analogue of the Hopf-Cole transformation. By letting $u = e^{-\frac{S}{\mu^2}}$ we can show that the above satisfies the heat equation (1.1), namely

$$\frac{\partial u}{\partial t} = \frac{\mu^2}{2} \Delta u + \frac{1}{\mu^2} V(\underline{x}) u.$$

Furthermore, if we now look at the transformation $\underline{v} = \nabla S$ then we obtain the Burgers equation (1.12) with a scalar potential $V(\underline{x})$, namely

$$\frac{\partial \underline{v}}{\partial t} + (\underline{v} \cdot \nabla) \underline{v} = \frac{\mu^2}{2} \Delta \underline{v} - \nabla V(\underline{x}). \quad (1.32)$$

We can see that our study of heat and Burgers equations essentially reduces to a study of the Hamilton-Jacobi equations with viscosity. Similar results to this are well known in quantum mechanics under the name of the Madelung fluid, if one uses the formal correspondence between the heat and Schrödinger equation indicated previously.

1.4 Classical Laplace Expansions

Later we shall be looking at integral solutions of the heat equation of the form

$$u(x, t) = \frac{1}{\sqrt{2\pi\mu^2 t}} \int_{\mathbb{R}} T_0(x_0) e^{-\frac{\phi(x, x_0, t)}{\mu^2}} dx_0,$$

where we have a convergence factor $T_0(x_0)$ and phase function $\phi(x, x_0, t)$. We see that in order to compute the integral, we must use the classical Laplace method for one dimensional integrals, see [11]. The following encapsulates the spirit of the Laplace result.

Theorem 1.4.1 (Laplace's Asymptotic Method).

Consider the integral

$$I(\lambda) = \int_a^b T(x) e^{-\lambda\phi(x)} dx,$$

where $T(x) \in C_0^\infty$ has support $[a, b]$, and we assume that $\phi(x) \in C^2$ attains a minimum at the point $x_0 \in (a, b)$ such that $\phi''(x_0) \geq 0$. Then in the limiting case as $\lambda \rightarrow \infty$ we have

$$\begin{aligned} I(\lambda) e^{\lambda\phi(x_0)} \sqrt{\lambda} &\rightarrow T(x_0) \int_{-\infty}^{\infty} e^{-\frac{y^2}{2} \phi''(x_0)} dy \\ &= T(x_0) \left(\frac{\phi''(x_0)}{2\pi} \right)^{-\frac{1}{2}} \end{aligned} \quad (1.33)$$

Proof.

We merely change the integration variables by setting

$$x = x_0 + \frac{y}{\sqrt{\lambda}}.$$

Then the integral becomes

$$I(\lambda) = \int_{\sqrt{\lambda}(a-x_0)}^{\sqrt{\lambda}(b-x_0)} T\left(x_0 + \frac{y}{\sqrt{\lambda}}\right) e^{-\lambda\phi\left(x_0 + \frac{y}{\sqrt{\lambda}}\right)} \frac{dy}{\sqrt{\lambda}},$$

therefore, we have

$$I(\lambda) e^{\lambda\phi(x_0)} \sqrt{\lambda} = \int_{\sqrt{\lambda}(a-x_0)}^{\sqrt{\lambda}(b-x_0)} T\left(x_0 + \frac{y}{\sqrt{\lambda}}\right) e^{-\lambda\left[\phi\left(x_0 + \frac{y}{\sqrt{\lambda}}\right) - \phi(x_0)\right]} dy.$$

Now we observe that, according to Taylor's theorem, we have

$$\phi\left(x_0 + \frac{y}{\sqrt{\lambda}}\right) = \phi(x_0) + \frac{y}{\sqrt{\lambda}}\phi'(x_0) + \frac{1}{2}\frac{y^2}{\lambda}\phi''\left(x_0 + \frac{\theta y}{\sqrt{\lambda}}\right),$$

for $0 < \theta < 1$. Then, since ϕ attains a minimum at x_0 , we have

$$-\lambda\left[\phi\left(x_0 + \frac{y}{\sqrt{\lambda}}\right) - \phi(x_0)\right] = -\frac{y^2}{2}\phi''\left(x_0 + \frac{\theta y}{\sqrt{\lambda}}\right).$$

Therefore, we have

$$I(\lambda) e^{\lambda\phi(x_0)} \sqrt{\lambda} = \int_{\sqrt{\lambda}(a-x_0)}^{\sqrt{\lambda}(b-x_0)} T\left(x_0 + \frac{y}{\sqrt{\lambda}}\right) e^{-\frac{y^2}{2}\phi''\left(x_0 + \frac{\theta y}{\sqrt{\lambda}}\right)} dy,$$

where $\phi''\left(x_0 + \frac{\theta y}{\sqrt{\lambda}}\right) > 0$ for sufficiently large λ . By the dominated convergence theorem, the result follows. \square

It is important to remember that the classical asymptotic Laplace expansion is dominated by the quadratic terms in the exponential and higher order terms are of little importance here.

1.5 Wavefronts and Caustics

We are interested in the wavefronts of the heat equation (1.1) and the caustics of the Burgers equation (1.12) that appear in the limiting case of vanishing viscosity $\mu^2 \rightarrow 0$. Consider a general heat equation of the form

$$\frac{\partial u_t}{\partial t} = \frac{\mu^2}{2} \Delta u_t + \frac{V(\underline{x})}{\mu^2} u_t,$$

with initial condition $u_0(\cdot) = T_0(\cdot) e^{-\frac{S_0(\cdot)}{\mu^2}}$ where T_0 is a convergence factor in the integral below. Let $V = 0$, then this has a solution of the form⁴

$$u(\underline{x}, t) = \frac{1}{(2\pi\mu^2 t)^{\frac{3}{2}}} \int_{\mathbb{R}^3} T_0(\underline{x}_0) e^{-\frac{\phi(\underline{x}, \underline{x}_0, t)}{\mu^2}} dx_0 dy_0 dz_0,$$

where we have a phase function defined in the zero potential case as

$$\phi(\underline{x}, \underline{x}_0, t) = \frac{(\underline{x} - \underline{x}_0)^2}{2t} + S_0(\underline{x}_0).$$

The corresponding solution of the Burgers' equation is given by

$$\begin{aligned} \underline{v}(\underline{x}, t) &= -\mu^2 \nabla \ln u(\underline{x}, t) \\ &= -\mu^2 \nabla \ln \int_{\mathbb{R}^3} T_0(\underline{x}_0) e^{-\frac{\phi(\underline{x}, \underline{x}_0, t)}{\mu^2}} dx_0 dy_0 dz_0. \end{aligned}$$

Eventually we will have to set $T_0(\underline{x}_0) = 1$ since we have the initial condition of the solution of the Burgers' equation as

$$\begin{aligned} \underline{v}^\mu(\underline{x}_0, 0) &= -\mu^2 \nabla \ln u^\mu(\underline{x}_0, 0) \\ &= \nabla S_0(\underline{x}_0) - \mu^2 \nabla \ln T_0(\underline{x}_0), \end{aligned}$$

where we are primarily interested in the case as $\mu^2 \rightarrow 0$. In this limiting case we must use the Laplace method for classical Laplace expansions to evaluate the integral solution of the heat equation, we have

$$u(\underline{x}, t) = \frac{M^{\frac{1}{\mu^2}}}{(2\pi\mu^2 t)^{\frac{3}{2}}} \int_{\mathbb{R}^3} T_0(\underline{x}_0) \left(\frac{e^{-\phi(\underline{x}, \underline{x}_0, t)}}{M} \right)^{\frac{1}{\mu^2}} dx_0 dy_0 dz_0,$$

for

$$M = \max_{\underline{x}_0 \in \mathbb{R}^3} e^{-\phi(\underline{x}, \underline{x}_0, t)}.$$

We have to find the main contribution to this integral bearing in mind that $\frac{1}{\mu^2} \rightarrow \infty$. This is equivalent to finding

$$\tilde{\phi}(\underline{x}, \underline{x}_0, t) = \min_{\underline{x}_0 \in \mathbb{R}^3} \phi(\underline{x}, \underline{x}_0, t),$$

for the minimum being achieved at the point, or set of points, $\tilde{\underline{x}}_0$. This clearly occurs at the points \underline{x}_0 satisfying

$$\nabla_{\underline{x}_0} \phi(\underline{x}, \underline{x}_0, t) = 0,$$

which defines our classical mechanical flow, denoted by $\Phi_t(\underline{x}_0)$.

⁴In Chapter 2 we calculate exactly such solutions for several cases.

Now look at the derivatives of $\phi(\underline{x}, \underline{x}_0, t)$ with respect to \underline{x} and t , we have

$$\nabla_{\underline{x}}\phi = \frac{(\underline{x} - \underline{x}_0)}{t} + \nabla_{\underline{x}_0}\phi \cdot \nabla_{\underline{x}}\underline{x}_0 = \frac{(\underline{x} - \underline{x}_0)}{t},$$

and

$$\frac{\partial\phi}{\partial t} = -\frac{(\underline{x} - \underline{x}_0)^2}{t^2} + \nabla_{\underline{x}_0}\phi \cdot \frac{\partial\underline{x}_0}{\partial t} = -\frac{(\underline{x} - \underline{x}_0)^2}{2t^2},$$

which satisfies the Hamilton Jacobi equation

$$\frac{\partial\phi}{\partial t} + \frac{1}{2}|\nabla_{\underline{x}}\phi|^2 = 0.$$

However this is just

$$S(\underline{x}, t) = \min_{\underline{x}_0 \in \mathbb{R}^3} \phi(\underline{x}, \underline{x}_0, t),$$

which is the Hamilton characteristic function corresponding to the initial momentum $\nabla S_0(\underline{x}_0)$, i.e. the solution of the Hamilton Jacobi equation

$$\frac{\partial S}{\partial t} + \frac{|\nabla S|^2}{2} + V(\underline{x}) = \frac{\mu^2}{2}\Delta S,$$

with initial condition $S(\underline{x}, 0) = S_0(\underline{x})$ and for the case of $\mu^2 \rightarrow 0$ and $V(\underline{x}) = 0$. The wavefronts of the heat equation can be defined as the points that lie on the surface $S(\underline{x}, t) = 0$ where $u(\underline{x}, t)$ switches from being exponentially large to exponentially small.⁵ We can find the pre-wavefronts by eliminating the \underline{x} terms in the expression $S(\underline{x}, t) = 0$, and the wavefronts by eliminating \underline{x}_0 . Now, if we expand $\phi(\underline{x}, \underline{x}_0, t)$ about $\underline{x}_0 \rightarrow \tilde{\underline{x}}_0$ by Taylor's theorem, then we have

$$\phi(\underline{x}, \underline{x}_0, t) = \phi(\underline{x}, \tilde{\underline{x}}_0, t) + (\underline{x}_0 - \tilde{\underline{x}}_0)^T \frac{\partial\phi}{\partial\underline{x}_0} \Big|_{\tilde{\underline{x}}_0} + \frac{(\underline{x}_0 - \tilde{\underline{x}}_0)^T}{2} \frac{\partial^2\phi}{\partial\underline{x}_0^2} \Big|_{\tilde{\underline{x}}_0} (\underline{x}_0 - \tilde{\underline{x}}_0) + \mathcal{O}(\tilde{\underline{x}}_0^3),$$

where $\frac{\partial^2\phi}{\partial\underline{x}_0^2}$ is the Hessian matrix of second order derivatives. But, recall that we have already demanded that

$$\frac{\partial\phi}{\partial\underline{x}_0} \Big|_{\tilde{\underline{x}}_0} = \nabla\phi|_{\tilde{\underline{x}}_0} = 0,$$

so the leading behaviour of the solution of the heat equation must be of the form

$$u(\underline{x}, t) = \frac{e^{-\frac{\phi(\underline{x}, \tilde{\underline{x}}_0, t)}{\mu^2}}}{(2\pi\mu^2 t)^{\frac{3}{2}}} \int_{\mathbb{R}^3} e^{-\frac{(\underline{x}_0 - \tilde{\underline{x}}_0)^T}{2\mu^2} \frac{\partial^2\phi}{\partial\underline{x}_0^2} \Big|_{\tilde{\underline{x}}_0} (\underline{x}_0 - \tilde{\underline{x}}_0)} dx_0 dy_0 dz_0.$$

⁵Recent work by Davies, Truman and Zhao, see [12], has required a more precise definition of a wavefront, but for the purpose of this work it is sufficient to use our definition.

Clearly then, this will become infinite when one of the eigenvalues of $\frac{\partial^2 \phi}{\partial \underline{x}_0^2}$ becomes zero, i.e. when

$$\text{Det} \left| \frac{\partial^2 \phi}{\partial \underline{x}_0^2} \right| = 0,$$

for $\underline{x}_0 = \tilde{\underline{x}}_0(\underline{x}, t)$ and where we must emphasize that $\frac{\partial^2 \phi}{\partial \underline{x}_0^2}$ is a matrix of second order derivatives with respect to the components of \underline{x}_0 . Then the caustics of the heat equation can be defined as the points where this occurs, and we would eliminate the \underline{x}_0 terms to get the caustic and the \underline{x} terms to get the pre-caustic.

1.5.1 Other Cases

We can show that in the case of a general potential $V = V(\underline{x})$ we have similar results for the wavefronts of the heat equation

$$\frac{\partial u}{\partial t} = \frac{\mu^2}{2} \Delta u + \frac{V(\underline{x})}{\mu^2} u,$$

with initial condition $u_0(\cdot) = T_0(\cdot) e^{-\frac{S_0(\cdot)}{\mu^2}}$, and caustics of the Burgers' equation

$$\frac{\partial \underline{v}}{\partial t} + (\underline{v} \cdot \nabla) \underline{v} = \frac{\mu^2}{2} \Delta \underline{v} - \nabla V(\underline{x}),$$

with initial condition

$$\underline{v}(\cdot, 0) = \nabla S_0(\cdot) - \mu^2 \nabla \ln T_0(\cdot).$$

We can assume that the heat equation has a solution of the form

$$u(\underline{x}, t) = \frac{1}{(2\pi\mu^2 t)^{\frac{3}{2}}} \int_{\mathbb{R}^3} T_0(\underline{x}_0) e^{-\frac{1}{\mu^2} \phi(\underline{x}, \underline{x}_0, t)} d x_0 d y_0 d z_0,$$

where we have a phase function of the form

$$\phi(\underline{x}, \underline{x}_0, t) = A[\underline{x}, \underline{x}_0, t] + S_0(\underline{x}_0),$$

and $A[\underline{x}, \underline{x}_0, t]$ is the classical action of a classical mechanical path starting from \underline{x}_0 and getting to \underline{x} in time t , i.e.

$$A[\underline{x}, \underline{X}(0), t] = \inf_{\substack{\underline{X}(s) \\ \underline{X}(t) = \underline{x}}} \left\{ \frac{1}{2} \int_0^t \dot{\underline{X}}^2 ds - \int_0^t V(\underline{X}(s)) ds \right\}.$$

We shall see later, in Chapter 2, that for the case of a linear potential, where $V(x) = -Kx$, we obtain a phase function of the form

$$\phi(x, x_0, t) = \frac{(x - x_0)^2}{2t} + \frac{Kt}{2} (x + x_0) - \frac{K^2 t^3}{24} + S_0(x_0), \quad (1.34)$$

and for the case of a harmonic oscillator potential, where $V(x) = \frac{w^2}{2}x^2$, we have phase function

$$\phi(x, x_0, t) = \frac{w}{2} \left[\frac{(x^2 + x_0^2) \cos(wt) - 2xx_0}{\sin(wt)} \right] + S_0(x_0). \quad (1.35)$$

1.6 Adding Noise

In the previous sections we discussed the relationships between the heat and Burgers' equation and the Hamilton-Jacobi theory. We shall now see that all of the previous work still holds in a noisy environment, i.e. if we add noise in time, as long as we use the Stratonovich stochastic integral.

1.6.1 Stochastic Heat and Burgers' Equations and the Hopf-Cole Transformation

Consider now a stochastic version of the heat equation

$$\partial u = \frac{\mu^2}{2} \Delta u \partial t + V(\underline{x}) \frac{u}{\mu^2} \partial t + U(\underline{x}, t) \frac{u}{\mu^2} \circ \partial W_t, \quad (1.36)$$

for the Wiener process W_t and with \circ representing a stochastic Stratonovich integral rather than an Itô integral, see Appendix B.1. For the Stratonovich integral, the normal rules of calculus apply and there are no Itô corrections required. We can use the usual Hopf-Cole transformation, as discussed earlier,

$$\underline{v}(\underline{x}, t) = -\mu^2 \nabla \ln u(\underline{x}, t),$$

to obtain the stochastic version of the Burgers' equation,

$$\partial \underline{v} + (\underline{v} \cdot \nabla) \underline{v} \partial t = \frac{\mu^2}{2} \Delta \underline{v} \partial t - \nabla V(\underline{x}) \partial t - \nabla U(\underline{x}, t) \circ \partial W_t. \quad (1.37)$$

We prove this formally in the one dimensional case.

Theorem 1.6.1.

Consider the stochastic heat equation with a classical potential $V(x)$ and a random potential $U(x, t) \circ \dot{W}_t$

$$\partial u = \frac{\mu^2}{2} \frac{\partial^2 u}{\partial x^2} \partial t + V(x) \frac{u}{\mu^2} \partial t + U(x, t) \frac{u}{\mu^2} \circ \partial W_t. \quad (1.38)$$

where $u = u(x, t)$. Then the Hopf-Cole transformation for $v = v(x, t)$

$$v = -\mu^2 \frac{\partial}{\partial x} \ln u = -\frac{\mu^2}{u} \frac{\partial u}{\partial x}, \quad (1.39)$$

satisfies the Burgers' equation in one dimension

$$\partial v + v \frac{\partial v}{\partial x} \partial t = \frac{\mu^2}{2} \frac{\partial^2 v}{\partial x^2} \partial t - \frac{\partial V}{\partial x} - \frac{\partial U}{\partial x} \circ \partial W_t. \quad (1.40)$$

Proof.

The first derivative of v with respect to time t is, by the Hopf-Cole transformation, just

$$\frac{\partial v}{\partial t} = \frac{\mu^2}{2} \frac{\partial u}{\partial t} \frac{\partial u}{\partial x} - \frac{\mu^2}{u} \frac{\partial^2 u}{\partial t \partial x},$$

and by the Hopf-Cole transformation (1.39), we have

$$\frac{\partial v}{\partial t} = -\frac{v}{u} \frac{\partial u}{\partial t} - \frac{\mu^2}{u} \frac{\partial^2 u}{\partial t \partial x}. \quad (1.41)$$

With respect to space x , the first derivative of v by the Hopf-Cole transformation (1.39) is

$$\frac{\partial v}{\partial x} = \frac{\mu^2}{u^2} \left(\frac{\partial u}{\partial x} \right)^2 - \frac{\mu^2}{u} \frac{\partial^2 u}{\partial x^2}.$$

But, recalling the above simplification of the Hopf-Cole transformation (1.39) and also by using the heat equation (1.38), we have

$$\frac{\partial v}{\partial x} = \frac{v^2}{\mu^2} - \frac{2}{u} \frac{\partial u}{\partial t} + \frac{2}{\mu^2} \left(V + U \circ \dot{W}_t \right). \quad (1.42)$$

Now we are primarily concerned with the second derivative of v with respect to x , i.e.

$$\frac{\partial^2 v}{\partial x^2} = 2 \frac{v}{\mu^2} \frac{\partial v}{\partial x} + \frac{2}{u^2} \frac{\partial u}{\partial x} \frac{\partial u}{\partial t} - \frac{2}{u} \frac{\partial^2 u}{\partial x \partial t} + \frac{2}{\mu^2} \left(\frac{\partial V}{\partial x} + \frac{\partial U}{\partial x} \circ \dot{W}_t \right).$$

Once again, using the Hopf-Cole transformation (1.39), we have

$$\frac{\partial^2 v}{\partial x^2} = 2 \frac{v}{\mu^2} \frac{\partial v}{\partial x} + \frac{2}{\mu^2} \frac{v}{u} \frac{\partial u}{\partial t} - \frac{2}{u} \frac{\partial^2 u}{\partial x \partial t} + \frac{2}{\mu^2} \left(\frac{\partial V}{\partial x} + \frac{\partial U}{\partial x} \circ \dot{W}_t \right).$$

We also assume that u is sufficiently well-behaved such that we have continuous second derivatives, so that

$$\frac{\partial^2 u}{\partial t \partial x} = \frac{\partial^2 u}{\partial x \partial t},$$

then we have, from the heat equation (1.38),

$$\frac{\partial^2 v}{\partial x^2} = 2 \frac{v}{\mu^2} \frac{\partial v}{\partial x} + \frac{2}{\mu^2} \frac{\partial v}{\partial t} + \frac{2}{\mu^2} \left(\frac{\partial V}{\partial x} + \frac{\partial U}{\partial x} \circ \dot{W}_t \right), \quad (1.43)$$

which is just the stochastic Burgers' equation in one dimension with a potential $V(x) + U(x, t) \circ \dot{W}_t$, i.e.

$$\partial v + v \frac{\partial v}{\partial x} \partial t = \frac{\mu^2}{2} \frac{\partial^2 v}{\partial x^2} \partial t - \frac{\partial V}{\partial x} - \frac{\partial U}{\partial x} \circ \partial W_t.$$

□

1.6.2 Stochastic Hamilton-Jacobi Theory

Earlier we showed how the classical heat equation (1.1) and Burgers' equations (1.12) can be transformed into the classical Hamilton-Jacobi equations. We now look at a stochastic version of this. Consider the stochastic Burgers' equation (1.37) with a potential $V(\underline{x})$,

$$\partial \underline{v} + (\underline{v} \cdot \nabla) \underline{v} \partial t = \frac{\mu^2}{2} \Delta \underline{v} \partial t - \nabla V(\underline{x}) \partial t - \nabla U(\underline{x}, t) \circ \partial W_t,$$

then by using the same transformation as in the classical case, $\underline{v} = \nabla S$, we can derive the stochastic Hamilton-Jacobi equation

$$\partial S + \frac{1}{2} |\nabla S|^2 \partial t + V(\underline{x}) \partial t + U(\underline{x}, t) \circ \partial W_t = \frac{\mu^2}{2} \Delta S \partial t. \quad (1.44)$$

For a proof of this, as well as a more rigorous account of the stochastic Hamilton-Jacobi theory, see [10].

1.6.3 Noisy Wavefronts and Caustics

Consider the stochastic heat equation (1.36) with a potential $V(\underline{x})$ for $u = u(\underline{x}, t)$ and with the coefficient of the stochastic term as $U(\underline{x}, t) = -x$,

$$\partial u = \frac{\mu^2}{2} \Delta u \partial t + V(\underline{x}) \frac{u}{\mu^2} \partial t - \frac{x}{\mu^2} u \circ \partial W_t,$$

with initial condition $u(\cdot, 0) = T_0(\cdot) e^{-\frac{S_0(\cdot)}{\mu^2}}$. This choice of $U(\underline{x}, t) = -x$ introduces the stochastic term as a random linear acceleration. As we have shown, the corresponding Burgers' equation (1.37) with a potential $V(\underline{x})$ is,

$$\partial \underline{v} + (\underline{v} \cdot \nabla) \underline{v} \partial t = \frac{\mu^2}{2} \Delta \underline{v} \partial t - \nabla V(\underline{x}) \partial t + \nabla(x) \circ \partial W_t,$$

with initial condition $\underline{v}(\cdot, 0) = \nabla S_0(\cdot)$. We shall assume that the stochastic heat equation has a solution of the form

$$u(\underline{x}, t) = \frac{1}{(2\pi\mu^2 t)^{\frac{3}{2}}} \int_{\mathbb{R}^3} T_0(\underline{x}_0) e^{-\frac{\phi(\underline{x}, \underline{x}_0, t)}{\mu^2}} dx_0 dy_0 dz_0,$$

where we have a phase function of the form

$$\phi(\underline{x}, \underline{x}_0, t) = A[\underline{x}, \underline{x}_0, t] + S_0(\underline{x}_0),$$

and $A[\underline{x}, \underline{x}_0, t]$ is the stochastic action of a classical mechanical path starting from \underline{x}_0 and getting to \underline{x} in time t , i.e.

$$A[\underline{x}, \underline{X}(0), t] = \inf_{\substack{\underline{X}(s) \\ \underline{X}(t) = \underline{x}}} \left\{ \frac{1}{2} \int_0^t \dot{\underline{X}}(s) \cdot \dot{\underline{X}}(s) ds - \int_0^t V(\underline{X}(s)) ds + \int_0^t \underline{X}(s) \circ dW_s \right\}.$$

Chapter 2

Stochastic Mehler Kernel Formulae

2.1 On Some Recent Papers

In this section we review some recent papers on the subject of stochastic analysis of heat and Burgers' equations. We shall present some of the results of A. Truman and H.Z. Zhao [10], A. Truman and T. Zastawniak [1, 5].

2.1.1 Stochastic Mehler Kernels and Path Integrals

In A. Truman and T. Zastawniak [1], they consider the one dimensional stochastic Schrödinger equation,

$$i\partial\psi(x,t) = \left(-\frac{1}{2}\frac{\partial^2}{\partial x^2} + \frac{a^2}{2}x^2\right)\psi(x,t)dt + (K\psi(x,t))(x) \circ dW_t, \quad (2.1)$$

for the Wiener process W_t with \circ representing a Stratonovich integral rather than an Itô integral¹. Specifically they look at the cases of the position operator $K(x) = x$ and the momentum operator case $K(x) = -i\frac{d}{dx}$, applying extensions of the Itô-Albeverio-Høegh-Krohn Feynman path integral approach [13, 14] to compute the stochastic Mehler kernels of the corresponding Schrödinger equations.

We are mainly interested in the position operator case, where the solution is found by using configuration space path integrals and the Green's function of the stochastic Schrödinger equation,

$$i\partial\psi(x,t) = \left(-\frac{1}{2}\frac{\partial^2}{\partial x^2} + \frac{a^2}{2}x^2\right)\psi(x,t)dt + x\psi(x,t) \circ dW_t, \quad (2.2)$$

¹We discuss the relationship between Stratonovich and Itô calculus in Appendix B.1.

is shown to be

$$\begin{aligned} G(x, x_0, t) &= \sqrt{\frac{a}{2\pi i \sin(at)}} e^{\frac{ia}{2\sin(at)} [(x^2 + x_0^2) \cos(at) - 2xx_0]} \\ &\quad \times e^{-i \int_0^t \frac{[x \sin(ar) - x_0 \sin(ar-at)]}{\sin(at)} \circ dW_r} \\ &\quad \times e^{i \int_0^t \int_0^r \frac{\sin(as) \sin(ar-at)}{a \sin(at)} \circ dW_s \circ dW_r}. \end{aligned}$$

for all $t \in \mathbb{R}^+$, $t \neq \frac{k\pi}{a}$ and $k \in \mathbb{N}$.

As we saw in Section 1.1.1, we may easily convert from a Schrödinger type equation to a heat equation by mapping $t \mapsto it$. This is a standard technique from Complex Variables where we are essentially moving from real to complex time. We may further extend this by setting $t \mapsto i\mu^2 t$ and $w = \mu^2 a$ such that we obtain a corresponding stochastic heat equation for $u(x, t) = \psi(x, t)$ as

$$\partial u(x, t) = \left(\frac{\mu^2}{2} \frac{\partial^2}{\partial x^2} - \frac{w^2 x^2}{2\mu^2} \right) u(x, t) dt - xu(x, t) \circ dW_t, \quad (2.3)$$

which in turn gives the stochastic Green's function as

$$G(x, x_0, t) = \sqrt{\frac{w}{2\pi\mu^2 \sinh(wt)}} e^{\frac{-w}{2\mu^2 \sinh(wt)} [(x^2 + x_0^2) \cosh(wt) - 2xx_0]} \quad (2.4)$$

$$\times e^{-\int_0^t \frac{[x \sinh(wr) - x_0 \sinh(wr-wt)]}{\mu^2 \sinh(wt)} \circ dW_r} \quad (2.5)$$

$$\times e^{-\int_0^t \int_0^r \frac{\sinh(ws) \sinh(wr-wt)}{\mu^2 w \sinh(wt)} \circ dW_s \circ dW_r}. \quad (2.6)$$

Later we shall consider the stochastic heat equation with a harmonic oscillator potential as

$$\partial u(x, t) = \left(\frac{\mu^2}{2} \frac{\partial^2}{\partial x^2} + \frac{w^2 x^2}{2\mu^2} \right) u(x, t) dt - xu(x, t) \circ dW_t, \quad (2.7)$$

where we simply let $w \rightarrow iw$ to provide us with interesting periodic results. We also look at the limiting case $w \rightarrow 0$ to examine the effects of noise on the zero potential case.

2.2 Classical Green Functions

In this section, we consider the classical heat equation (1.1) and examine the respective solutions via the use of Green's functions. We also discuss the singularities of the heat and Burgers' equations in each case and we begin by taking a look at the case of the classical heat and Burgers' equations, under three different potentials: the zero; harmonic oscillator; and the linear potential cases. The simplest case that we shall

cover is the classical case with a zero potential. Later on, in Chapters 3 and 4, we give some explicit examples of the singularities of Burgers' equation and wavefronts of the heat equation with and without noise terms. We also take time to discuss the nature of these singularities in relation to the corresponding Thom catastrophes. In this section we shall discuss how we go about computing the singularities, discussing the different approaches required for cases of different potentials.

2.2.1 Zero Potential Case

Theorem 2.2.1.

The one dimensional heat equation with no potential term

$$\frac{\partial u_t}{\partial t} = \frac{\mu^2}{2} \frac{\partial^2 u_t}{\partial x^2}, \quad (2.8)$$

where $u_t(x) = u(x, t)$ for position x and time t , has solution

$$u(x, t) = \int_{-\infty}^{\infty} G(x, x_0, t) u_0(x_0) dx_0, \quad (2.9)$$

with

$$\lim_{t \rightarrow 0^+} u(x, t) = u_0(x),$$

for $u_0(x_0) \in C_0^\infty(\mathbb{R})$ and with Green's function given by

$$G(x, x_0, t) = \frac{1}{\sqrt{2\pi\mu^2 t}} e^{-\frac{(x-x_0)^2}{2\mu^2 t}}. \quad (2.10)$$

Proof.

To begin we show that the Green's function (2.10) is actually a solution of the partial differential equation (2.8). Taking the natural logarithm of the Green's function (2.10), then we obtain

$$\ln G = -\frac{1}{2} \ln(2\pi\mu^2 t) - \frac{(x-x_0)^2}{2\mu^2 t},$$

and differentiating with respect to time t gives

$$\frac{\partial G}{\partial t} = \left[\frac{(x-x_0)^2}{2\mu^2 t^2} - \frac{1}{2t} \right] G.$$

Now differentiating $\ln G$ with respect to x gives us

$$\frac{\partial G}{\partial x} = -\frac{(x-x_0)}{\mu^2 t} G,$$

and looking at the second derivative of $\ln G$ with respect to x , we have

$$\frac{\partial^2 G}{\partial x^2} = \left[\frac{(x - x_0)^2}{\mu^4 t^2} - \frac{1}{\mu^2 t} \right] G.$$

Putting these terms into our heat equation above, we obtain,

$$\left[\frac{(x - x_0)^2}{2\mu^2 t^2} - \frac{1}{2t} \right] G = \frac{\mu^2}{2} \left[\frac{(x - x_0)^2}{\mu^4 t^2} - \frac{1}{\mu^2 t} \right] G.$$

This shows that the Green's function (2.10) satisfies the heat equation (2.8). We may also see that, for $u_0 \in C_0^\infty(\mathbb{R})$,

$$\int_{-\infty}^{\infty} G(x, x_0, t) u_0(x_0) dx_0,$$

is also a solution of the heat equation 2.8. All that remains to be shown is that

$$\lim_{t \rightarrow 0^+} u(x, t) = u_0(x).$$

Making the substitution $x_0 = x + z\mu\sqrt{t}$ in $u(x, t)$ yields

$$\begin{aligned} u(x, t) &= \frac{1}{\sqrt{2\pi\mu^2 t}} \int_{-\infty}^{\infty} e^{-\frac{z^2}{2}} u_0(x + z\mu\sqrt{t}) \mu\sqrt{t} dz \\ &= \frac{1}{\sqrt{2\pi}} \int_{-\infty}^{\infty} e^{-\frac{z^2}{2}} u_0(x + z\mu\sqrt{t}) dz. \end{aligned}$$

Then by the dominated convergence theorem, we may deduce that

$$\begin{aligned} \lim_{t \rightarrow 0^+} u(x, t) &= \frac{1}{\sqrt{2\pi}} \int_{-\infty}^{\infty} e^{-\frac{z^2}{2}} \lim_{t \rightarrow 0^+} u_0(x + z\mu\sqrt{t}) dz \\ &= u_0(x), \end{aligned}$$

as required. \square

We observe that, by the dominated convergence theorem, the above proof works when u_0 is bounded and continuous. Now we need to consider

$$u_0 = T_0 e^{-\frac{s_0}{\mu^2}},$$

for some convergence factor $T_0 > 0$. From Theorem 1.2.1, we can consider $\lim_{\mu \rightarrow 0} \underline{v}^\mu$, where

$$\frac{\partial \underline{v}^\mu}{\partial t} + (\underline{v}^\mu \cdot \nabla) \underline{v}^\mu = \frac{\mu^2}{2} \Delta \underline{v}^\mu,$$

with the initial condition $\underline{v}_0^\mu = \nabla S_0 - \mu^2 \nabla \ln T_0$. Formally this limit is

$$\frac{\partial \underline{v}}{\partial t} + (\underline{v} \cdot \nabla) \underline{v} = 0,$$

for initial condition $\underline{v}_0 = \nabla S_0$, but the latter equation does not have a unique solution. Hence, our limit provides a method of selecting a solution which should be the physically interesting case corresponding to the minimal classical action. Now, extending the solution of the heat equation to \mathbb{R}^3 , we have a phase function given by

$$\phi(\underline{x}, \underline{x}_0, t) = \frac{(x - x_0)^2}{2t} + \frac{(y - y_0)^2}{2t} + \frac{(z - z_0)^2}{2t} + S_0(\underline{x}_0). \quad (2.11)$$

As we saw earlier, the singularities of the inviscid limit of the Burgers' velocity field

$$\frac{\partial \underline{v}^\mu}{\partial t} + (\underline{v}^\mu \cdot \nabla) \cdot \underline{v}^\mu = \frac{\mu^2}{2} \Delta \underline{v}^\mu,$$

are given by the determinant of the Hessian matrix of the phase function (2.11). We eliminate \underline{x} to obtain the pre-caustic, and \underline{x}_0 to obtain the caustic, by means of the classical mechanical flow $\nabla_{\underline{x}_0} \phi(\underline{x}, \underline{x}_0, t) = 0$. This tells us that the zero potential pre-caustic will be determined by

$$\left| \frac{1}{t} I_3 + \frac{\partial^2 S_0}{\partial \underline{x}_0^2} \right| = 0, \quad (2.12)$$

which contains no terms in \underline{x} . In order to calculate the caustic, one must apply the flow $\nabla_{\underline{x}_0} \phi = 0$, which in this case, simplifies to

$$\underline{x} = \underline{x}_0 + t \nabla_{\underline{x}_0} S_0(\underline{x}_0). \quad (2.13)$$

If the expression for the pre-caustic (2.12) is linear in one component of \underline{x}_0 , then we could easily obtain a parametric expression of the caustic. One may also attempt to directly eliminate the \underline{x}_0 variables from the set of equations (2.12) and (2.13).

Now for the heat equation

$$\frac{\partial u}{\partial t} = \frac{\mu^2}{2} \Delta u, \quad (2.14)$$

the wave-fronts are given by

$$\inf_{\underline{x}_0 \in \mathbb{R}^3} \phi(\underline{x}, \underline{x}_0, t) = 0, \quad (2.15)$$

where we eliminate \underline{x} for the pre-wavefront, and \underline{x}_0 for the wavefront. We may simplify the expression for the pre-wavefront by making use of the flow (2.13) to eliminate \underline{x} , this provides a nice expression for the pre-wavefront as the Eikonal equation

$$\frac{t}{2} |\nabla_{\underline{x}_0} S_0(\underline{x}_0)|^2 + S_0(\underline{x}_0) = 0. \quad (2.16)$$

The wavefront, on the other hand, can be quite complex, when we attempt to eliminate \underline{x} . Even when using simple polynomial based functions, we shall see that we can soon run into some difficulties investigating these singularities.

2.2.2 Linear Potential Case

Theorem 2.2.2.

The heat equation with a linear potential,

$$\frac{\partial u}{\partial t} = \frac{\mu^2}{2} \frac{\partial^2 u}{\partial x^2} - \frac{k}{\mu^2} x u, \quad (2.17)$$

has solution

$$u(x, t) = \int_{-\infty}^{\infty} G(x, x_0, t) u_0(x_0) dx_0,$$

with initial condition

$$\lim_{t \rightarrow 0^+} u(x, t) = u_0(x),$$

where we have $u_0 \in C_0^\infty$ and Green's function

$$G(x, x_0, t) = \frac{1}{\sqrt{2\pi\mu^2 t}} e^{-\frac{(x-x_0)^2}{2\mu^2 t} - \frac{kt}{2\mu^2}(x+x_0) + \frac{k^2 t^3}{24\mu^2}}. \quad (2.18)$$

Proof.

Taking the natural logarithm of the Green's function (2.18), we see that

$$\ln G = -\frac{1}{2} \ln(2\pi\mu^2 t) - \frac{(x-x_0)^2}{2\mu^2 t} - \frac{kt}{2\mu^2}(x+x_0) + \frac{k^2 t^3}{24\mu^2},$$

so that the first derivative of $\ln G$ with respect to time t is given by

$$\frac{\partial G}{\partial t} = \left[\frac{k^2 t^2}{8\mu^2} - \frac{k}{2\mu^2}(x+x_0) + \frac{(x-x_0)^2}{2\mu^2 t^2} - \frac{1}{2t} \right] G.$$

Now, looking at the first derivative with respect to position x , we obtain

$$\frac{\partial G}{\partial x} = \left[-\frac{kt}{2\mu^2} - \frac{(x-x_0)}{\mu^2 t} \right] G,$$

which gives the second derivative with respect to position x as

$$\frac{\partial^2 G}{\partial x^2} = \left[\frac{k^2 t^2}{4\mu^4} + \frac{k}{\mu^4}(x-x_0) + \frac{(x-x_0)^2}{\mu^4 t^4} - \frac{1}{\mu^2 t} \right] G.$$

Then putting the above expressions into the heat equation with the linear potential (2.17), we have

$$\begin{aligned} & \frac{k^2 t^2}{8\mu^2} - \frac{k}{2\mu^2}(x+x_0) + \frac{(x-x_0)^2}{2\mu^2 t^2} - \frac{1}{2t} \\ &= \frac{\mu^2}{2} \left[\frac{k^2 t^2}{4\mu^4} + \frac{k}{\mu^4}(x-x_0) + \frac{(x-x_0)^2}{\mu^4 t^4} - \frac{1}{\mu^2 t} \right] - \frac{kx}{\mu^2}, \end{aligned}$$

as required. Hence, the Green's function (2.18) solves the heat equation with the linear potential (2.17). Now we must verify that we have the initial condition

$$\lim_{t \rightarrow 0^+} u(x, t) = u_0(x).$$

In the case of small t we see that

$$-\frac{(x-x_0)^2}{2\mu^2 t} - \frac{kt}{2\mu^2}(x+x_0) + \frac{k^2 t^3}{24\mu^2} \approx -\frac{(x-x_0)^2}{2\mu^2 t},$$

since the terms involving positive powers of t will vanish as $t \rightarrow 0$. Hence we may reduce this to our zero potential case. \square

Consider the following heat equation in \mathbb{R}^3 with a linear potential $\underline{K} = (k_1, k_2, k_3)$,

$$\frac{\partial u_t}{\partial t} = \frac{\mu^2}{2} \Delta u_t - \frac{\underline{K} \cdot \underline{x}}{\mu^2} u_t, \quad (2.19)$$

with initial condition $u_0 = e^{-\frac{S_0}{\mu^2}}$ and where \cdot represents the standard scalar product of a pair of vectors in \mathbb{R}^3 . Then from the one dimensional case, equation (2.18), we derive its Green's function to be

$$G(x, x_0, t) = \frac{1}{(2\pi\mu^2 t)^{\frac{3}{2}}} \exp \left\{ -\frac{(\underline{x} - \underline{x}_0)^2}{2\mu^2 t} - \frac{t}{2\mu^2} \underline{K} \cdot (\underline{x} - \underline{x}_0) + \frac{t^3}{24\mu^2} \underline{K}^2 \right\}, \quad (2.20)$$

which gives the solution of the heat equation with a linear potential (2.19) as

$$u(x, t) = \frac{1}{(2\pi\mu^2 t)^{\frac{3}{2}}} \int \int \int_{\mathbb{R}^3} e^{-\frac{\phi(\underline{x}, \underline{x}_0, t)}{\mu^2}} dx_0 dy_0 dz_0,$$

where the phase function $\phi = \phi(\underline{x}, \underline{x}_0, t)$ is

$$\phi(\underline{x}, \underline{x}_0, t) = \frac{(\underline{x} - \underline{x}_0)^2}{2t} + \frac{t}{2} \underline{K} \cdot (\underline{x} + \underline{x}_0) - \frac{t^3}{24} \underline{K}^2 + S_0(\underline{x}_0). \quad (2.21)$$

We can calculate the classical mechanical flow by looking at $\nabla_{\underline{x}_0} \phi(\underline{x}, \underline{x}_0, t) = 0$, which gives us

$$\underline{x} = \underline{x}_0 + \frac{t^2}{2} \underline{K} + t \nabla_{\underline{x}_0} S_0(\underline{x}_0). \quad (2.22)$$

Now, recall that the pre-caustic is calculated by looking at the zeros of the determinant of the Hessian matrix of $\phi(\underline{x}, \underline{x}_0, t)$, in this case this simplifies to exactly the case of the zero potential, i.e.

$$\left| \frac{1}{t} I_3 + \frac{\partial^2 S_0}{\partial \underline{x}_0^2} \right| = 0, \quad (2.23)$$

and the caustic will come from applying the above classical mechanical flow to eliminate the \underline{x}_0 terms. Recall also that the pre-wavefront is given by the zeros of $\phi(\underline{x}, \underline{x}_0, t)$, where we eliminate the \underline{x} terms by using the classical mechanical flow, and we have the pre-wavefront for the linear potential case given by

$$\frac{t}{2} \left(\frac{t}{2} \underline{K} + \nabla_{\underline{x}_0} S_0 \right)^2 + \frac{t}{2} \underline{K} \cdot \left(2\underline{x}_0 + \frac{t^2}{2} \underline{K} + t \nabla_{\underline{x}_0} S_0 \right) - \frac{t^3}{24} \underline{K}^2 + S_0(\underline{x}_0) = 0. \quad (2.24)$$

2.2.3 Harmonic Oscillator Potential Case

Theorem 2.2.3.

The one dimensional heat equation with harmonic oscillator potential

$$\frac{\partial u}{\partial t} = \frac{\mu^2}{2} \frac{\partial^2 u}{\partial x^2} + \frac{w^2}{2\mu^2} x^2 u, \quad (2.25)$$

has solution

$$u(x, t) = \int_{-\infty}^{\infty} G(x, x_0, t) u_0(x_0) dx_0,$$

with

$$\lim_{t \rightarrow 0^+} u(x, t) = u_0(x),$$

for $u_0 \in C_0^\infty(\mathbb{R})$ and with Green's function given by

$$G(x, x_0, t) = \sqrt{\frac{w}{2\pi\mu^2 \sin(wt)}} e^{-\frac{w}{2\mu^2} \left[\frac{(x^2 + x_0^2) \cos(wt) - 2xx_0}{\sin(wt)} \right]}. \quad (2.26)$$

We must take care here as the solution $u(x, t)$ will become unstable for large time t . That is, we need $\sin(wt) > 0$ such that $t < \frac{\pi}{w}$, or in the \mathbb{R}^3 case, we require $t < \frac{\Pi}{\max(w_i)}$.

Proof.

We should begin by verifying that the Green's function (2.26) is actually a solution of the heat equation (2.25). We look at the natural logarithm of the Green's function (2.26),

$$\ln G = -\frac{1}{2} \ln \left(\frac{2\pi\mu^2}{w} \sin(wt) \right) - \frac{w}{2\mu^2} \left[\frac{(x^2 + x_0^2) \cos(wt) - 2xx_0}{\sin(wt)} \right],$$

and differentiating with respect to time gives us

$$\frac{\partial G}{\partial t} = \left[-\frac{w}{2 \tan(wt)} + \frac{w^2}{2\mu^2} (x^2 + x_0^2) + \frac{w^2 (x^2 + x_0^2)}{2\mu^2 \tan^2(wt)} - \frac{w^2 x x_0}{\mu^2 \sin(wt) \tan(wt)} \right] G.$$

Now differentiating with respect to space x we obtain

$$\frac{\partial G}{\partial x} = \left[-\frac{wx}{\mu^2 \tan(wt)} + \frac{wx_0}{\mu^2 \sin(wt)} \right] G,$$

which gives second derivative as

$$\frac{\partial^2 G}{\partial x^2} = \left[-\frac{w}{\mu^2 \tan(wt)} + \left(-\frac{wx}{\mu^2 \tan(wt)} + \frac{wx_0}{\mu^2 \sin(wt)} \right)^2 \right] G.$$

Then putting this into our harmonic oscillator heat equation (2.25), we have

$$\begin{aligned} & -\frac{w}{2 \tan(wt)} + \frac{w^2}{2\mu^2} (x^2 + x_0^2) + \frac{w^2 (x^2 + x_0^2)}{2\mu^2 \tan^2(wt)} - \frac{w^2 x x_0}{\mu^2 \sin(wt) \tan(wt)} \\ &= \frac{\mu^2}{2} \left[-\frac{w}{\mu^2 \tan(wt)} + \frac{w^2 x^2}{\mu^4 \tan^2(wt)} + \frac{w^2 x_0^2}{\mu^4 \sin^2(wt)} - \frac{2w^2 x x_0}{\mu^4 \sin(wt) \tan(wt)} \right] + \frac{w^2 x^2}{2\mu^2}. \end{aligned}$$

This simplifies to the well known trigonometric identity

$$1 + \frac{1}{\tan^2(wt)} = \frac{1}{\sin^2(wt)}.$$

Now we need to show that

$$\lim_{t \rightarrow 0^+} u(x, t) = u_0(x).$$

Clearly in the case of small t we have $\sin(wt) \approx wt$ and $\cos(wt) \approx 1$ which reduces us to the zero potential case, since our solution behaves like

$$u(x, t) \approx \frac{1}{\sqrt{2\pi\mu^2 t}} \int_{-\infty}^{\infty} e^{-\frac{(x-x_0)^2}{2\mu^2 t}} u_0(x_0) dx_0.$$

Then, we may use the same approach that we applied in the previous proof to show that

$$\lim_{t \rightarrow 0^+} u(x, t) = u_0(x).$$

□

We can now go onto consider a three dimensional heat equation of the type (2.25), i.e.

$$\frac{\partial u_t}{\partial t} = \frac{\mu^2}{2} \Delta u_t + \frac{1}{2\mu^2} (w_1^2 x^2 + w_2^2 y^2 + w_3^2 z^2) u_t, \quad (2.27)$$

with initial condition $u_0 = e^{-\frac{S_0}{\mu^2}}$. We may then examine the phase function for the harmonic oscillator potential, namely

$$\begin{aligned} \phi(\underline{x}, \underline{x}_0, t) &= \frac{w_1}{2} \left[\frac{(x^2 + x_0^2) \cos(w_1 t) - 2xx_0}{\sin(w_1 t)} \right] + \frac{w_2}{2} \left[\frac{(y^2 + y_0^2) \cos(w_2 t) - 2yy_0}{\sin(w_2 t)} \right] \\ &\quad + \frac{w_3}{2} \left[\frac{(z^2 + z_0^2) \cos(w_3 t) - 2zz_0}{\sin(w_3 t)} \right] + S_0(\underline{x}_0). \end{aligned} \quad (2.28)$$

It may easily be shown that the classical mechanical flow $\nabla_{\underline{x}_0} \phi(\underline{x}, \underline{x}_0, t) = 0$ is given by

$$\begin{pmatrix} x \\ y \\ z \end{pmatrix} = \begin{pmatrix} x_0 \cos(w_1 t) \\ y_0 \cos(w_2 t) \\ z_0 \cos(w_3 t) \end{pmatrix} + \begin{pmatrix} \frac{\sin(w_1 t)}{w_1} \frac{\partial S_0}{\partial x_0} \\ \frac{\sin(w_2 t)}{w_2} \frac{\partial S_0}{\partial y_0} \\ \frac{\sin(w_3 t)}{w_3} \frac{\partial S_0}{\partial z_0} \end{pmatrix}. \quad (2.29)$$

Recall that the pre-caustic is given by the zeros of the determinant of the Hessian matrix, with respect to \underline{x}_0 , of $\phi(\underline{x}, \underline{x}_0, t)$, namely

$$\text{Det} \left| \frac{\partial^2 \phi}{\partial \underline{x}_0^2} \right| = 0.$$

Looking at the second derivative with respect to x_0 we have

$$\frac{\partial^2 \phi}{\partial x_0^2} = \frac{w_1}{\tan(w_1 t)} + \frac{\partial^2 S_0}{\partial x_0^2},$$

and similarly for the y_0 and z_0 derivatives, where the second order derivatives are continuous. Then we see that the pre-caustic is given by

$$\left| \begin{pmatrix} \frac{w_1}{\tan(w_1 t)} & 0 & 0 \\ 0 & \frac{w_2}{\tan(w_2 t)} & 0 \\ 0 & 0 & \frac{w_3}{\tan(w_3 t)} \end{pmatrix} + \begin{pmatrix} \frac{\partial^2 S_0}{\partial x_0^2} & \frac{\partial^2 S_0}{\partial y_0 \partial x_0} & \frac{\partial^2 S_0}{\partial z_0 \partial x_0} \\ \frac{\partial^2 S_0}{\partial x_0 \partial y_0} & \frac{\partial^2 S_0}{\partial y_0^2} & \frac{\partial^2 S_0}{\partial z_0 \partial y_0} \\ \frac{\partial^2 S_0}{\partial x_0 \partial z_0} & \frac{\partial^2 S_0}{\partial y_0 \partial z_0} & \frac{\partial^2 S_0}{\partial z_0^2} \end{pmatrix} \right| = 0. \quad (2.30)$$

Observe that in the case where w_1 , w_2 and w_3 tend to zero we obtain the earlier zero potential case,

$$\left| \frac{1}{t} I_3 + \frac{\partial^2 S_0}{\partial \underline{x}_0^2} \right| = 0,$$

as in equation (2.12). We can calculate the caustic by applying the flow to the pre-caustic and eliminating the terms x_0 , y_0 and z_0 for our specific $S_0(\underline{x}_0)$, which, as we shall see later, is easier to compute in a specific example. The pre-wavefront is given by $\phi(\underline{x}_0, t) = 0$ where we reduce $\phi(\underline{x}, \underline{x}_0, t) = \phi(\underline{x}_0, t)$ by using the flow to eliminate

the terms x , y and z in the phase function, hence we have $\phi(\underline{x}_0, t) = 0$ as

$$\begin{aligned}
& \frac{w_1}{2 \sin(w_1 t)} \left\{ \left[\left(x_0 \cos(w_1 t) + \frac{\sin(w_1 t)}{w_1} \frac{\partial S_0}{\partial x_0} \right)^2 + x_0^2 \right] \cos(w_1 t) \right. \\
& \quad \left. - 2 \left(x_0 \cos(w_1 t) + \frac{\sin(w_1 t)}{w_1} \frac{\partial S_0}{\partial x_0} \right) x_0 \right\} \\
& + \frac{w_2}{2 \sin(w_2 t)} \left\{ \left[\left(y_0 \cos(w_2 t) + \frac{\sin(w_2 t)}{w_2} \frac{\partial S_0}{\partial y_0} \right)^2 + y_0^2 \right] \cos(w_2 t) \right. \\
& \quad \left. - 2 \left(y_0 \cos(w_2 t) + \frac{\sin(w_2 t)}{w_2} \frac{\partial S_0}{\partial y_0} \right) y_0 \right\} \\
& + \frac{w_3}{2 \sin(w_3 t)} \left\{ \left[\left(z_0 \cos(w_3 t) + \frac{\sin(w_3 t)}{w_3} \frac{\partial S_0}{\partial z_0} \right)^2 + z_0^2 \right] \cos(w_3 t) \right. \\
& \quad \left. - 2 \left(z_0 \cos(w_3 t) + \frac{\sin(w_3 t)}{w_3} \frac{\partial S_0}{\partial z_0} \right) z_0 \right\} + S_0(\underline{x}_0) = 0.
\end{aligned} \tag{2.31}$$

Again, we can see that as we let the potential tend to zero we obtain the zero potential case,

$$\frac{t}{2} |\nabla_{\underline{x}_0} S_0(\underline{x}_0)|^2 + S_0(\underline{x}_0) = 0, \tag{2.32}$$

as in equation (2.16).

In order to calculate the wavefront we must apply the flow to the pre-wavefront so that we can eliminate the terms x_0 , y_0 and z_0 . In some cases, however, this is not possible directly, as we shall see in the zero potential case of the butterfly and fish. This we overcome by applying the classical mechanical flow numerically.

2.3 Noisy Green Function

2.3.1 Zero Potential Case

Consider the stochastic heat equation under a harmonic oscillator potential that we obtained earlier in (2.3),

$$\partial u = \left(\frac{\mu^2}{2} \frac{\partial^2}{\partial x^2} - \frac{w^2}{2\mu^2} x^2 \right) u \partial t - \frac{x}{\mu^2} u \circ dW_t,$$

where $\circ dW_t$ denotes a Stratonovich integral with respect to the Wiener process W_t and $u = u(x, t)$. We know, from Section 2.1.1, that the stochastic heat Mehler kernel

is given by

$$\begin{aligned}
G(x, x_0, t) = & \sqrt{\frac{w}{2\pi\mu^2 \sinh wt}} e^{\frac{-w}{2\mu^2 \sinh(wt)} [(x^2 + x_0^2) \cosh(wt) - 2x_0]} \\
& \times e^{-\int_0^t \frac{x \sinh(wr) - x_0 \sinh(w(r-t))}{\mu^2 \sinh(wt)} \circ dW_r} \\
& \times e^{-\int_0^t \int_0^r \frac{\sinh(ws) \sinh(w(r-t))}{\mu^2 w \sinh(wt)} \circ dW_s \circ dW_r}. \quad (2.33)
\end{aligned}$$

We are particularly interested in the case of $w \rightarrow 0$. We begin by looking at small w , so that by virtue of small angles, we have

$$\begin{aligned}
G(x, x_0, t) = & \frac{1}{\sqrt{2\pi\mu^2 t}} e^{-\frac{(x-x_0)^2}{2\mu^2 t}} e^{-\frac{1}{\mu^2 t} \int_0^t [xr - x_0(r-t)] \circ dW_r} \\
& \times e^{-\frac{1}{\mu^2 t} \int_0^t \int_0^r s(r-t) \circ dW_s \circ dW_r}.
\end{aligned}$$

Since we are dealing with a smooth function, we may calculate the first Stratonovich integral by a simple application of Itô's formula,

$$\int_0^t [xr - x_0(r-t)] \circ dW_r = xtW_t - (x-x_0) \int_0^t W_s ds.$$

Note that $W_s(\omega)$ is the position of a one dimensional Brownian motion at time s , or the value of a Wiener process at time s , and the integral $\int_0^t W_s ds$ is the integral of the Wiener process from time 0 to t . Both of these are stochastic processes and their values will depend upon the specific sample path taken by the Wiener process. Since this is random it will make an exact calculation impossible, but there are several options available to help with this. For example, we may work with expectations, or approximations based on a chosen sample path. Details of how we deal with this for the purposes of this work are given in Appendix B.3. The second stochastic integral in this heat kernel is quite complex so for the meantime we simply represent it by

$$\zeta(t) = \int_0^t \int_0^r s(r-t) \circ dW_s \circ dW_r. \quad (2.34)$$

A more detailed treatment may be found in Appendix B.2. Re-capping over what we have just shown, we can prove, by using the dominated convergence theorem:

Theorem 2.3.1.

The one dimensional stochastic heat equation

$$\partial u = \frac{\mu^2}{2} \frac{\partial^2 u}{\partial x^2} \partial t - \frac{x}{\mu^2} u \circ dW_t, \quad (2.35)$$

has solution

$$u(x, t) = \int_{-\infty}^{\infty} G(x, x_0, t) u_0(x_0) dx_0,$$

with initial condition

$$\lim_{t \rightarrow 0^+} u(x, t) = u_0(x),$$

for deterministic $u_0 \in C_0^\infty(\mathbb{R})$ where we have the stochastic Green's function

$$G(x, x_0, t) = \frac{1}{\sqrt{2\pi\mu^2 t}} e^{\left(-\frac{(x-x_0)^2}{2\mu^2 t} - \frac{xW_t}{\mu^2} + \frac{(x-x_0)}{\mu^2 t} \int_0^t W_s ds\right)} e^{-\frac{\zeta(t)}{\mu^2 t}}, \quad (2.36)$$

and $\zeta(t)$ is given by

$$\zeta(t) = \zeta(t, \omega) := \int_0^t \int_0^r s(r-t) \circ dW_s \circ dW_r.$$

Proof.

All that we have to prove is that the above $G(x, x_0, t)$ is indeed the Green's function for the stochastic heat equation (2.35). Observe that taking the natural logarithm of the Green's function (2.36) gives

$$\ln G(x, x_0, t) = -\frac{1}{2} \ln(2\pi\mu^2 t) - \frac{(x-x_0)^2}{2\mu^2 t} - \frac{xW_t}{\mu^2} + \frac{(x-x_0)}{\mu^2 t} \int_0^t W_s ds - \frac{\zeta(t)}{\mu^2 t},$$

and differentiating with respect to time t yields the Stratonovich derivative as

$$\begin{aligned} \partial G = & \left[-\frac{1}{2t} + \frac{(x-x_0)^2}{2\mu^2 t^2} - \frac{x}{\mu^2} \frac{\partial W_t}{\partial t} - \frac{(x-x_0)}{\mu^2 t^2} \int_0^t W_s ds \right. \\ & \left. + \frac{(x-x_0)}{\mu^2 t} W_t + \frac{\zeta(t)}{\mu^2 t^2} - \frac{\dot{\zeta}(t)}{\mu^2 t} \right] G \partial t. \end{aligned}$$

Now differentiating $\ln G$ with respect to space x gives

$$\frac{\partial G}{\partial x} = \left[-\frac{(x-x_0)}{\mu^2 t} - \frac{W_t}{\mu^2} + \frac{1}{\mu^2 t} \int_0^t W_s ds \right] G,$$

and the second derivative with respect to space x is

$$\frac{\partial^2 G}{\partial x^2} = \left[-\frac{1}{\mu^2 t} + \left(-\frac{(x-x_0)}{\mu^2 t} - \frac{W_t}{\mu^2} + \frac{1}{\mu^2 t} \int_0^t W_s ds \right) \right] G.$$

Then inserting these derivatives into the stochastic heat equation (2.35), we have, after some cancellation of terms

$$\frac{\zeta(t)}{\mu^2 t^2} - \frac{\dot{\zeta}(t)}{\mu^2 t} = \frac{W_t^2}{2\mu^2} - \frac{W_t}{\mu^2 t} \int_0^t W_s ds + \frac{1}{2\mu^2 t^2} \left(\int_0^t W_s ds \right)^2.$$

Namely

$$-\frac{\partial}{\partial t} \left(\frac{\zeta(t)}{t} \right) = \frac{1}{2t^2} \left(\int_0^t r \circ dW_r \right)^2.$$

Then we see that in order for the Green's function to solve the stochastic heat equation (2.35), we must have the following

$$-\frac{\zeta(t)}{t} = \frac{1}{2} \int_0^t \frac{1}{r^2} \left(\int_0^r s \circ dW_s \right)^2 dr.$$

In a forthcoming work by Chris Reynolds, [15], this has been proved, so we assume that the above holds. Then we see that the Green's function (2.36) indeed solves the stochastic heat equation (2.35), and the proof is complete. \square

In full, for $u_0 = e^{-\frac{S_0}{\mu^2}}$, the solution of the zero potential stochastic heat equation (2.35) is

$$u(x, t) = \frac{e^{-\frac{\zeta(t)}{\mu^2 t}}}{\sqrt{2\pi\mu^2 t}} \int_{\mathbb{R}} e^{-\frac{1}{\mu^2} \left[\frac{(x-x_0)^2}{2t} + xW_t - \frac{(x-x_0)}{t} \int_0^t W_s ds \right]} e^{-\frac{S_0(x_0)}{\mu^2}} dx_0.$$

Hence, in this case we shall write our phase function as

$$\phi(x, x_0, t) = \frac{(x-x_0)^2}{2t} + xW_t - \frac{(x-x_0)}{t} \int_0^t W_s ds + \frac{\zeta(t)}{t} + S_0(x_0).$$

Now, consider the stochastic heat equation in \mathbb{R}^3 with a noise term in one dimension only, i.e.

$$\partial u_t = \frac{\mu^2}{2} \Delta u_t \partial t - \frac{x}{\mu^2} u_t \circ dW_t,$$

with initial condition $u_0 = e^{-\frac{S_0}{\mu^2}}$ and where $\circ dW_t$ represents a Stratonovich integral. The corresponding stochastic Burgers' equation is

$$\partial \underline{v} + (\underline{v} \cdot \nabla) \underline{v} \partial t = \frac{\mu^2}{2} \Delta \underline{v} \partial t + \nabla(x) \circ dW_t.$$

The solution of the stochastic heat equation is given by

$$u(\underline{x}, t) \simeq \frac{1}{(2\pi\mu^2 t)^{\frac{3}{2}}} \int_{\mathbb{R}^3} e^{-\frac{1}{\mu^2} \phi(\underline{x}, \underline{x}_0, t)} dx_0 dy_0 dz_0,$$

where the phase function $\phi(\underline{x}, \underline{x}_0, t)$ is

$$\begin{aligned} \phi(\underline{x}, \underline{x}_0, t) &= \frac{(x-x_0)^2}{2t} + \frac{(y-y_0)^2}{2t} + \frac{(z-z_0)^2}{2t} + xW_t \\ &\quad - \frac{(x-x_0)}{t} \int_0^t W_s ds + \frac{\zeta(t)}{t} + S_0(\underline{x}_0). \end{aligned}$$

We shall look at the wavefronts of the stochastic heat equation and the caustics of the stochastic Burgers' equation for the corresponding initial $S_0(\underline{x}_0)$ functions of the classical case, so that we may compare the resulting singularities. Now the pre-caustic of the heat equation are given by the zeros of the determinant of the Hessian matrix of $\phi(\underline{x}, \underline{x}_0, t)$, with respect to \underline{x}_0 . This is exactly the same as in the case without noise, i.e.

$$\left| \frac{\partial^2 \phi}{\partial \underline{x}_0^2} \right| = \left| I_3 + t \frac{\partial^2 S_0}{\partial \underline{x}_0^2} \right| = 0.$$

Next, the caustic for the heat equation comes from setting $\nabla_{\underline{x}_0} \phi(\underline{x}, \underline{x}_0, t) = 0$, which gives the flow

$$\underline{x} = \underline{x}_0 + t \nabla_{\underline{x}_0} S_0(\underline{x}_0) + \begin{pmatrix} \int_0^t W_s ds \\ 0 \\ 0 \end{pmatrix}.$$

If the pre-caustic may be solved explicitly to obtain $z_0 = z_0(x_0, y_0, t)$, then we may obtain the caustic as a set of parametric equations, making plotting much easier. If we are looking at a relatively simple $S_0(\underline{x}_0)$, then we may be able to form an explicit equation for the caustic. For the corresponding heat equation the pre-wavefront is given by

$$\inf_{\underline{x}_0 \in \mathbb{R}^3} \phi(\underline{x}, \underline{x}_0, t) = 0,$$

where we can use the flow to eliminate the terms in x , y and z to obtain

$$\begin{aligned} \frac{1}{2t} \left[\left(t \frac{\partial S_0}{\partial x_0} + \int_0^t W_s ds \right)^2 + \left(t \frac{\partial S_0}{\partial y_0} \right)^2 + \left(t \frac{\partial S_0}{\partial z_0} \right)^2 \right] \\ + \left(x_0 + t \frac{\partial S_0}{\partial x_0} + \int_0^t W_s ds \right) W_t - \frac{1}{t} \left(t \frac{\partial S_0}{\partial x_0} + \int_0^t W_s ds \right) \int_0^t W_s ds \\ + \frac{\zeta(t)}{t} + S_0(\underline{x}_0) = 0, \end{aligned}$$

or more simply,

$$\begin{aligned} \frac{t}{2} |\nabla_{\underline{x}_0} S_0(\underline{x}_0)|^2 + S_0(\underline{x}_0) + \left(x_0 + t \frac{\partial S_0}{\partial x_0} + \int_0^t W_s ds \right) W_t \\ - \frac{1}{2t} \left(\int_0^t W_s ds \right)^2 + \frac{\zeta(t)}{t} = 0. \quad (2.37) \end{aligned}$$

Then we can find the wavefront by eliminating x_0 , y_0 and z_0 by using the flow equations that arise from setting $\nabla_{\underline{x}_0} \phi(\underline{x}, \underline{x}_0, t) = 0$. This is often much easier to compute in a specific example.

2.3.2 Linear Potential Case

Consider the stochastic heat equation in one dimension with a linear potential, namely,

$$\frac{\partial u}{\partial t} = \frac{\mu^2}{2} \frac{\partial^2 u}{\partial x^2} - \frac{K}{\mu^2} x u - \frac{\alpha}{\mu^2} x u \circ \dot{W}_t, \quad (2.38)$$

where \dot{W}_t is white noise, K and α are constants, μ^2 is the viscosity and $u = u(x, t)$. We shall look for a solution of the form

$$u(x, t) = \int_{-\infty}^{\infty} G(x, x_0, t) e^{-\frac{S_0(x_0)}{\mu^2}} dx_0,$$

where the Green's function is given by

$$G(x, x_0, t) = \frac{1}{\sqrt{2\pi\mu^2 t}} e^{-\frac{1}{\mu^2} \left[\frac{(x-x_0)^2}{2t} + F(t)x + k(t)x_0 + l(t) \right]}, \quad (2.39)$$

and F , k and l are to be determined.

Now take the natural logarithm of the Green's function (2.39) to get,

$$\ln G = -\frac{1}{2} \ln(2\pi\mu^2 t) - \frac{(x-x_0)^2}{2\mu^2 t} - \frac{F(t)}{\mu^2} x - \frac{k(t)}{\mu^2} x_0 - \frac{l(t)}{\mu^2}. \quad (2.40)$$

Taking the Stratonovich derivative of (2.40) with respect to time t we obtain

$$\partial G = \left(-\frac{1}{2t} + \frac{(x-x_0)^2}{2\mu^2 t^2} \right) G \partial t - G \frac{\partial F}{\mu^2} x - G \frac{\partial k}{\mu^2} x_0 - G \frac{\partial l}{\mu^2}.$$

Differentiating (2.40) with respect to space x yields

$$\frac{\partial G}{\partial x} = \left(-\frac{(x-x_0)}{\mu^2 t} - \frac{F}{\mu^2} \right) G,$$

so that the second derivative of (2.40) with respect to space x is given by

$$\frac{\partial^2 G}{\partial x^2} = \left(-\frac{1}{\mu^2 t} + \frac{(x-x_0)^2}{\mu^4 t^2} + \frac{2F}{\mu^4 t} (x-x_0) + \frac{F^2}{\mu^4} \right) G.$$

Inserting these derivatives into our stochastic heat equation (2.38) we obtain, after eliminating the common terms in G ,

$$\begin{aligned} & \left(-\frac{1}{2t} + \frac{(x-x_0)^2}{2\mu^2 t^2} \right) \partial t - \frac{\partial F}{\mu^2} x - \frac{\partial k}{\mu^2} x_0 - \frac{\partial l}{\mu^2} \\ & = \left(-\frac{1}{2t} + \frac{(x-x_0)^2}{2\mu^2 t^2} + \frac{F}{\mu^2 t} (x-x_0) + \frac{F^2}{2\mu^2} - \frac{K}{\mu^2} x \right) \partial t - \frac{\alpha}{\mu^2} x \circ dW_t. \end{aligned}$$

After cancellation of terms, this gives

$$-x \partial F - x_0 \partial k - \partial l = \left(\frac{F}{t} x - \frac{F}{t} x_0 + \frac{F^2}{2} - Kx \right) \partial t - \alpha x \circ dW_t.$$

We may now calculate the functions of time $F(t)$, $k(t)$ and $l(t)$ by comparing coefficients. Looking at the coefficients of x , we have a first order stochastic differential equation,

$$\partial F + \frac{F}{t} \partial t = K \partial t + \alpha \circ dW_t,$$

i.e.

$$\partial (tF) = Kt \partial t + t\alpha \circ dW_t.$$

Assuming the $F(0) = 0$, this can be solved to give

$$F(t) = \frac{Kt}{2} + \frac{\alpha}{t} \int_0^t s \circ dW_s. \quad (2.41)$$

Now comparing the coefficients of x_0 and observing that F is continuous, we have the first order differential equation,

$$\frac{dk}{dt} = \frac{F}{t},$$

i.e.

$$\frac{dk}{dt} = \frac{K}{2} + \frac{\alpha}{t^2} \int_0^t s \circ dW_s,$$

which admits the solution

$$k(t) = \frac{Kt}{2} + \int_0^t \frac{\alpha}{r^2} \int_0^r s \circ dW_s \, dr. \quad (2.42)$$

Finally, comparing the constant terms, we have

$$\frac{dl}{dt} = -\frac{F^2}{2},$$

i.e.

$$\frac{dl}{dt} = -\frac{1}{2} \left(\frac{Kt}{2} + \frac{\alpha}{t} \int_0^t s \circ dW_s \right)^2,$$

which has the solution

$$l(t) = -\frac{K^2 t^3}{24} - \frac{\alpha K}{2} \int_0^t \int_0^r s \circ dW_s \, dr - \frac{\alpha^2}{2} \int_0^t \frac{1}{r^2} \left(\int_0^r s \circ dW_s \right)^2 \, dr. \quad (2.43)$$

Summarising the above we arrive at the following theorem

Theorem 2.3.2.

The one dimensional stochastic heat equation with a linear potential,

$$\partial u = \left(\frac{\mu^2}{2} \frac{\partial^2 u}{\partial x^2} - \frac{K}{\mu^2} x u \right) \partial t - \frac{\alpha}{\mu^2} x u \circ dW_t, \quad (2.44)$$

has solution

$$u(x, t) = \int_{-\infty}^{\infty} G(x, x_0, t) u_0(x_0) dx_0,$$

with initial condition

$$\lim_{t \rightarrow 0^+} u(x, t) = u_0(x),$$

for $u_0 \in C_0^\infty(\mathbb{R})$ where the Green's function is given by

$$\begin{aligned} G(x, x_0, t) = & \frac{1}{\sqrt{2\pi\mu^2 t}} \exp \left\{ -\frac{1}{\mu^2} \left(\frac{(x-x_0)^2}{2t} + \frac{Kt}{2} (x+x_0) - \frac{K^2 t^3}{24} \right) \right. \\ & + \frac{\alpha}{t} \int_0^t s \circ dW_s x + \alpha x_0 \int_0^t \int_0^r \frac{s}{r^2} \circ dW_s dr \\ & \left. - \frac{\alpha K}{2} \int_0^t \int_0^r s \circ dW_s dr - \frac{\alpha^2}{2} \int_0^t \frac{1}{r^2} \left(\int_0^r s \circ dW_s \right)^2 dr \right\}. \end{aligned} \quad (2.45)$$

Clearly as $\alpha \rightarrow 0$ we obtain the classical solution to the linear potential problem, see Section 2.2.2, namely

$$G(x, x_0, t) = \frac{1}{\sqrt{2\pi\mu^2 t}} e^{-\frac{(x-x_0)^2}{2\mu^2 t} - \frac{Kt}{2\mu^2} (x-x_0) + \frac{K^2 t^3}{24\mu^2}}.$$

However, if we instead take the limit as $K \rightarrow 1$ and $\alpha \rightarrow 0$, we obtain

$$\begin{aligned} G(x, x_0, t) = & \frac{1}{\sqrt{2\pi\mu^2 t}} e^{-\frac{(x-x_0)^2}{2\mu^2 t} - \frac{x}{\mu^2 t} \int_0^t s \circ dW_s - \frac{x_0}{\mu^2} \int_0^t \int_0^r \frac{s}{r^2} \circ dW_s dr} \\ & \times e^{\frac{1}{2\mu^2} \int_0^t \frac{1}{r^2} \left(\int_0^r s \circ dW_s \right)^2 dr}. \end{aligned}$$

This agrees with the result obtained for the zero potential noisy case, see Section 2.3.1, except for the last term. However, in a forthcoming work, [15], it has been shown that

$$\frac{1}{2} \int_0^t \frac{1}{r^2} \left(\int_0^r s \circ dW_s \right)^2 dr = -\frac{1}{t} \int_0^t \int_0^r s(r-t) \circ dW_s \circ dW_r,$$

and this reflects the different approaches used in calculating the Green's functions. We can process the functions $F(t)$, $k(t)$ and $l(t)$ a little further to obtain,

$$F(t) = \frac{Kt}{2} - \alpha W_t + \frac{\alpha}{t} \int_0^t W_s ds, \quad (2.46)$$

$$k(t) = \frac{Kt}{2} + \alpha \int_0^t \frac{W_r}{r} dr - \alpha \int_0^t \int_0^r \frac{W_s}{r^2} ds dr, \quad (2.47)$$

$$\begin{aligned} l(t) = & -\frac{K^2 t^3}{24} - \frac{\alpha K}{2} \int_0^t r W_r dr + \frac{\alpha K}{2} \int_0^t \int_0^r W_s ds dr \\ & - \frac{\alpha^2}{2} \int_0^t W_r^2 dr + \alpha^2 \int_0^t \int_0^r \frac{W_r W_s}{r} ds dr - \frac{\alpha^2}{2} \int_0^t \frac{1}{r^2} \left(\int_0^r W_s ds \right)^2 dr, \end{aligned} \quad (2.48)$$

which, for computation of wavefronts and caustics, are much easier to deal with. Hence we shall write our one dimensional phase function as

$$\phi(x, x_0, t) = \frac{(x - x_0)^2}{2t} + F(t)x + k(t)x_0 + l(t) + S_0(x_0).$$

Now consider the stochastic heat equation in \mathbb{R}^3 with linear potential $\underline{K} = (K, 0, 0)$ and noise in one dimension only,

$$\partial u = \left(\frac{\mu^2}{2} \Delta u + \frac{\underline{K} \cdot \underline{x}}{\mu^2} u \right) \partial t + \frac{\alpha}{\mu^2} x u \circ dW_t. \quad (2.49)$$

This choice of $\underline{K} = (K, 0, 0)$ denotes that we are only considering a linear acceleration in one direction, that being along the x-axis.

The corresponding Burgers' equation is given by

$$\partial \underline{v} + (\underline{v} \cdot \nabla) \underline{v} \partial t = \left(\frac{\mu^2}{2} \Delta \underline{v} - \underline{K} \right) \partial t - \nabla(x) \circ dW_t,$$

and our phase function in \mathbb{R}^3 is given by

$$\phi(x, x_0, t) = \frac{(\underline{x} - \underline{x}_0)^2}{2t} + F(t)x + k(t)x_0 + l(t) + S_0(\underline{x}_0), \quad (2.50)$$

where we know F , k and l from above. We may easily calculate the classical mechanical flow $\nabla_{\underline{x}_0} \phi = 0$, to obtain

$$\underline{x} = \underline{x}_0 + t \begin{pmatrix} k(t) \\ 0 \\ 0 \end{pmatrix} + t \nabla_{\underline{x}_0} S_0(\underline{x}_0). \quad (2.51)$$

From this it may be easily seen that the pre-caustic is simply

$$\left| \frac{\partial^2 \phi}{\partial x_0^2} \right| = \left| \frac{1}{t} I_3 + \frac{\partial^2 S_0}{\partial x_0^2} \right| = 0,$$

which is identical to the classical case with zero potential, as expected. To compute the caustic, we use the classical mechanical flow to eliminate the terms in x_0 , y_0 and z_0 . Furthermore, we may calculate the pre-wavefront as

$$\begin{aligned} 0 = & \frac{t}{2} |\nabla_{\underline{x}_0} S_0(\underline{x}_0)|^2 + S_0(\underline{x}_0) + (F(t) + k(t)) \left(t \frac{\partial S_0}{\partial x_0} + x_0 \right) \\ & + tk(t) \left(F(t) + \frac{1}{2} k(t) \right) + l(t). \end{aligned} \quad (2.52)$$

By using the classical mechanical flow to eliminate the \underline{x}_0 term, we may calculate the wavefront.

2.3.3 Harmonic Oscillator Potential Case

Consider the stochastic heat equation (2.3) under a harmonic oscillator potential

$$\partial u = \left(\frac{\mu^2}{2} \frac{\partial^2}{\partial x^2} - \frac{w^2 x^2}{2\mu^2} \right) u dt - xu \circ dW_t,$$

where we know from equation (2.4) that the Green's function is

$$\begin{aligned} G(x, x_0, t) = & \sqrt{\frac{w}{2\pi\mu^2 \sinh(wt)}} e^{\frac{-w}{2\mu^2 \sinh(wt)} [(x^2 + x_0^2) \cosh(wt) - 2xx_0]} \\ & \times e^{-\int_0^t \frac{[x \sinh(wr) - x_0 \sinh(wr - wt)]}{\mu^2 \sinh(wt)} \circ dW_r} \\ & \times e^{-\int_0^t \int_0^r \frac{\sinh(ws) \sinh(wr - wt)}{\mu^2 w \sinh(wt)} \circ dW_s \circ dW_r}. \end{aligned}$$

We are interested in generating a system whereby we have periodic solutions. This may be achieved by letting $w \mapsto iw$ which will give the stochastic heat equation

$$\partial u = \left(\frac{\mu^2}{2} \frac{\partial^2}{\partial x^2} + \frac{w^2 x^2}{2\mu^2} \right) u dt - xu \circ dW_t. \quad (2.53)$$

We may calculate the stochastic Green's function of (2.53) by simply applying the transformation $w \mapsto iw$ in (2.4), i.e.

$$\begin{aligned} G(x, x_0, t) = & \sqrt{\frac{iw}{2\pi\mu^2 \sinh(iwt)}} e^{\frac{-iw}{2\mu^2 \sinh(iwt)} [(x^2 + x_0^2) \cosh(iwt) - 2xx_0]} \\ & \times e^{-\int_0^t \frac{[x \sinh(iwr) - x_0 \sinh(iwr - iwt)]}{\mu^2 \sinh(iwt)} \circ dW_r} \\ & \times e^{-\int_0^t \int_0^r \frac{\sinh(iws) \sinh(iwr - iwt)}{\mu^2 iw \sinh(iwt)} \circ dW_s \circ dW_r}. \end{aligned}$$

Moreover, using the identities $\sinh(iwt) = i \sin(wt)$ and $\cosh(iwt) = \cos(wt)$ we see that the stochastic Green's function of the stochastic heat equation (2.53) is

$$\begin{aligned} G(x, x_0, t) &= \sqrt{\frac{w}{2\pi\mu^2 \sin(wt)}} e^{\frac{-w}{2\mu^2 \sin(wt)}} [(x^2 + x_0^2) \cos(wt) - 2xx_0] \\ &\times e^{-\int_0^t \frac{[x \sin(wr) - x_0 \sin(wr - wt)]}{\mu^2 \sin(wt)} \circ dW_r} \\ &\times e^{-\int_0^t \int_0^r \frac{\sin(ws) \sin(wr - wt)}{\mu^2 w \sin(wt)} \circ dW_s \circ dW_r}. \end{aligned} \quad (2.54)$$

This leads to the following theorem,

Theorem 2.3.3.

The one dimensional stochastic heat equation with harmonic oscillator potential

$$\partial u_t = \left(\frac{\mu^2}{2} \frac{\partial^2}{\partial x^2} + \frac{w^2 x^2}{2\mu^2} \right) u_t dt - x u_t \circ dW_t,$$

has solution

$$u(x, t) = \int_{-\infty}^{\infty} G(x, x_0, t) u_0(x_0) dx_0,$$

with initial condition

$$\lim_{t \rightarrow 0^+} u(x, t) = u_0(x),$$

for $u_0 \in C_0^\infty(\mathbb{R})$ where we have Green's function,

$$\begin{aligned} G(x, x_0, t) &= \sqrt{\frac{w}{2\pi\mu^2 \sin(wt)}} e^{\frac{-w}{2\mu^2 \sin(wt)}} [(x^2 + x_0^2) \cos(wt) - 2xx_0] \\ &\times e^{-\int_0^t \frac{[x \sin(wr) - x_0 \sin(wr - wt)]}{\mu^2 \sin(wt)} \circ dW_r} \\ &\times e^{-\int_0^t \int_0^r \frac{\sin(ws) \sin(wr - wt)}{\mu^2 w \sin(wt)} \circ dW_s \circ dW_r}. \end{aligned}$$

We can simplify some of the stochastic terms in the above Green's function a little. If we write

$$\begin{aligned} &-\int_0^t \frac{x \sin(wr) - x_0 \sin(wr - wt)}{\sin(wt)} \circ dW_r \\ &= -\frac{x}{\sin(wt)} \int_0^t \sin(wr) \circ dW_r + \frac{x_0}{\sin(wt)} \int_0^t \sin(wr - wt) \circ dW_r, \end{aligned}$$

then we can see that we only have to evaluate some straightforward Stratonovich integrals, namely,

$$\int_0^t \sin(wr) \circ dW_r \quad \text{and} \quad \int_0^t \sin(wr - wt) \circ dW_r.$$

Since $\sin(\cdot)$ is a smooth function, we see that our Stratonovich integrals may be evaluated as Itô integrals, and we have

$$\int_0^t \sin(wr) \circ dW_r = W_t \sin(wt) - w \int_0^t W_r \cos(wr) dr,$$

and

$$\int_0^t \sin(wr - wt) \circ dW_r = -w \int_0^t W_r \cos(wr - wt) dr.$$

Hence we obtain

$$\begin{aligned} - \int_0^t \frac{x \sin(wr) - x_0 \sin(wr - wt)}{\sin(wt)} \circ dW_r \\ = -xW_t + \frac{w}{\sin(wt)} \int_0^t W_r [x \cos(wr) - x_0 \cos(wr - wt)] dr. \end{aligned}$$

For now we shall denote the double Stratonovich integral by

$$\eta(t) = \eta(t, \omega) = \int_0^t \int_0^r \frac{\sin(ws) \sin(wr - wt)}{w \sin(wt)} \circ dW_s \circ dW_r. \quad (2.55)$$

Hence we shall write the phase function for the stochastic harmonic oscillator in three dimensions as

$$\begin{aligned} \phi(\underline{x}, \underline{x}_0, t) &= \frac{w_1}{2} \left[\frac{(x^2 + x_0^2) \cos(w_1 t) - 2xx_0}{\sin(w_1 t)} \right] + \frac{w_2}{2} \left[\frac{(y^2 + y_0^2) \cos(w_2 t) - 2yy_0}{\sin(w_2 t)} \right] \\ &+ \frac{w_3}{2} \left[\frac{(z^2 + z_0^2) \cos(w_3 t) - 2zz_0}{\sin(w_3 t)} \right] + xW_t + \eta(t) \\ &- \frac{w_1}{\sin(w_1 t)} \int_0^t W_r [x \cos(w_1 r) - x_0 \cos(w_1 r - w_1 t)] dr + S_0(\underline{x}_0). \end{aligned} \quad (2.56)$$

Using this we are able to calculate explicitly the equations that govern the caustics and wavefronts. The classical mechanical flow for this system, given by $\nabla_{\underline{x}_0} \phi = 0$, is just

$$\begin{pmatrix} x \\ y \\ z \end{pmatrix} = \begin{pmatrix} x_0 \cos(w_1 t) \\ y_0 \cos(w_2 t) \\ z_0 \cos(w_3 t) \end{pmatrix} + \begin{pmatrix} \frac{\sin(w_1 t)}{w_1} \frac{\partial S_0}{\partial x_0} \\ \frac{\sin(w_2 t)}{w_2} \frac{\partial S_0}{\partial y_0} \\ \frac{\sin(w_3 t)}{w_3} \frac{\partial S_0}{\partial z_0} \end{pmatrix} + \begin{pmatrix} \int_0^t W_r \cos(w_1 r - w_1 t) dr \\ 0 \\ 0 \end{pmatrix}. \quad (2.57)$$

Recall that the pre-caustics are given by zeros of the determinant of the Hessian matrix of $\phi(\underline{x}, \underline{x}_0, t)$, i.e.

$$\text{Det} \left| \frac{\partial^2 \phi}{\partial \underline{x}_0^2} \right| = 0,$$

which, for our phase function, reduces to the classical case of the harmonic oscillator potential, namely

$$\left| \left(\begin{array}{ccc} \frac{w_1}{\tan(w_1 t)} & 0 & 0 \\ 0 & \frac{w_2}{\tan(w_2 t)} & 0 \\ 0 & 0 & \frac{w_3}{\tan(w_3 t)} \end{array} \right) + \left(\begin{array}{ccc} \frac{\partial^2 S_0}{\partial x_0^2} & \frac{\partial^2 S_0}{\partial y_0 \partial x_0} & \frac{\partial^2 S_0}{\partial z_0 \partial x_0} \\ \frac{\partial^2 S_0}{\partial x_0 \partial y_0} & \frac{\partial^2 S_0}{\partial y_0^2} & \frac{\partial^2 S_0}{\partial z_0 \partial y_0} \\ \frac{\partial^2 S_0}{\partial x_0 \partial z_0} & \frac{\partial^2 S_0}{\partial y_0 \partial z_0} & \frac{\partial^2 S_0}{\partial z_0^2} \end{array} \right) \right| = 0. \quad (2.58)$$

The pre-wavefront is given by $\phi(\underline{x}_0, t) = 0$ where we reduce $\phi(\underline{x}, \underline{x}_0, t) = \phi(\underline{x}_0, t)$ by using the flow to eliminate the \underline{x} terms in the phase function. Hence we see the equation of the pre-wavefront is given by

$$\begin{aligned} & \frac{w_1}{2 \sin(w_1 t)} \left\{ \left[\left(x_0 \cos(w_1 t) + \frac{\sin(w_1 t)}{w_1} \frac{\partial S_0}{\partial x_0} + \int_0^t W_r \cos(w_1 r - w_1 t) dr \right)^2 + x_0^2 \right] \cos(w_1 t) \right. \\ & \quad \left. - 2 \left(x_0 \cos(w_1 t) + \frac{\sin(w_1 t)}{w_1} \frac{\partial S_0}{\partial x_0} + \int_0^t W_r \cos(w_1 r - w_1 t) dr \right) x_0 \right\} \\ & + \frac{w_2}{2 \sin(w_2 t)} \left\{ \left[\left(y_0 \cos(w_2 t) + \frac{\sin(w_2 t)}{w_2} \frac{\partial S_0}{\partial y_0} \right)^2 + y_0^2 \right] \cos(w_2 t) \right. \\ & \quad \left. - 2 \left(y_0 \cos(w_2 t) + \frac{\sin(w_2 t)}{w_2} \frac{\partial S_0}{\partial y_0} \right) y_0 \right\} \\ & + \frac{w_3}{2 \sin(w_3 t)} \left\{ \left[\left(z_0 \cos(w_3 t) + \frac{\sin(w_3 t)}{w_3} \frac{\partial S_0}{\partial z_0} \right)^2 + z_0^2 \right] \cos(w_3 t) \right. \\ & \quad \left. - 2 \left(z_0 \cos(w_3 t) + \frac{\sin(w_3 t)}{w_3} \frac{\partial S_0}{\partial z_0} \right) z_0 \right\} \\ & + \left(x_0 \cos(w_1 t) + \frac{\sin(w_1 t)}{w_1} \frac{\partial S_0}{\partial x_0} + \int_0^t W_r \cos(w_1 r - w_1 t) dr \right) \\ & \quad \times \left(W_t - \frac{w_1}{\sin(w_1 t)} \int_0^t W_r \cos(wr) dr \right) \\ & + \frac{w_1 x_0}{\sin(w_1 t)} \int_0^t W_r \cos(w_1 r - w_1 t) dr + \eta(t) + S_0(\underline{x}_0) = 0 \quad (2.59) \end{aligned}$$

Part II
Explicit Examples Using
Mathematica

Chapter 3

Cusp and Tricorn

We give some explicit examples of singularities of the Burgers' equation and the corresponding wavefronts of the heat equation with and without noise terms for the case $S_0(\underline{x}_0) = \frac{1}{2}x_0^2y_0$. In part we follow the treatment of I.M. Davies, A. Truman and H.Z. Zhao in [16].

3.1 Classical Case

In this section we look at the singularities of the classical heat and Burgers' equations that appear in the cases of the zero potential $V(\underline{x}) = 0$, the linear potential $V(\underline{x}) = -kx$ and the harmonic oscillator potential $V(\underline{x}) = -\frac{1}{2}(w_1^2x^2 + w_2^2y^2 + w_3^2z^2)$. Using the initial condition $S_0(\underline{x}_0) = \frac{1}{2}x_0^2y_0$, we discover that the generic caustic is the cusp catastrophe as covered in [3] and the introduction of a potential term does little to effect the overall geometry of the cusp.

3.1.1 Zero Potential

For the case of the cusp singularity in two dimensions, the polynomial phase function is determined by taking $S_0(\underline{x}_0) = \frac{1}{2}x_0^2y_0$. Omitting the z and z_0 terms we see that in the two dimensional case the phase function is given by

$$\phi(\underline{x}, \underline{x}_0, t) = \frac{(x - x_0)^2}{2t} + \frac{(y - y_0)^2}{2t} + \frac{1}{2}x_0^2y_0. \quad (3.1)$$

Then the pre-caustic for the Burgers equation is given by

$$\begin{vmatrix} 1 + ty_0 & tx_0 \\ tx_0 & 1 \end{vmatrix} = 0,$$

which we may rearrange as the expression for the pre-caustic $y_0 = y_0(x_0, t)$, i.e.

$$y_0 = tx_0^2 - \frac{1}{t}. \quad (3.2)$$

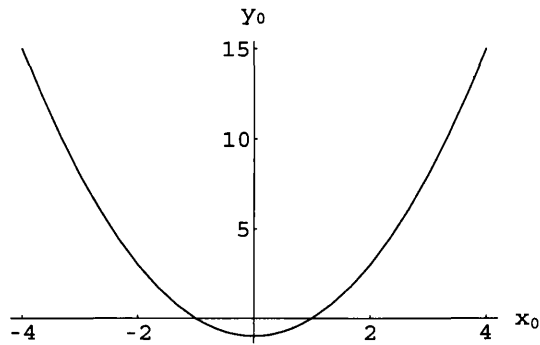


Figure 3.1: Zero potential pre-caustic for $S_0 = \frac{1}{2}x_0^2y_0$.

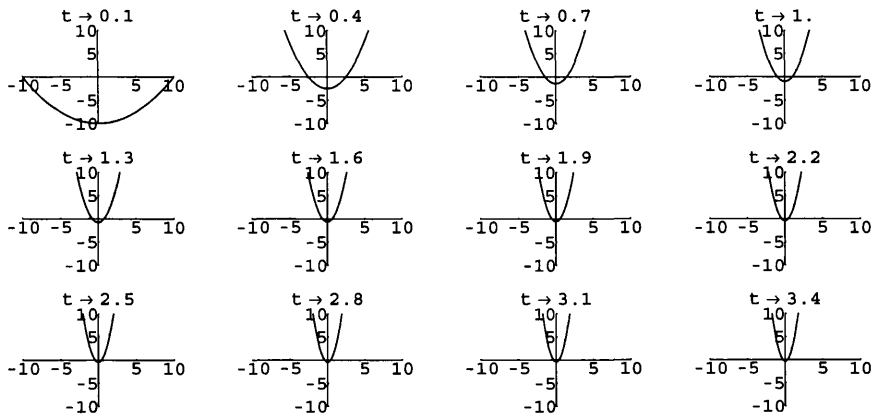


Figure 3.2: Evolving zero potential pre-caustics for $S_0 = \frac{1}{2}x_0^2y_0$.

This is just a parabola and, for some instant of time $t > 0$, we have the pre-caustic as in Figure 3.1. We can show a time evolution of this, see Figure 3.2. Observe that as time $t \rightarrow 0$ we have a horizontal line at $y_0 \rightarrow -\infty$, and as time $t \rightarrow \infty$ we see that the parabola folds into the $y_0 \geq 0$ part of the vertical line $x_0 = 0$. We can also obtain the above by repeated integration.

Recall that for $S_0(\underline{x}_0) = \frac{1}{2}x_0^2 y_0$ our phase function is given by equation (3.1), then $\frac{\partial}{\partial y_0} \phi(\underline{x}, \underline{x}_0, t) = 0$ tells us that

$$-\frac{(y - y_0)}{t} + \frac{x_0^2}{2} = 0.$$

This gives us $y_0 = y - \frac{1}{2}tx_0^2$, and, after using this result to do the integral in y_0 by the Laplace method, see Section 1.4, the phase function becomes

$$\tilde{\phi}(x, x_0, t) = -\frac{t}{8}x_0^4 + \frac{1}{2}\left(y + \frac{1}{t}\right)x_0^2 - \frac{x}{t}x_0 + \frac{x^2}{2t}.$$

If we look now at the solution of the heat equation after computing the y_0 integral, we have

$$\begin{aligned} u(\underline{x}, t) &\simeq \frac{1}{2\pi\mu^2 t} \int_{\mathbb{R}} T_0(x_0) e^{-\frac{1}{\mu^2} \left\{ -\frac{t}{8}x_0^4 + \frac{1}{2}\left(y + \frac{1}{t}\right)x_0^2 - \frac{x}{t}x_0 + \frac{x^2}{2t} \right\}} dx_0 \\ &\simeq \frac{1}{2\pi\mu^2 t} \int_{\mathbb{R}} T_0(x_0) e^{Ax_0^4 + Bx_0^2 + Cx_0 + D} dx_0 \end{aligned} \quad (3.3)$$

where $T_0(x_0)$ is a convergence factor and we emphasize that

$$A = \frac{t}{8\mu^2}, \quad B = -\frac{1}{2\mu^2} \left(y + \frac{1}{t} \right), \quad C = \frac{x}{\mu^2 t}, \quad D = -\frac{x^2}{2\mu^2 t}.$$

We see immediately that the polynomial in the exponential term of equation (3.3) is the canonical form of the cusp catastrophe, as described in [3], which is distinctive in that it is a quartic with no cubic term. Later on, we shall be dealing with the far more difficult case of the butterfly catastrophe. In order to integrate over x_0 we need to look at $\frac{\partial \phi}{\partial x_0}$ where the main contribution comes from the x_0 satisfying $\frac{\partial \phi}{\partial x_0} = 0$, i.e. the solution x_0 of

$$-\frac{t}{2}x_0^3 + \left(y + \frac{1}{t}\right)x_0 - \frac{x}{t} = 0.$$

The condition for a singularity to appear is that $\frac{\partial^2 \phi}{\partial x_0^2} = 0$, i.e.

$$\frac{3tx_0^2}{2} = y + \frac{1}{t}, \quad (3.4)$$

where from above

$$y = y_0 + \frac{tx_0^2}{2}. \quad (3.5)$$

Eliminating y from equation (3.4) and (3.5) we obtain the pre-caustic as in equation (3.2), namely

$$y_0 = tx_0^2 - \frac{1}{t}.$$

Comparing this to what we obtained for y_0 from $\frac{\partial\phi}{\partial y_0} = 0$ we have

$$y - \frac{1}{2}tx_0^2 = tx_0^2 - \frac{1}{t},$$

admitting solution

$$x_0 = \pm \sqrt{\frac{2}{3t} \left(y + \frac{1}{t} \right)},$$

which determines the position of the singularities. Putting this into our condition that $\frac{\partial\phi}{\partial x_0} = 0$ yields

$$\mp \frac{t}{2} \frac{2}{3t} \left(y + \frac{1}{t} \right) \sqrt{\frac{2}{3t} \left(y + \frac{1}{t} \right)} \pm \left(y + \frac{1}{t} \right) \sqrt{\frac{2}{3t} \left(y + \frac{1}{t} \right)} - \frac{x}{t} = 0.$$

Simplifying the above, we discover that the caustic is the following semi-cubical parabola

$$\frac{8}{27} \left(y + \frac{1}{t} \right)^3 = \frac{x^2}{t},$$

which may be solved explicitly for $y = y(x, t)$ as

$$y = \frac{3}{2} \left(\frac{x^2}{t} \right)^{\frac{1}{3}} - \frac{1}{t}. \quad (3.6)$$

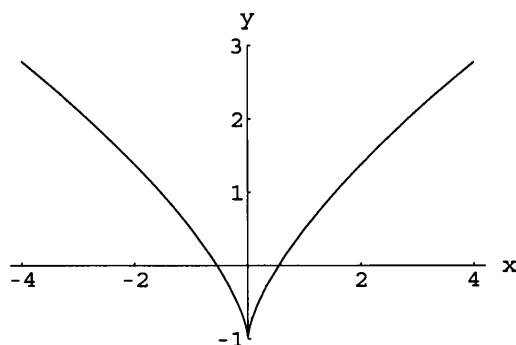


Figure 3.3: Zero potential caustic for $S_0 = \frac{1}{2}x_0^2y_0$.

This is the cusp catastrophe classified by Thom's catastrophe theory, shown in Figure 3.3, at an instance of time $t > 0$. Furthermore, we may show a time evolution of the

caustic for $S_0(\underline{x}_0) = \frac{1}{2}x_0^2y_0$, see Figure 3.4, where we see that as $t \rightarrow \infty$, the caustic tends to the horizontal straight line $y = 0$ and as $t \rightarrow 0$ we have the vertical line $x = 0$.

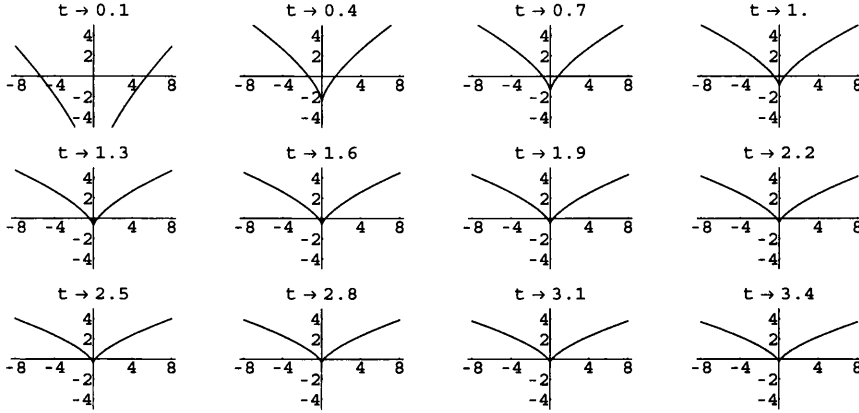


Figure 3.4: Evolving zero potential caustics for $S_0 = \frac{1}{2}x_0^2y_0$.

Now, returning to the heat equation, recall that the pre-wavefront is determined by

$$\frac{t}{2} |\nabla_{\underline{x}_0} S_0(\underline{x}_0)|^2 + S_0(\underline{x}_0) = 0,$$

i.e.

$$\frac{t}{2} \left[(x_0 y_0)^2 + \left(\frac{1}{2} x_0^2 \right)^2 \right] + \frac{1}{2} x_0^2 y_0 = 0,$$

so that the pre-wavefront of the heat equation is given by

$$\frac{t}{8} x_0^4 + \frac{1}{2} x_0^2 y_0 + \frac{t}{2} x_0^2 y_0^2 = 0, \quad (3.7)$$

namely

$$\frac{x_0^2}{8t} \left[\frac{(y_0 + \frac{1}{2t})^2}{(\frac{1}{2t})^2} + \frac{x_0^2}{(\frac{1}{t})^2} - 1 \right] = 0.$$

This is simply the straight vertical line $x_0 = 0$ repeated, and an ellipse centred at $(0, -\frac{1}{2t})$ with semi-major axis $\frac{1}{t}$ and semi-minor axis $\frac{1}{2t}$, as in Figure 3.5. In Figure 3.6 we observe the behaviour of the ellipse with respect to time. As $t \rightarrow 0$ this settles down to $S_0(\underline{x}_0) = \frac{1}{2}x_0^2y_0 = 0$ so the ellipse has infinite axis corresponding to the horizontal line $y_0 = 0$, and also the vertical line $x_0 = 0$. We see that as $t \rightarrow \infty$ the centre of the ellipse moves to the origin so the pre-wavefront focuses down to a point at the origin and the straight vertical line $x_0 = 0$.

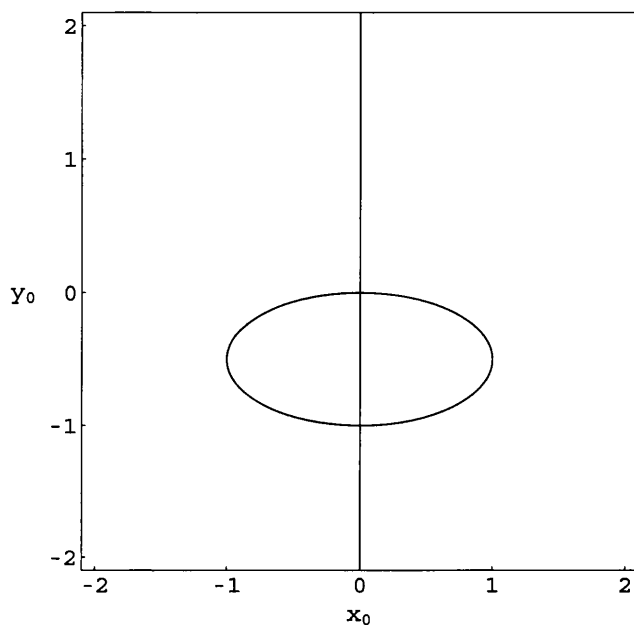


Figure 3.5: Zero potential pre-wavefront for $S_0 = \frac{1}{2}x_0^2y_0$.

One interesting point here is that we may reduce the pre-wavefront (3.7) to a quadratic in y_0 , i.e.

$$y_0^2 + \frac{1}{t}y_0 + \frac{x_0^2}{4} = 0,$$

so that we may find explicitly the solution as

$$y_0 = \frac{1}{2t} \left(-1 \pm \sqrt{1 - t^2x_0^2} \right).$$

Hence we can see that the existence of the pre-wavefront is entirely dependent on the inequality $1 - t^2x_0^2 \geq 0$. Namely $y_0(x_0) \in \mathbb{R}$ if, and only if,

$$-\frac{1}{t} \leq x_0 \leq \frac{1}{t}.$$

This tells us that as time increases, the pre-wavefront focuses down to the point $(0, 0)$, since x_0 is bounded by the above inequality. Recall that the wavefront for the heat equation is given by the level surfaces of $S(\underline{x}, t) = 0$, i.e.

$$S(\underline{x}, t) = \inf_{\underline{x}_0 \in \mathbb{R}^3} \phi(\underline{x}, \underline{x}_0, t) = 0.$$

The infimum of $\phi(\underline{x}, \underline{x}_0, t)$ is achieved at the points \underline{x}_0 satisfying $\nabla_{\underline{x}_0} \phi(\underline{x}, \underline{x}_0, t) = 0$. Thus we must solve $\phi(\underline{x}, \underline{x}_0, t) = 0$ and $\nabla_{\underline{x}_0} \phi(\underline{x}, \underline{x}_0, t) = 0$ simultaneously. This gives

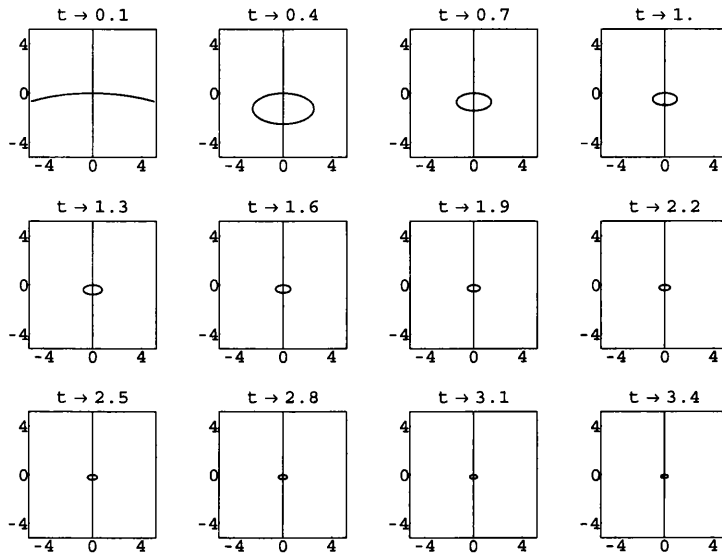


Figure 3.6: Evolving zero potential pre-wavefronts for $S_0 = \frac{1}{2}x^2y_0$.

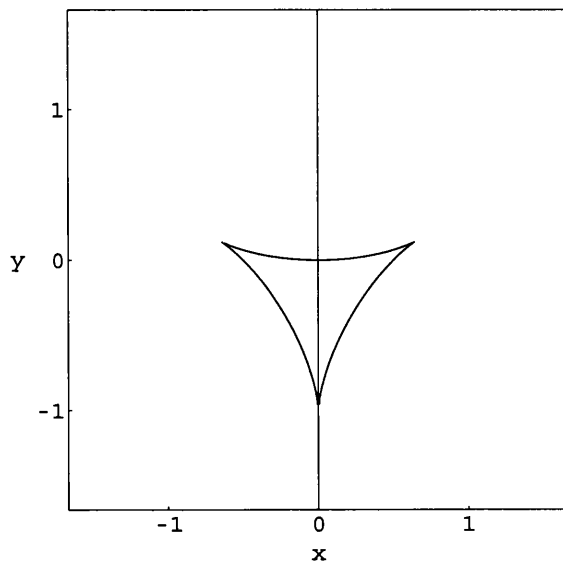


Figure 3.7: Zero potential wavefront for $S_0 = \frac{1}{2}x^2y_0$.

the equation of the wavefront as

$$x^2 \left[4x^4 + x^2 \left(8y^2 - \frac{20}{t}y - \frac{1}{t^2} \right) + 4y \left(y + \frac{1}{t} \right)^3 \right] = 0, \quad (3.8)$$

which is the straight line pair $x = 0$ and the tricorn, see [16]. This triple cusped hypo-cycloid, is shown in Figure 3.7. In Figure 3.8 we look at the wavefront for $S_0 = \frac{1}{2}x_0^2y_0$ evolving with time and we notice that as $t \rightarrow 0$ the wavefront tends to the lines $y = 0$ and $x = 0$. Furthermore, as $t \rightarrow \infty$, the triple cusped hypo-cycloid focuses to a point at the origin, leaving the wavefront as the vertical line $x = 0$.

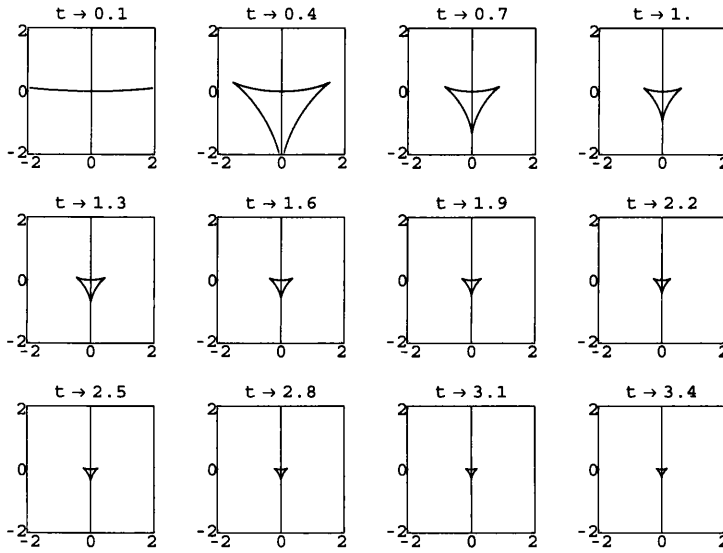


Figure 3.8: Evolving zero potential wavefronts for $S_0 = \frac{1}{2}x_0^2y_0$.

Returning to the pre-wavefront (3.7), we may use the parametric equation of an ellipse to simplify the earlier equation thus reducing it to the pair of parametric equations

$$\begin{pmatrix} x_0 \\ y_0 \end{pmatrix} = \begin{pmatrix} \frac{\cos \theta}{t} \\ \frac{\sin \theta - 1}{2t} \end{pmatrix}, \quad (3.9)$$

where $\theta \in [0, 2\pi)$. Now, in order to calculate the wavefront we must apply the classical mechanical flow

$$\begin{pmatrix} x \\ y \end{pmatrix} = \begin{pmatrix} x_0 \\ y_0 \end{pmatrix} + t \begin{pmatrix} x_0 y_0 \\ \frac{x_0^2}{2} \end{pmatrix},$$

which yields the wavefront as the pair of parametric equations

$$\begin{pmatrix} x \\ y \end{pmatrix} = \begin{pmatrix} \frac{\cos \theta}{2t} (1 + \sin \theta) \\ \frac{\sin \theta}{2t} (1 - \sin \theta) \end{pmatrix}. \quad (3.10)$$

This provides us with an alternate way of computing the pre-wavefront and wavefront that can be a more efficient for plotting purposes.

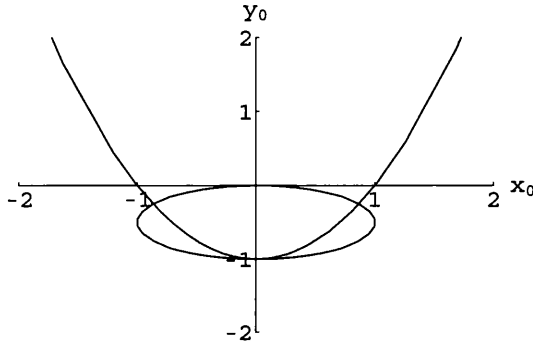


Figure 3.9: Zero potential pre-caustic and pre-wavefront for $S_0 = \frac{1}{2}x_0^2y_0$.

It is interesting to look at a plot of the pre-curves on common axes as in Figure 3.9. We can calculate exactly the meeting points of the pre-caustic and pre-wavefront by substituting into $\phi(\underline{x}_0, t) = 0$ the explicit expression $y_0 = y_0(x_0, t)$ of the pre-caustic (3.2). Hence the pre-curves will meet at the solutions x_0 of $\phi(x_0, y_0(x_0, t), t) = 0$. Evaluating this yields a polynomial of order six in x_0 , namely

$$\frac{t}{2}x_0^4 \left(t^2x_0^2 - \frac{3t}{4} \right) = 0.$$

This is easily solved for $x_0 = x_0(t)$ and substituting these solutions into our pre-caustic allows us to express the meeting points of the pre-caustic and pre-wavefront as $(0, -\frac{1}{t})$, $(-\frac{\sqrt{3}}{2t}, -\frac{1}{4t})$ and $(\frac{\sqrt{3}}{2t}, -\frac{1}{4t})$, where the first occurs with multiplicity 4.

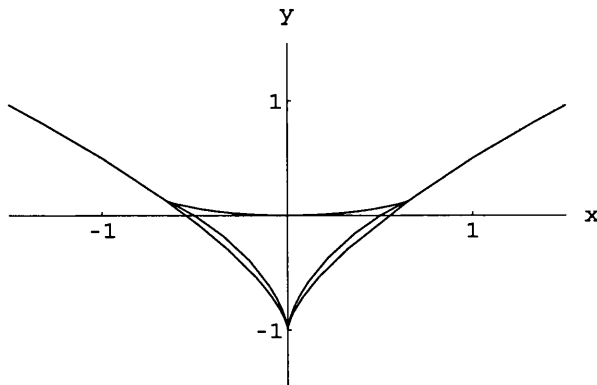


Figure 3.10: Zero potential caustic and wavefront for $S_0 = \frac{1}{2}x_0^2y_0$.

We may also compare the wavefront of the heat equation to the caustic of Burgers' equation, as in Figure 3.10. In a similar fashion, we can calculate the meeting points by substituting the caustic equation $y = y(x, t)$ into the wavefront expression $\phi(\underline{x}, t) = 0$. Doing so we obtain, after a little simplification,

$$x^4 \left(4x^2 + \frac{18}{t^{\frac{2}{3}}} x^{\frac{4}{3}} - \frac{135}{4t^{\frac{4}{3}}} x^{\frac{2}{3}} + \frac{27}{2t^2} \right) = 0. \quad (3.11)$$

Solving for $x = x(t)$ and putting these solutions into our caustic $y = y(x, t)$ gives the positions of the meeting points as $(0, -\frac{1}{t})$, $(-\frac{3\sqrt{3}}{8t}, \frac{1}{8t})$ and $(\frac{3\sqrt{3}}{8t}, \frac{1}{8t})$. Clearly we are not concerned with the complex solutions of equation (3.11), since these give rise to a pair of complex points.

3.1.2 Linear Potential

We shall consider the case of a linear potential of the form $V(\underline{x}) = kx$, then the heat equation becomes,

$$\frac{\partial u}{\partial t} = \frac{\mu^2}{2} \Delta u - \frac{k}{\mu^2} xu.$$

The Green's function for this case of the linear potential is given by equation (2.20) as

$$G(\underline{x}, \underline{x}_0, t) = \frac{1}{2\pi\mu^2 t} e^{-\frac{(x-x_0)^2}{2\mu^2 t} - \frac{(y-y_0)^2}{2\mu^2 t} - \frac{kt}{2\mu^2} (x+x_0) + \frac{k^2 t^3}{24\mu^2}},$$

which yields the phase function as

$$\phi(\underline{x}, \underline{x}_0, t) = \frac{(x-x_0)^2}{2t} + \frac{(y-y_0)^2}{2t} + \frac{kt}{2} (x+x_0) - \frac{k^2 t^3}{24} + \frac{x_0^2 y_0}{2}. \quad (3.12)$$

Then as discussed earlier in Section 2.2.2, the pre-caustic is given by equation (2.23), namely

$$\text{Det} \left| \frac{1}{t} I_3 + \frac{\partial^2 S_0}{\partial \underline{x}_0^2} \right| = 0,$$

which for our case of $S_0(\underline{x}_0) = \frac{1}{2} x_0^2 y_0$ simply becomes

$$y_0 = tx_0^2 - \frac{1}{t}. \quad (3.13)$$

Observe that this is exactly the same as the pre-caustic in the zero potential case, equation (3.2) in Section 3.1.1, and we refer the reader to Figures 3.1 and 3.2. We are now presented with two options for calculating the caustic of the Burgers' equation. We may substitute into the classical mechanical flow

$$\begin{pmatrix} x \\ y \end{pmatrix} = \begin{pmatrix} x_0 \\ y_0 \end{pmatrix} + \frac{t^2}{2} \begin{pmatrix} k \\ 0 \end{pmatrix} + t \begin{pmatrix} x_0 y_0 \\ \frac{1}{2} x_0^2 \end{pmatrix}, \quad (3.14)$$

the y_0 in equation (3.13), to give a parametric form of the caustic as

$$\begin{pmatrix} x \\ y \end{pmatrix} = \begin{pmatrix} x_0 \\ tx_0^2 - \frac{1}{t} \end{pmatrix} + \frac{t^2}{2} \begin{pmatrix} k \\ 0 \end{pmatrix} + t \begin{pmatrix} tx_0^3 - \frac{1}{t}x_0 \\ \frac{1}{2}x_0^2 \end{pmatrix}.$$

Alternatively, since we are dealing with a relatively simple $S_0(\underline{x}_0)$, we may eliminate the x_0 and y_0 variables from the pre-caustic (3.13) and the classical mechanical flow equation (3.14). This yields the equation for the caustic as a semi-cubical parabola

$$32 \left(y + \frac{1}{t} \right)^3 = \frac{27}{t} (2x - t^2k)^2,$$

which gives the explicit equation for the caustic as

$$y = \frac{3}{2t^{\frac{1}{3}}} \left(x - \frac{t^2}{2}k \right)^{\frac{2}{3}} - \frac{1}{t}. \quad (3.15)$$

If we look at doing the y_0 integral by the Laplace method, see Section 1.4, then we will obtain a solution of the form,

$$\begin{aligned} u(\underline{x}, t) &\simeq \frac{1}{2\pi\mu^2 t} \int_{\mathbb{R}} T_0(x_0) e^{-\frac{1}{\mu^2} \left\{ -\frac{1}{8}x_0^4 + \frac{1}{2}(y + \frac{1}{t})x_0^2 - \left(\frac{x}{t} - \frac{kt}{2}\right)x_0 + \frac{x^2}{2t} + \frac{xkt}{2} - \frac{k^2t^3}{24} \right\}} dx_0 \\ &\simeq \frac{1}{2\pi\mu^2 t} \int_{\mathbb{R}} T_0(x_0) e^{Ax_0^4 + Bx_0^2 + Cx_0 + D} dx_0, \end{aligned} \quad (3.16)$$

where $T_0(x_0)$ is a convergence factor and we have

$$\begin{aligned} A &= \frac{t}{8\mu^2}, & B &= -\frac{1}{2\mu^2} \left(y + \frac{1}{t} \right), \\ C &= +\frac{1}{\mu^2} \left(\frac{x}{t} - \frac{kt}{2} \right), & D &= -\frac{1}{\mu^2} \left(\frac{x^2}{2t} + \frac{kt}{2}x - \frac{k^2t^3}{24} \right). \end{aligned}$$

Once again we see that we have the canonical form of the the cusp catastrophe, the distinctive quartic polynomial with no cubic term, see [3]. It is easier, in this case, to work with the explicit equation rather than the parametric form. We shall now choose a value of $k = 5$, then Figure 3.11 shows the movement of the cusp while under the linear acceleration in the x direction.

Next, by equation (2.24), we may calculate the pre-wavefront as

$$\frac{t}{8}x_0^4 + \frac{y_0}{2}(1 + ty_0)x_0^2 + kt(1 + ty_0)x_0 + \frac{k^2t^3}{3} = 0. \quad (3.17)$$

Note that, as expected, when $k \rightarrow 0$ we obtain the zero potential case of the pre-wavefront, see equation (3.7). Observe that the pre-wavefront is simply a quadratic in y_0 which may be solved to give

$$y_0 = -\frac{tk}{x_0} - \frac{1}{2t} \pm \frac{1}{2\sqrt{3}tx_0} \sqrt{4t^4k^2 - 12t^2kx_0 + 3x_0^2 - 3t^2x_0^4}.$$

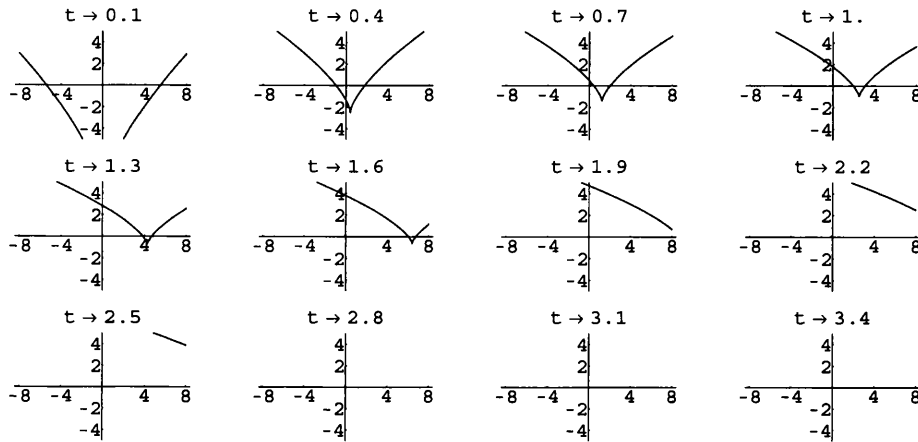


Figure 3.11: Evolving linear potential caustics for $S_0 = \frac{1}{2}x_0^2 y_0$ with $k = 5$.

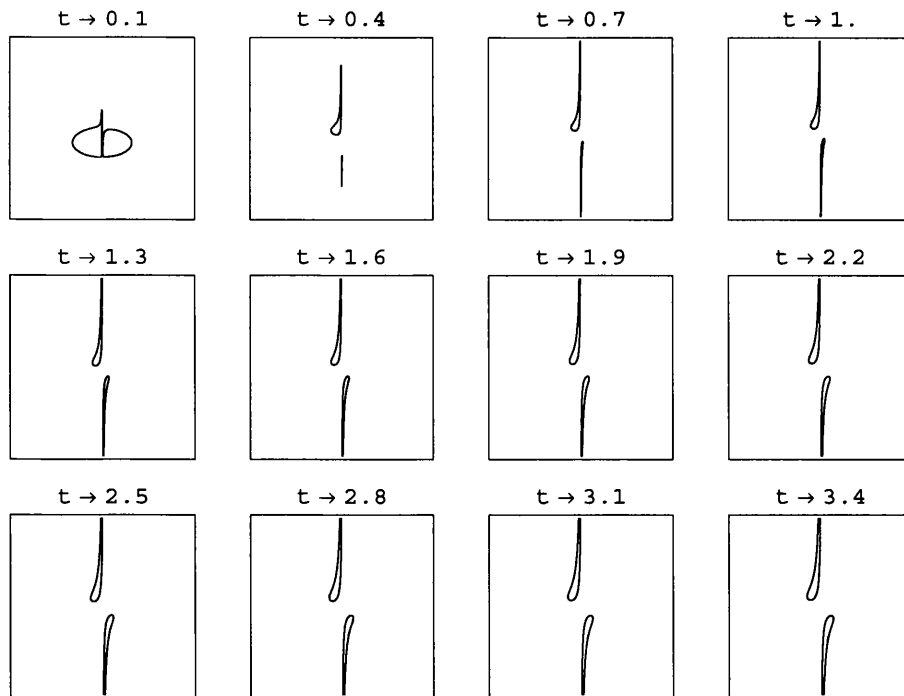


Figure 3.12: Evolving linear potential pre-wavefronts for $S_0 = \frac{1}{2}x_0^2 y_0$ with $k = 5$.

Then the pre-wavefront can only exist for the values of x_0 and t satisfying the inequality

$$4t^4k^2 - 12t^2kx_0 + 3x_0^2 - 3t^2x_0^4 \geq 0,$$

for a chosen value of k . Choosing a values of $k = 5$ gives the pre-wavefront, shown in Figure 3.12, as

$$\frac{t}{8}x_0^4 + \frac{y_0}{2}(1 + ty_0)x_0^2 + 5t(1 + ty_0)x_0 + \frac{25t^3}{3} = 0.$$

Notice that the pre-wavefront splits into a pair of regions, one tending to $y_0 = \infty$ and the other to $y_0 = -\infty$ as we approach $x_0 = 0$ from either side. We can give an interpretation of this. Recall that the pre-wavefront may be expressed as a quadratic in y_0 which we solved above, so that in our example $k = 5$ we have the solutions

$$y_0 = -\frac{5t}{x_0} - \frac{1}{2t} \pm \frac{1}{2\sqrt{3}tx_0} \sqrt{100t^4 - 60t^2x_0 + 3x_0^2 - 3t^2x_0^4}.$$

This tells us that the pre-wavefront can only exist for x_0 and t satisfying the inequality

$$100t^4 - 60t^2x_0 + 3x_0^2 - 3t^2x_0^4 \geq 0.$$

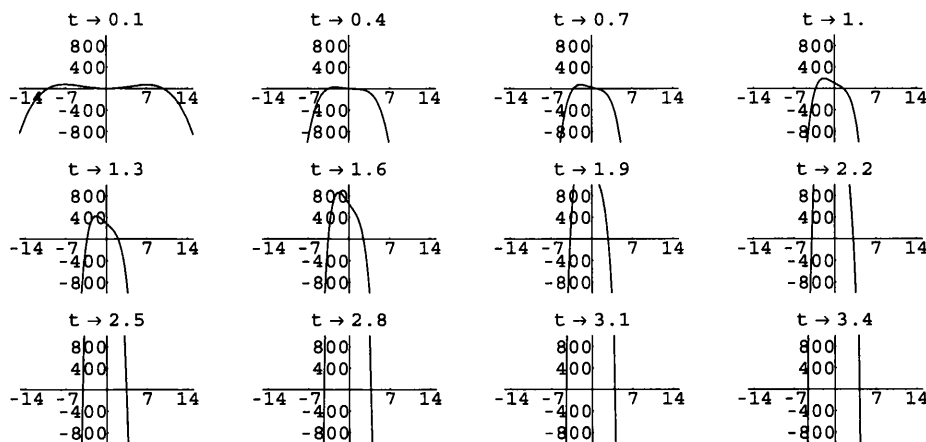


Figure 3.13: Linear potential pre-wavefront generator for $S_0 = \frac{1}{2}x_0^2y_0$ with $k = 5$.

We may look at the behaviour of this function over time, as shown in Figure 3.13, where the positive parts represent the regions on which the pre-wavefront is well defined. However we see that, in some instances, we have only one interval, yet the pre-wavefront has split into a two parts. This is due to the factor of $\frac{1}{x_0}$ which creates a problem point at $x_0 = 0$, giving $y_0 \rightarrow \infty$ as $x_0 \rightarrow 0^-$ and $y_0 \rightarrow -\infty$ as $x_0 \rightarrow 0^+$. We

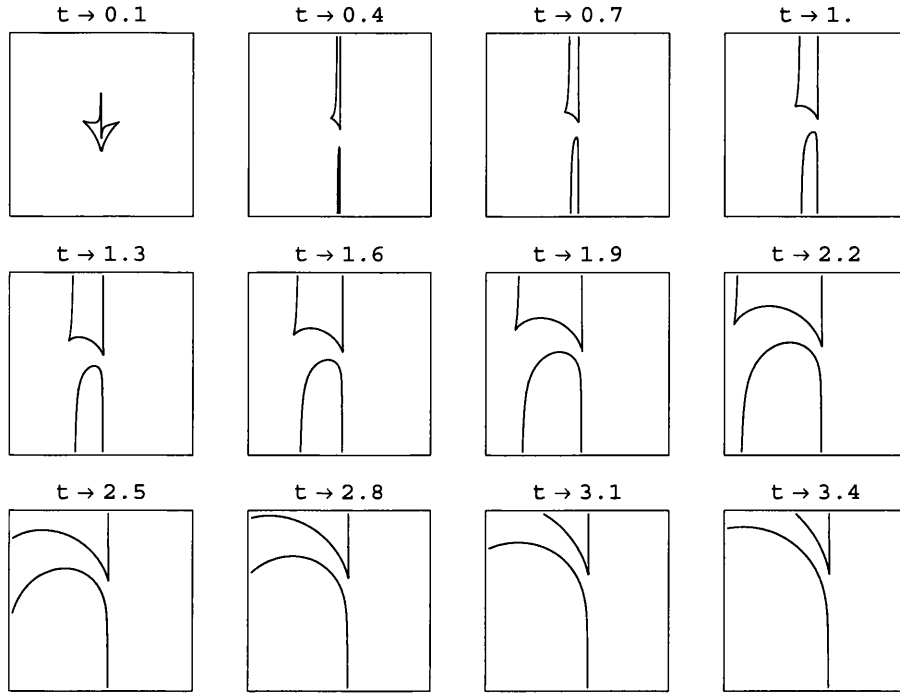


Figure 3.14: Evolving linear potential wavefronts for $S_0 = \frac{1}{2}x_0^2 y_0$ with $k = 5$.

can calculate exactly the zero points of the inequality in terms of time t , but solving a quartic can become rather clumsy.

We are fortunate that we may calculate the wavefront exactly by eliminating x_0 and y_0 from the pre-wavefront by using the classical mechanical flow. Hence we obtain the implicit form of the wavefront as

$$\begin{aligned}
 & 1728x^6 + 5184kt^2x^5 + \frac{432}{t^2} (8t^2y^2 - 20ty - 1 + 11k^2t^6) x^4 \\
 & + 864k [8(1+ty)^2 - 27 + k^2t^6] x^3 \\
 & + \frac{36}{t^3} [48y(1+ty)^3 + 2k^2t^5 (40t^2y^2 + 260ty + 463) - 11k^4t^{11}] x^2 \\
 & + \frac{36k}{t^2} [48(1+ty)^3 (2+ty) - 2k^2t^6 (8t^2y^2 + 88ty + 161) + k^4t^{12}] x \\
 & - k^2 [144(1+ty)^3 (4+ty) - 3k^2t^6 (8t^2y^2 + 124ty + 359) + k^4t^{12}] = 0,
 \end{aligned} \tag{3.18}$$

which is shown in Figure 3.14. On comparison of the pre-curves, see Figure 3.15, we see that for our example $t = 1$ there are only two meeting points, and these have been calculated numerically to be at the positions $(-2.14973, 3.62135)$ and

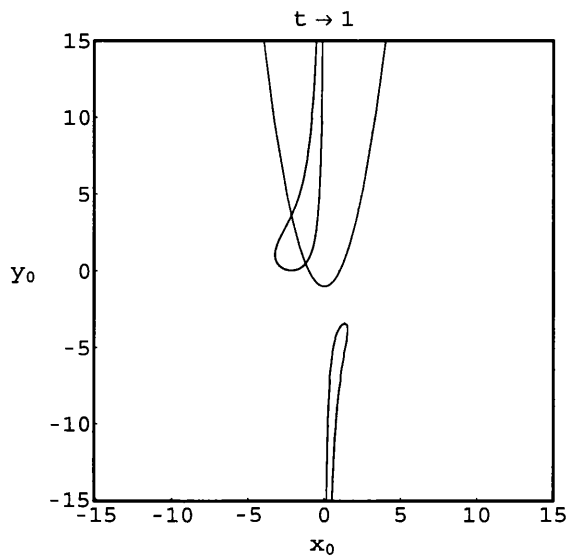


Figure 3.15: Linear potential pre-caustic and pre-wavefront for $S_0 = \frac{1}{2}x_0^2 y_0$ with $k = 5$.

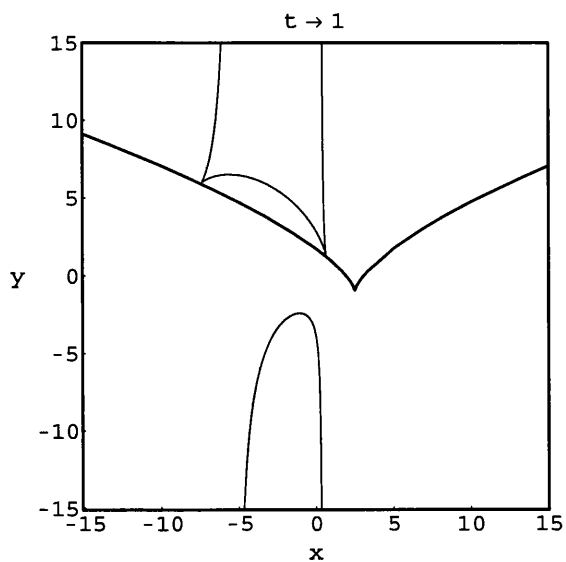


Figure 3.16: Linear potential caustic and wavefront for $S_0 = \frac{1}{2}x_0^2 y_0$ with $k = 5$.

$(-1.22424, 0.498774)$. Also, in the case of the meeting points of the caustic and wavefront, see Figure 3.16, we see that they meet at two points which may be found numerically to be approximately $(-7.43467, 5.93203)$ and $(0.665134, 1.24816)$ to 5 decimal places.

3.1.3 Harmonic Oscillator Potential

Consider the two dimensional heat equation with a harmonic oscillator potential, namely

$$\frac{\partial u}{\partial t} = \frac{\mu^2}{2} \Delta u + \frac{1}{2\mu^2} (w_1^2 x^2 + w_2^2 y^2) u.$$

We know the Mehler heat kernel from Section 2.2.3 is given by

$$G(\underline{x}, \underline{x}_0, t) = \sqrt{\frac{w_1 w_2}{(2\pi\mu^2)^2 \sin(w_1 t) \sin(w_2 t)}} \times \exp \left[-\frac{w_1}{2\mu^2} \left(\frac{(x^2 + x_0^2) \cos(w_1 t) - 2xx_0}{\sin(w_1 t)} \right) - \frac{w_2}{2\mu^2} \left(\frac{(y^2 + y_0^2) \cos(w_2 t) - 2yy_0}{\sin(w_2 t)} \right) \right].$$

Now recall that the solution of the heat equation for $S_0(\underline{x}_0) = \frac{1}{2}x_0^2 y_0$ is

$$u(\underline{x}, t) = \int_{\mathbb{R}} \int_{\mathbb{R}} G(\underline{x}, \underline{x}_0, t) e^{-\frac{x_0^2 y_0}{2\mu^2}} dx_0 dy_0,$$

i.e.

$$u(\underline{x}, t) = \sqrt{\frac{w_1 w_2}{(2\pi\mu^2)^2 \sin(w_1 t) \sin(w_2 t)}} \int_{\mathbb{R}} \int_{\mathbb{R}} e^{-\frac{\phi(\underline{x}, \underline{x}_0, t)}{\mu^2}} dx_0 dy_0,$$

where the phase function $\phi = \phi(\underline{x}, \underline{x}_0, t)$ is

$$\begin{aligned} \phi(\underline{x}, \underline{x}_0, t) &= \frac{w_1}{2 \sin(w_1 t)} [(x^2 + x_0^2) \cos(w_1 t) - 2xx_0] \\ &\quad + \frac{w_2}{2 \sin(w_2 t)} [(y^2 + y_0^2) \cos(w_2 t) - 2yy_0] + \frac{x_0^2 y_0}{2}. \end{aligned} \quad (3.19)$$

The pre-caustic is given by

$$\left| \left(\begin{array}{cc} \frac{w_1}{\tan(w_1 t)} & 0 \\ 0 & \frac{w_2}{\tan(w_2 t)} \end{array} \right) + \left(\begin{array}{cc} y_0 & x_0 \\ x_0 & 0 \end{array} \right) \right| = 0.$$

Evaluating this and re-arranging to obtain $y_0 = y_0(x_0, t)$ yields the pre-caustic as

$$y_0 = \frac{x_0^2}{w_2} \tan(w_2 t) - \frac{w_1}{\tan(w_1 t)}. \quad (3.20)$$

In Figure 3.17, we have looked at this in the example of a periodic case, where we have taken $w_1 = 2$ and $w_2 = 3$, looking at times from $t = 0.1$ in steps of 0.1. Care has been taken to ensure that t is sufficiently small as to allow our simulations to hold. Note that in the case of a vanishing potential, i.e. when $\underline{w} = (w_1, w_2) \rightarrow 0$, we have the same pre-caustic as in the zero potential case, namely

$$y_0 = tx_0^2 - \frac{1}{t}.$$

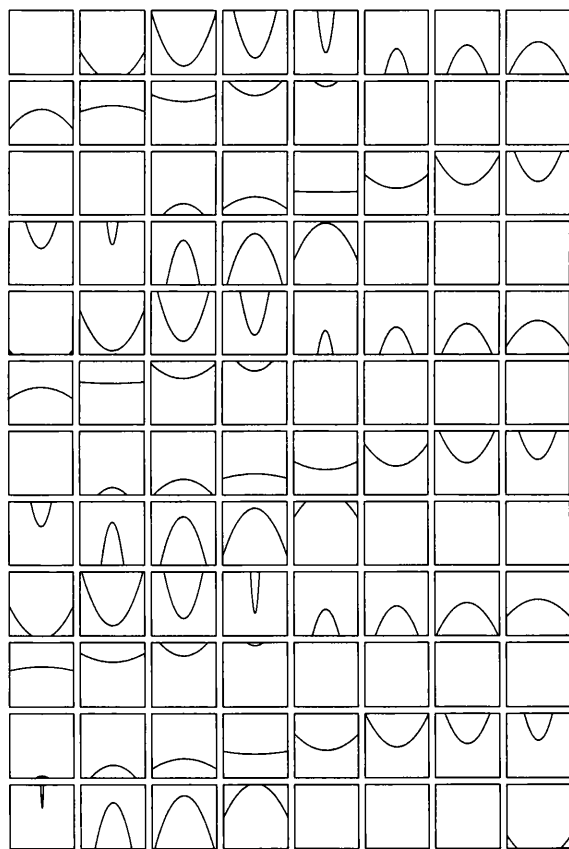


Figure 3.17: Periodic harmonic oscillator pre-caustics for $S_0 = \frac{1}{2}x_0^2y_0$ with $w_1 = 2$ and $w_2 = 3$.

In this case the classical mechanical flow is given by

$$\begin{pmatrix} x \\ y \end{pmatrix} = \begin{pmatrix} x_0 \cos(w_1 t) \\ y_0 \cos(w_2 t) \end{pmatrix} + \begin{pmatrix} x_0 y_0 \frac{\sin(w_1 t)}{w_1} \\ \frac{x_0^2 \sin(w_2 t)}{2 w_2} \end{pmatrix}. \quad (3.21)$$

We may calculate the caustic as $y = y(x, t)$ by observing that we must eliminate the variables x_0 and y_0 from the flow and pre-caustic equations. Doing so will give us the caustic $y = y(x, t)$ as

$$y = \frac{3}{2}x^{\frac{2}{3}} \left(\frac{w_1^2}{\sin^2(w_1t)} \cdot \frac{\tan(w_2t)}{w_2 \cos(w_2t)} \right)^{\frac{1}{3}} - \frac{w_1}{\tan(w_1t)} \cos(w_2t). \quad (3.22)$$

If we return to our solution of the heat equation and compute the y_0 integral by the Laplace method, see Section 1.4, then we have

$$\begin{aligned} u(\underline{x}, t) &\simeq \frac{1}{2\pi\mu^2} \sqrt{\frac{w_1 w_2}{\sin(w_1t) \sin(w_2t)}} \int_{\mathbb{R}} T_0(x_0) \\ &\quad \times \exp \left[\frac{\tan(w_2t)}{8\mu^2 w_2} x_0^4 - \frac{1}{2\mu^2} \left(\frac{y}{\cos(w_2t)} + \frac{w_1}{\tan(w_1t)} \right) x_0^2 \right. \\ &\quad \left. + \frac{w_1 x}{\mu^2 \sin(w_1t)} x_0 - \frac{w_1 x^2}{2\mu^2 \tan(w_1t)} \right] dx_0 \\ &\simeq \frac{1}{2\pi\mu^2} \sqrt{\frac{w_1 w_2}{\sin(w_1t) \sin(w_2t)}} \int_{\mathbb{R}} T_0(x_0) e^{Ax_0^4 + Bx_0^2 + Cx_0 + D} dx_0, \end{aligned}$$

for a convergence factor $T_0(x_0)$ and where the functions A , B , C and D are defined in the natural sense. This again is just the canonical form of the cusp catastrophe, see [3], where we see that the effect of the addition of the harmonic oscillator potential was to make it periodic. We illustrate an example of a periodic case in Figure 3.18, where we look at the caustic for $w_1 = 2$ and $w_2 = 3$ and for various times in steps of 0.1 from $t = 0.1$. We can clearly see that as w_1 and w_2 tend to zero our caustic tends to the zero potential caustic, namely

$$y = \frac{3}{2} \left(\frac{x^2}{t} \right)^{\frac{1}{3}} - \frac{1}{t}.$$

It is easy to compute the equation of the pre-wavefront as

$$\begin{aligned} &\frac{w_1}{2 \sin(w_1t)} \left\{ \left[\left(x_0 \cos(w_1t) + \frac{\sin(w_1t)}{w_1} x_0 y_0 \right)^2 + x_0^2 \right] \cos(w_1t) \right. \\ &\quad \left. - 2 \left(x_0 \cos(w_1t) + \frac{\sin(w_1t)}{w_1} x_0 y_0 \right) x_0 \right\} \\ &+ \frac{w_2}{2 \sin(w_2t)} \left\{ \left[\left(y_0 \cos(w_2t) + \frac{\sin(w_2t)}{w_2} \frac{x_0^2}{2} \right)^2 + y_0^2 \right] \cos(w_2t) \right. \\ &\quad \left. - 2 \left(y_0 \cos(w_2t) + \frac{\sin(w_2t)}{w_2} \frac{x_0^2}{2} \right) y_0 \right\} + \frac{1}{2} x_0^2 y_0 = 0. \end{aligned}$$

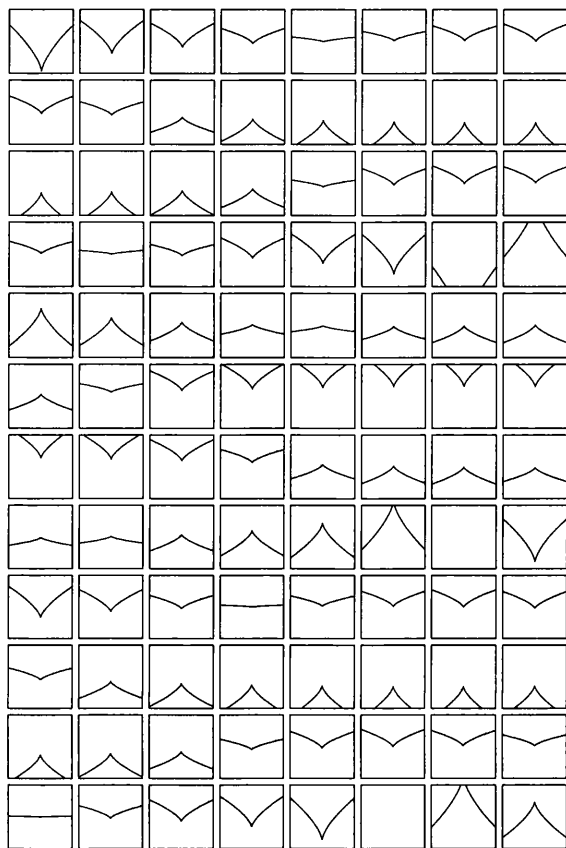


Figure 3.18: Periodic harmonic oscillator caustics for $S_0 = \frac{1}{2}x_0^2y_0$ with $w_1 = 2$ and $w_2 = 3$.

The condition for this to be periodic in time is that

$$\frac{w_1}{w_2} = \frac{p}{q},$$

where p and q are co-prime integers, the time period being $pT_1 = qT_2$, with

$$T_1 = \frac{2\pi}{w_1}, \quad \text{and} \quad T_2 = \frac{2\pi}{w_2}.$$

This may be simplified to obtain the following equation which may be considered as

a quadratic in x_0^2 or y_0 ,

$$\begin{aligned} & \frac{\sin(w_2 t) \cos(w_2 t)}{8w_2} x_0^4 + \frac{\sin(w_1 t)}{2w_1} \cos(w_1 t) x_0^2 y_0^2 \\ & + \left(\frac{1}{2} - \sin^2(w_1 t) - \frac{\sin^2(w_2 t)}{2} \right) x_0^2 y_0 - \frac{w_1}{2} \sin(w_1 t) \cos(w_1 t) x_0^2 \\ & - \frac{w_2}{2} \sin(w_2 t) \cos(w_2 t) y_0^2 = 0, \end{aligned} \quad (3.23)$$

and it is a simple matter to show that as w_1 and w_2 tend to zero we obtain the corresponding zero potential pre-wavefront, namely equation (3.7)

$$\frac{t}{8} x_0^4 + \frac{t}{2} x_0^2 y_0^2 + \frac{1}{2} x_0^2 y_0 = 0.$$

Figure 3.19 shows our periodic case of the pre-wavefront, where we notice that, for certain times, the pre-wavefront is a deformed ellipse which is similar to the zero potential case. We shall call this deformed ellipse shape, caused by fusing the line pair with the ellipse, the “kneecap singularity”. Let us illustrate how we may calculate directly the times for which the kneecap singularity may exist. If we let $y_0 \rightarrow 0$ in the expression for the pre-wavefront then this reduces to a quartic in x_0 , namely

$$\frac{\sin(w_2 t) \cos(w_2 t)}{8w_2} x_0^4 - \frac{w_1}{2} \sin(w_1 t) \cos(w_1 t) x_0^2 = 0.$$

Clearly then, two roots of the quartic occur at $x_0 = 0$ leaving the quadratic equation,

$$x_0^2 - 4w_1 w_2 \frac{\sin(w_1 t) \cos(w_1 t)}{\sin(w_2 t) \cos(w_2 t)} = 0,$$

which has roots

$$x_0 = \pm 2 \sqrt{w_1 w_2 \frac{\sin(w_1 t) \cos(w_1 t)}{\sin(w_2 t) \cos(w_2 t)}}.$$

Thus, we may only obtain a kneecap singularity when the following inequality is satisfied,

$$w_1 w_2 \frac{\sin(w_1 t) \cos(w_1 t)}{\sin(w_2 t) \cos(w_2 t)} > 0.$$

In the case of our example $w_1 = 2$ and $w_2 = 3$, we see that the kneecap can only occur for the times corresponding to the positive parts of Figure 3.20, which are the time intervals $(0, \frac{\pi}{6})$, $(\frac{\pi}{4}, \frac{\pi}{3})$, $(\frac{2\pi}{3}, \frac{3\pi}{4})$ and $(\frac{5\pi}{6}, \pi)$ with repetitions every π .

The wavefront is calculated by eliminating x_0 and y_0 from the equation of the pre-wavefront and the flow equations. This yields, after some re-arrangement, the equa-

tion,

$$\begin{aligned}
& \frac{4w_1^3}{\tan^3(w_1t)} \frac{w_2}{\tan(w_2t)} x^6 \\
& + \frac{w_1^2}{\tan^2(w_1t)} \left\{ \frac{4w_2^2 (3\cos^2(w_2t) - 1)}{\sin^2(w_2t)} y^2 + \frac{4w_1}{\tan(w_1t)} \frac{w_2^2}{\sin(w_2t)\tan(w_2t)} \left(4 - \frac{9}{\cos^2(w_1t)} \right) y \right. \\
& \quad \left. + \frac{w_1^2}{\tan^2(w_1t)} \frac{w_2^2}{\tan^2(w_2t)} \left(8 - \frac{36}{\cos^2(w_1t)} + \frac{27}{\cos^4(w_1t)} \right) \right\} x^4 \\
& + \frac{2w_1}{\tan(w_1t)} \left\{ \frac{2w_2^3 (3\cos^2(w_2t) - 2)}{\sin^2(w_2t)\tan(w_2t)} y^4 \right. \\
& \quad + \frac{2w_1}{\tan(w_1t)} \frac{w_2^3}{\sin^3(w_2t)} \left[4(2\cos^2(w_2t) - 1) + \frac{(8 - 9\cos^2(w_2t))}{\cos^2(w_1t)} \right] y^3 \\
& \quad + \frac{2w_1^2}{\tan^2(w_1t)} \frac{w_2^3}{\sin^2(w_2t)\tan(w_2t)} \left[4(3 - 2\sin^2(w_2t)) + \frac{3(6\sin^2(w_2t) - 2)}{\cos^2(w_1t)} \right] y^2 \\
& \quad \left. + \frac{2w_1^3}{\tan^3(w_1t)} \frac{w_2^3}{\sin(w_2t)\tan^2(w_2t)} \left(4 - \frac{3}{\cos^2(w_1t)} \right) y - \frac{2w_1^4}{\tan^2(w_1t)} \frac{w_2^3}{\tan^3(w_2t)} \right\} x^2 \\
& - \frac{4w_2^4}{\tan^2(w_2t)} \left\{ y^4 + \frac{4w_1}{\tan(w_1t)} \frac{y^3}{\cos(w_2t)} + \frac{2w_1^2}{\tan^2(w_1t)} \left(1 + \frac{2}{\cos^2(w_1t)} \right) y^2 \right. \\
& \quad \left. + \frac{4w_1^3}{\tan^3(w_1t)} \frac{y}{\cos(w_2t)} \frac{w_1^4}{\tan^4(w_1t)} \right\} = 0 \tag{3.24}
\end{aligned}$$

Again, this is periodic in time if $\frac{w_1}{w_2} = \frac{p}{q}$ with co-prime integers p and q . It is a little messy to show, but has actually been verified, that as w_1 and w_2 tend to zero, we obtain the same result as the zero potential case, namely equation (3.8)

$$\frac{x^2}{t^7} \left[4x^4 + \left(8y^2 - \frac{20y}{t} - \frac{1}{t^2} \right) + 4y \left(y + \frac{1}{t} \right)^3 \right] = 0.$$

Figure 3.21 shows the periodic wavefront in time steps of 0.1 starting at $t = 0.1$. The shape can be thought of as the fusing of the tricorn and the line pair witnessed in the zero potential case.

We may compute exactly the positions of the meeting points of the pre-caustic and pre-wavefront but the expression is quite complex. We shall only mention that to find these meeting points one must eliminate y_0 from the expressions of the pre-caustic, equation (3.20), and pre-wavefront, equation (3.23), and look at the zeros of the resulting cubic in x_0^2 . The real solutions, for x_0 , will give the x_0 position of the meeting points and the corresponding y_0 position may be easily found by substitution into the pre-caustic, equation (3.20). Figure 3.22 shows an example of the meeting points for $w_1 = 2$ and $w_2 = 3$ for time $t = 1$, where we can see that they cross at the points $(9.32998, 3.22084)$ and $(-9.32998, 3.22084)$ which are given approximately.

We may also consider the meeting points of the caustic and wavefront, as depicted for our periodic case at time $t = 1$ in Figure 3.23. Similarly to the meeting points of the

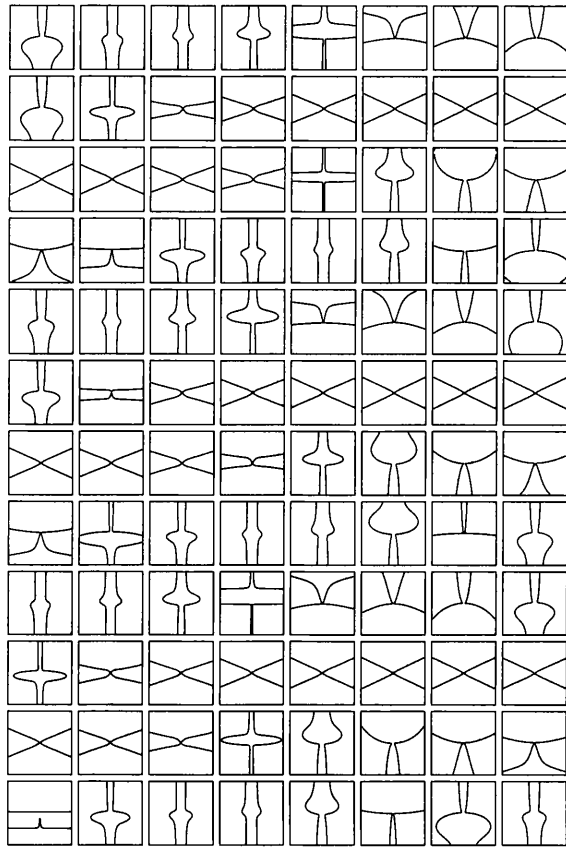


Figure 3.19: Periodic harmonic oscillator pre-wavefronts for $S_0 = \frac{1}{2}x_0^2y_0$ with $w_1 = 2$ and $w_2 = 3$.

pre-caustic and pre-wavefront, we may calculate the positions of intersection at approximately $(-17.545, 5.236)$, $(-0.022, -0.834)$, $(0.022, -0.834)$ and $(17.545, 5.236)$. This is an interesting case to look at. In the previous cases, we had the same amount of points of intersection of the pre-caustic and pre-wavefront as we had for the caustic and wavefront. However in the case we have only 2 points of intersection on the pre-curves, whilst we have 4 distinct points where the wavefront and caustic meet.

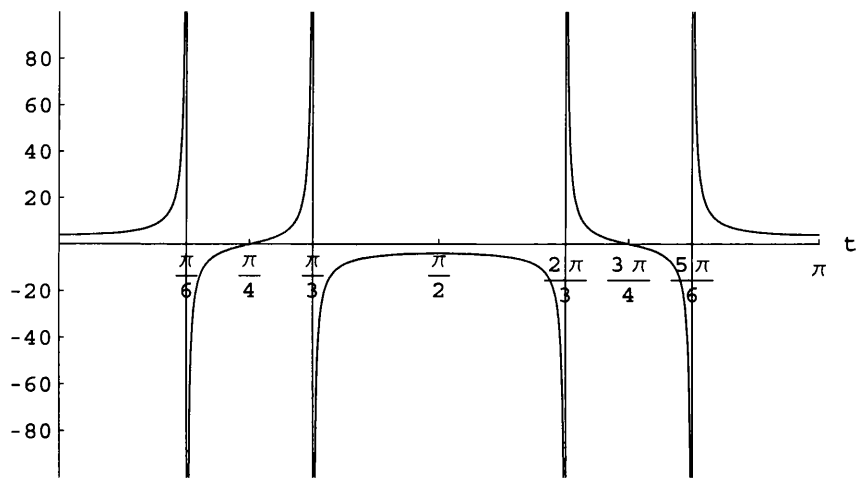


Figure 3.20:
Harmonic oscillator pre-wavefront generator for $S_0 = \frac{1}{2}x_0^2 y_0$ with $k = 5$.

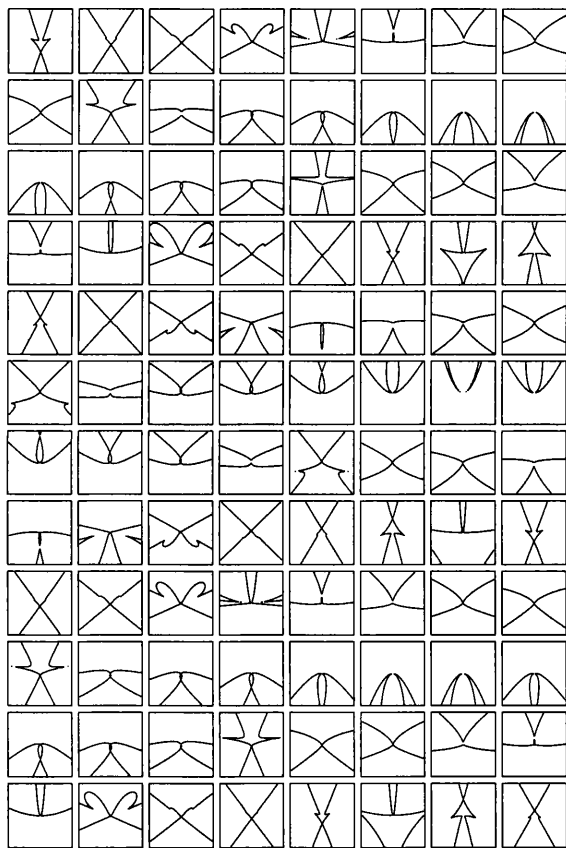


Figure 3.21: Periodic harmonic oscillator wavefronts for $S_0 = \frac{1}{2}x_0^2y_0$ with $w_1 = 2$ and $w_2 = 3$.

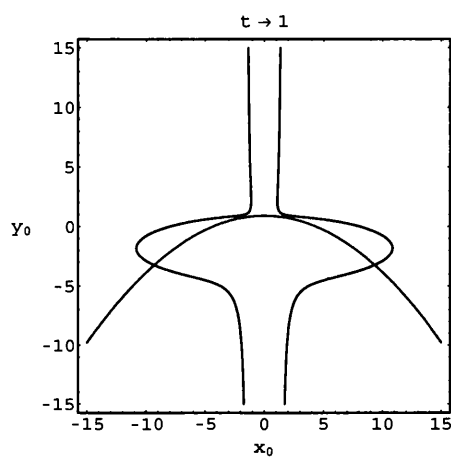


Figure 3.22: Harmonic oscillator pre-caustic and pre-wavefront for $S_0 = \frac{1}{2}x_0^2 y_0$ with $w_1 = 2$ and $w_2 = 3$.

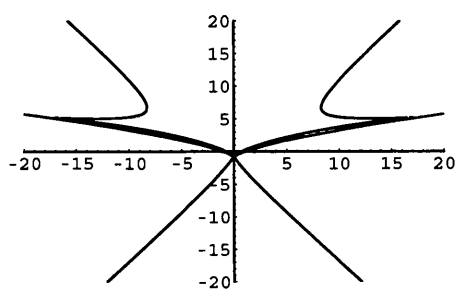


Figure 3.23: Harmonic oscillator caustic and wavefront for $S_0 = \frac{1}{2}x_0^2 y_0$ with $w_1 = 2$ and $w_2 = 3$.

3.2 The Noisy Case

We now study the effects of a linear noise term $-\frac{x}{\mu^2}u \circ \partial W_t$ upon the singularities in the previous section. We provide an analysis and produce exact formulae for the singularities of the stochastic heat and Burgers' equations for the same potentials as discussed previously. We shall see that the addition of a noisy term doesn't effect the overall geometry of the cusp caustic and moreover, there is no effect whatsoever upon the pre-caustic curves.

3.2.1 Zero Potential

In the case of our initial condition for the polynomial cusp, i.e. $S_0(\underline{x}_0) = \frac{1}{2}x_0^2 y_0$, the caustic of the stochastic Burgers' equation is given by

$$\begin{vmatrix} 1 + ty_0 & tx_0 \\ tx_0 & 1 \end{vmatrix} = 0,$$

as in the original case without noise. So the equation of the pre-caustic that we obtain is just the parabola

$$y_0 = tx_0^2 - \frac{1}{t}, \quad (3.25)$$

which we obtained earlier in the classical zero potential case, shown in Figure 3.1. Then $\nabla_{\underline{x}_0} \phi(\underline{x}, \underline{x}_0, t) = 0$ gives $y_0 = y - \frac{t}{2}x_0^2$, and after doing the y_0 integration we have phase function

$$\begin{aligned} \tilde{\phi}(\underline{x}, \underline{x}_0, t) &= -\frac{t}{8}x_0^4 + \frac{1}{2} \left(y + \frac{1}{t} \right) x_0^2 + \frac{1}{t} \left(\int_0^t W_s ds - x \right) x_0 \\ &\quad + \left(\frac{x^2}{2t} + xW_t - \frac{x}{t} \int_0^t W_s ds + \frac{\zeta(t)}{t} \right). \end{aligned}$$

This gives the solution of the stochastic heat equation with a zero potential as

$$\begin{aligned} u(\underline{x}, t) &\simeq \frac{1}{2\pi\mu^2 t} \int_{\mathbb{R}} T_0(x_0) e^{-\frac{\tilde{\phi}(\underline{x}, \underline{x}_0, t)}{\mu^2}} dx_0 \\ &\simeq \frac{1}{2\pi\mu^2 t} \int_{\mathbb{R}} T_0(x_0) e^{Ax_0^4 + Bx_0^2 + Cx_0 + D} dx_0, \end{aligned}$$

for the convergence factor $T_0(x_0)$ and where

$$\begin{aligned} A &= \frac{t}{8\mu^2}, & B &= -\frac{1}{2\mu^2} \left(y + \frac{1}{t} \right), & C &= -\frac{1}{\mu^2 t} \left(\int_0^t W_s ds - x \right), \\ D &= -\frac{1}{\mu^2} \left(\frac{x^2}{2t} + xW_t - \frac{x}{t} \int_0^t W_s ds + \frac{\zeta(t)}{t} \right). \end{aligned}$$

We see that the addition of a noisy terms has little effect upon the canonical form of the cusp catastrophe. Now, in order to perform the x_0 integration we need to look at the dominant term coming from $\frac{\partial \phi}{\partial x_0} = 0$, namely

$$\frac{\partial \phi}{\partial x_0} = -\frac{t}{2}x_0^3 + \left(y + \frac{1}{t}\right)x_0 + \frac{1}{t} \left(\int_0^t W_s ds - x\right) = 0.$$

Recall that the condition for caustics in the stochastic Burgers' equation is that $\left|\frac{\partial^2 \phi}{\partial x_0^2}\right| = 0$, which is just our pre-caustic $y_0 = tx_0^2 - \frac{1}{t}$, equation (3.25). Then eliminating y_0 from $\frac{\partial \phi}{\partial y_0} = 0$ gives us again that

$$x_0 = \pm \sqrt{\frac{2}{3t} \left(y + \frac{1}{t}\right)}.$$

Finally, substituting for x_0 into $\frac{\partial \phi}{\partial x_0} = 0$ we see that the caustic is governed by the equation

$$\left(y + \frac{1}{t}\right)^3 = \frac{27}{8t} \left(x - \int_0^t W_s ds\right)^2,$$

or for $y = y(x, t)$ we have the equation of the caustic as

$$y = \frac{3}{2t^{\frac{1}{3}}} \left(x - \int_0^t W_s ds\right)^{\frac{2}{3}} - \frac{1}{t}. \quad (3.26)$$

This has been calculated exactly, with no numerical analysis involved. Notice how it is similar to the original classical case but differs only by a random displacement of $-\frac{1}{t} \int_0^t W_s(\omega) ds$ in the x direction. Figure 3.24 is an example of what this may look like for some $t > 0$. For details of how this has been plotted, with regard to approximating the randomness of the function, see Appendix B.3.

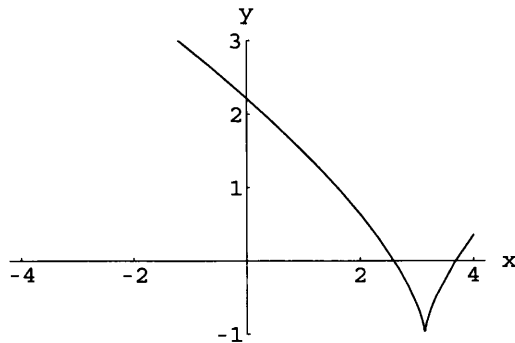


Figure 3.24: Zero potential caustic for $S_0 = \frac{1}{2}x_0^2 y_0$ with noise.

We may also look at the expectation and variance of this random displacement. The expectation is simply

$$\mathbb{E} \left[\int_0^t W_s(\omega) ds \right] = \int_0^t \mathbb{E} [W_s(\omega)] ds = 0,$$

whilst for the variance we have

$$\begin{aligned} \text{Var} \left[\int_0^t W_s(\omega) ds \right] &= \mathbb{E} \left[\left(\int_0^t W_s(\omega) ds \right)^2 \right] - \mathbb{E} \left[\int_0^t W_s(\omega) ds \right]^2 \\ &= \int_0^t \int_0^t \mathbb{E} [W_s(\omega) W_r(\omega)] ds dr \\ &= \int_0^t \int_0^t \inf\{s, r\} ds dr \\ &= \frac{t^3}{3}. \end{aligned}$$

Recall that in Section 2.3.1 we showed how to calculate a general pre-wavefront, given by equation (2.37). Applying this to our initial condition $S_0 = \frac{1}{2}x_0^2y_0$ gives the pre-wavefront for the solution to the above stochastic heat equation as equation (3.27), and Figure 3.25 is an example of this pre-wavefront.

$$\begin{aligned} \frac{t}{8}x_0^4 + \frac{t}{2}x_0^2y_0^2 + \frac{x_0^2y_0}{2} + \left(x_0 + tx_0y_0 + \int_0^t W_s ds \right) W_t \\ - \frac{1}{2t} \left(\int_0^t W_s ds \right)^2 + \frac{\zeta(t)}{t} = 0. \end{aligned} \quad (3.27)$$

Notice the similarities between Figure 3.5 and Figure 3.25, particularly that Figure 3.25 is equivalent to our ellipse and straight line from the classical case in Figure 3.5. We can see that the ellipse has been torn apart and that the straight line $x_0 = 0$ has been widened and, in fact, now forms a vertical asymptotic. Similarly to the classical case of zero potential, the pre-wavefront is a quadratic in y_0 and may be solved to give $y_0 = y_0(x_0, t)$ as

$$y_0 = - \left(\frac{1}{2t} + \frac{W_t}{x_0} \right) \pm \frac{1}{2tx_0} \sqrt{-t^2x_0^4 + x_0^2 - 4tx_0W_t + 4 \left(tW_t - \int_0^t W_s ds \right)^2 - 8\zeta(t)}.$$

Firstly, this explains the singularity as $x_0 \rightarrow 0$, why the pre-wavefront splits, and secondly, we see that the existence of the pre-wavefront is entirely dependent upon the inequality

$$-t^2x_0^4 + x_0^2 - 4tx_0W_t + 4 \left(tW_t - \int_0^t W_s ds \right)^2 - 8\zeta(t) \geq 0.$$

The equation for the wavefront of the heat equation is extremely untidy,

$$\begin{aligned}
& 4x^6 + 24 \left(tW_t - \int_0^t W_s ds \right) x^5 \\
& + \left[48 \left(tW_t - \int_0^t W_s ds \right)^2 + \frac{1}{t^2} (8t^2y^2 - 20ty - 1) + 24\zeta(t) \right] x^4 \\
& + 4 \left[24 \left(tW_t - \int_0^t W_s ds \right) \zeta(t) + \frac{2}{t} (4t^2y^2 - ty - 5) W_t \right. \\
& \quad \left. - \frac{1}{t^2} (8t^2y^2 - 20ty - 1) \int_0^t W_s ds + 8 \left(tW_t - \int_0^t W_s ds \right)^3 \right] x^3 \\
& + 2 \left[\frac{2y}{t^3} (1 + ty)^3 + 16 (1 + ty)^2 W_t^2 + \frac{1}{t^2} (16t^2y^2 - 58ty + 7) \left(\int_0^t W_s ds \right)^2 \right. \\
& \quad \left. - \frac{8}{t} (4t^2y^2 - ty - 5) W_t \int_0^t W_s ds + \frac{4}{t^2} (4t^2y^2 - ty - 5) \zeta(t) \right. \\
& \quad \left. + 48 \left(tW_t - \int_0^t W_s ds \right)^2 \zeta(t) + 24\zeta(t)^2 \right] x^2 \\
& + 4 \left[\frac{2}{t^3} (1 + ty)^4 W_t - \frac{2y}{t^3} (1 + ty)^3 W_t - \frac{18}{t} (1 + ty) W_t \left(\int_0^t W_s ds \right)^2 \right. \\
& \quad \left. - \frac{9}{t^2} (1 - 2ty) \left(\int_0^t W_s ds \right)^3 + \frac{16}{t} (1 + ty)^2 W_t \zeta(t) \right. \\
& \quad \left. - \frac{4}{t^2} (4t^2y^2 - ty - 5) \int_0^t W_s ds \zeta(t) + 24 \left(tW_t - \int_0^t W_s ds \right) \zeta(t)^2 \right] x \\
& + \left[\frac{8}{t^4} (1 + ty)^4 \zeta(t) - \frac{4}{t^4} (1 + ty)^3 \left(\int_0^t W_s ds \right)^2 + \frac{32}{t^2} (1 + ty)^2 \zeta(t)^2 \right. \\
& \quad \left. - \frac{72}{t^2} (1 + ty) \left(\int_0^t W_s ds \right)^2 \zeta(t) + \frac{27}{t^2} \left(\int_0^t W_s ds \right)^4 + 32\zeta(t)^3 \right] = 0. \quad (3.28)
\end{aligned}$$

This is depicted in Figure 3.26 for some $t > 0$.

It is interesting to look at a comparison of the pre-caustic and the pre-wavefront in this case as in Figure 3.27. We can calculate the position where the pre-caustic and pre-wavefront meet by eliminating y_0 from the equations of the pre-caustic (3.25) and pre-wavefront (3.27) to obtain a sixth order polynomial in x_0 ,

$$\frac{t^3}{2} x_0^6 - \frac{3}{8} t x_0^4 + t^2 W_t x_0^3 + W_t \int_0^t W_s ds - \frac{1}{2t} \left(\int_0^t W_s ds \right)^2 + \frac{\zeta(t)}{t} = 0.$$

We cannot directly solve a sixth order polynomial, but in the case of our example, we may numerically compute the x_0 positions of our meeting points and then use the computed values to calculate the y_0 position. Doing so gives the positions of the meeting points of the pre-caustic and pre-wavefront in our example as approximately $(-1.2952, 0.6775)$ and $(1.7867, 2.1922)$.

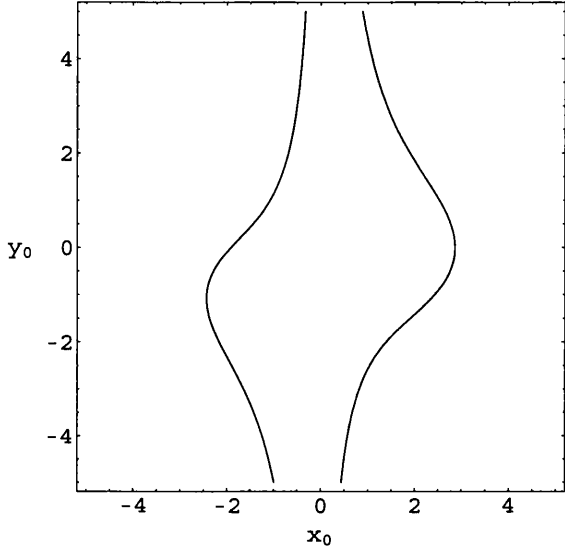


Figure 3.25: Zero potential pre-wavefront for $S_0 = \frac{1}{2}x_0^2y_0$ with noise.

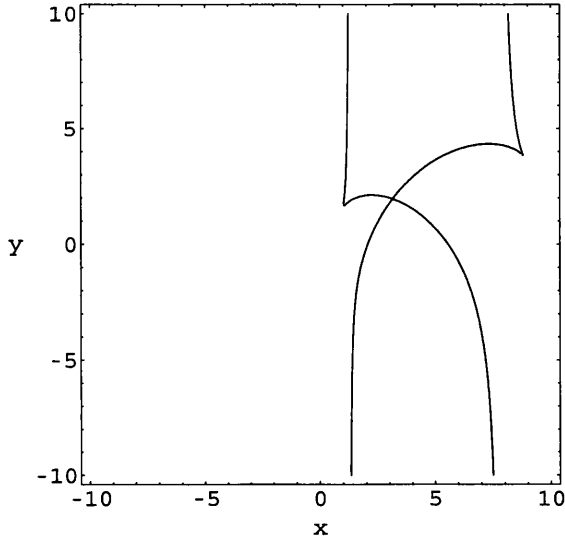


Figure 3.26: Zero potential wavefront for $S_0 = \frac{1}{2}x_0^2y_0$ with noise.

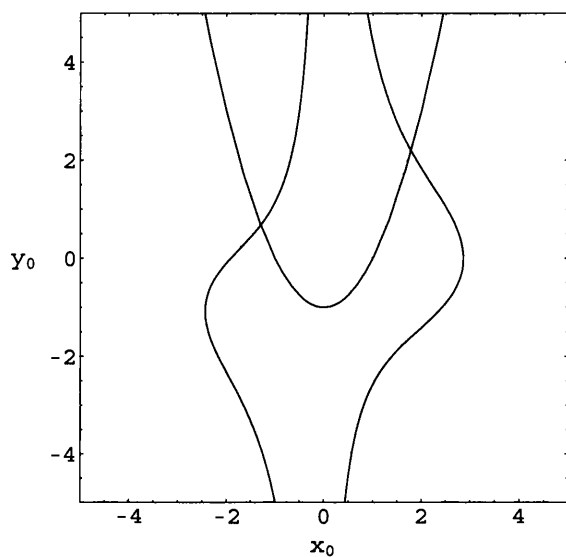


Figure 3.27: Zero potential pre-caustic and pre-wavefront for $S_0 = \frac{1}{2}x_0^2 y_0$ with noise.

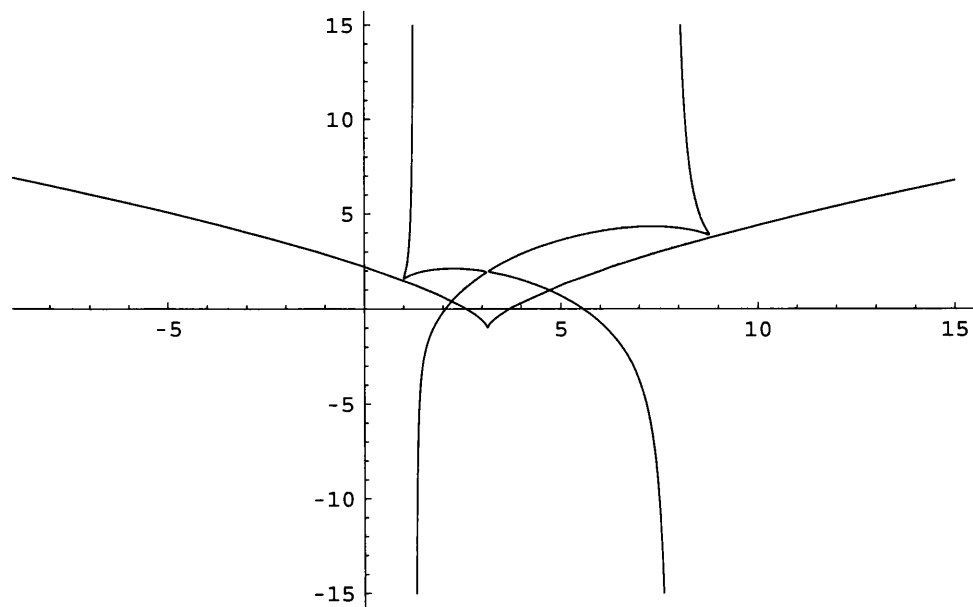


Figure 3.28: Zero potential caustic and wavefront for $S_0 = \frac{1}{2}x_0^2 y_0$ with noise.

We can also see how the wavefront of the heat equation fits in with the caustic for the Burgers' equation, Figure 3.28. Solving numerically we see that the curves in our example meet at $(0.9689, 1.5163)$, $(2.2266, 0.4138)$, $(4.6889, 1.0066)$ and $(8.8451, 3.7884)$ to 4 decimal places.

3.2.2 Linear Potential

In the noisy linear potential case with $S_0(\underline{x}_0) = \frac{1}{2}x_0^2y_0$, the pre-caustic of the stochastic heat equation (2.49) is given by exactly the same method used in the zero potential case, i.e.

$$\left| \frac{1}{t}I_3 + \frac{\partial^2 S_0}{\partial \underline{x}_0^2} \right| = 0.$$

Hence, the pre-caustic remains unchanged as

$$y_0 = tx_0^2 - \frac{1}{t}, \quad (3.29)$$

which is depicted in Figure 3.1. Now recall that we have phase function given by

$$\phi(\underline{x}, \underline{x}_0, t) = \frac{(x - x_0)^2}{2t} + \frac{(y - y_0)^2}{2t} + F(t)x + k(t)x_0 + l(t) + \frac{x_0^2 y_0}{2}, \quad (3.30)$$

for the $F(t)$, $k(t)$ and $l(t)$ calculated earlier in Section 2.3.2. Then our classical mechanical flow is given by equation (2.51) as

$$\begin{pmatrix} x \\ y \end{pmatrix} = \begin{pmatrix} x_0 \\ y_0 \end{pmatrix} + t \begin{pmatrix} k(t) \\ 0 \end{pmatrix} + t \begin{pmatrix} x_0 y_0 \\ \frac{x_0^2}{2} \end{pmatrix}. \quad (3.31)$$

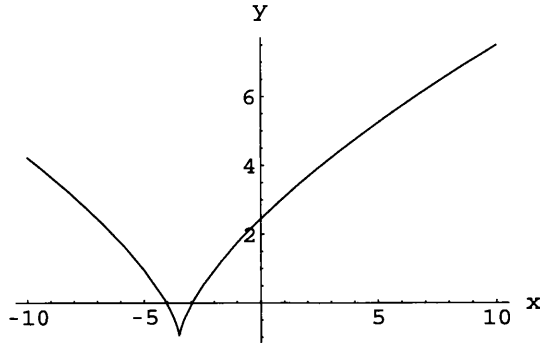


Figure 3.29: Linear potential caustic for $S_0 = \frac{1}{2}x_0^2y_0$ with $k = 5$ and noise for $\alpha \rightarrow 1$.

Using these simultaneous equations to eliminate the x_0 and y_0 variables from the pre-caustic (3.29), we obtain the caustic as

$$y = \frac{3}{2t^{\frac{1}{3}}}(x - tk(t))^{\frac{2}{3}} - \frac{1}{t}. \quad (3.32)$$

Going back to the solution of the heat equation, if we do the y_0 integral by the Laplace method, see section 1.4, then we have solution

$$\begin{aligned} u(\underline{x}, t) &\simeq \frac{1}{2\pi\mu^2 t} \int_{\mathbb{R}} T_0(x_0) e^{-\frac{1}{\mu^2} \left\{ -\frac{1}{8}x_0^4 + \frac{1}{2}(y + \frac{1}{t})x_0^2 + (k(t) - \frac{x}{t})x_0 + \frac{x^2}{2t} + F(t)x + l(t) \right\}} dx_0, \\ &\simeq \frac{1}{2\pi\mu^2 t} \int_{\mathbb{R}} T_0(x_0) e^{Ax_0^4 + Bx_0^2 + Cx_0 + D} dx_0, \end{aligned}$$

which again is just the canonical form of the cusp catastrophe.

By using the calculated value of $k(t)$ given in equation (2.47) we obtain the equation of the caustic as

$$y = \frac{3}{2t^{\frac{2}{3}}} \left(x - \frac{Kt^2}{2} - \alpha t \int_0^t \frac{W_r}{r} dr + \alpha t \int_0^t \int_0^r \frac{W_s}{r^2} ds dr \right)^{\frac{2}{3}} - \frac{1}{t}, \quad (3.33)$$

which, for our example, looks as in Figure 3.29. Recall that the pre-wavefront was given by equation (2.52), which for $S_0(\underline{x}_0) = \frac{1}{2}x_0^2 y_0$ is calculated as

$$\frac{tx_0^2}{2} \left(\frac{x_0^2}{4} + y_0^2 \right) + \frac{x_0^2 y_0}{2} + x_0 (F(t) + k(t)) (ty_0 + 1) + tk(t) \left(F(t) + \frac{k(t)}{2} \right) + l(t) = 0. \quad (3.34)$$

Using our values of $F(t)$, $k(t)$ and $l(t)$ from equations (2.46), (2.47), and (2.48), we can write the equation of the pre-wavefront for the noisy linear case, in full, as

$$\begin{aligned} 0 &= \frac{t}{8}x_0^4 + \frac{x_0^2 y_0}{2} (1 + ty_0) \\ &\quad + t \left(\frac{Kt}{2} + \alpha \int_0^t \frac{W_r}{r} dr - \alpha \int_0^t \int_0^r \frac{W_s}{r^2} ds dr \right) \\ &\quad \times \left(3\frac{Kt}{4} - \alpha W_t + \frac{\alpha}{t} \int_0^t W_s ds + \frac{\alpha}{2} \int_0^t \frac{W_r}{r} dr - \frac{\alpha}{2} \int_0^t \int_0^r \frac{W_s}{r^2} ds dr \right) \\ &\quad + x_0 (1 + ty_0) \left(Kt - \alpha W_t + \frac{\alpha}{t} \int_0^t W_s ds + \alpha \int_0^t \frac{W_r}{r} dr - \alpha \int_0^t \int_0^r \frac{W_s}{r^2} ds dr \right) \\ &\quad - \frac{K^2 t^3}{24} - \frac{\alpha K}{2} \int_0^t r W_r dr + \frac{\alpha K}{2} \int_0^t \int_0^r W_s ds dr - \frac{\alpha^2}{2} \int_0^t W_r^2 dr \\ &\quad + \alpha^2 \int_0^t \int_0^r \frac{W_r W_s}{r} ds dr - \frac{\alpha^2}{2} \int_0^t \frac{1}{r^2} \left(\int_0^r W_s ds \right)^2 dr. \quad (3.35) \end{aligned}$$

This is shown, for a sample Wiener process, in Figure 3.30, where we can see similarities between the previous cases. The wavefront is given by using the classical mechanical flow (3.31) to eliminate the x_0 and y_0 terms, see Figure 3.31, which gives

the equation of the wavefront as

$$\begin{aligned}
& \frac{4}{t^3}x^6 + \frac{24}{t^2}F(t)x^5 + \frac{1}{t}\left[\frac{8}{t^2}y^2 - \frac{20}{t^3}y - \frac{1}{t^4} + 48F(t)^2 + \frac{24}{t}l(t)\right]x^4 \\
& + 4\left\{\frac{8}{t^2}F(t)y^2 + \frac{2}{t^3}[9k(t) - F(t)]y + 8F(t)^3 + \frac{2}{t}F(t)\left[12l(t) - \frac{5}{t^3}\right] - \frac{9}{t^4}k(t)\right\}x^3 \\
& + 2\left\{\frac{2}{t^3}y^4 + \frac{6}{t^4}y^3 + \frac{2}{t}\left[\frac{3}{t^4} + 8F(t)^2 + \frac{8}{t}l(t)\right]y^2\right. \\
& \quad \left. + \frac{2}{t^2}\left[\frac{1}{t^4} + 16F(t)^2 + 36F(t)k(t) - 9k(t)^2 - \frac{2}{t}l(t)\right]y + \frac{16}{t^3}F(t)^2\right. \\
& \quad \left. + \frac{72}{t^3}F(t)k(t) + \frac{63}{t^3}k(t)^2 - \frac{20}{t^4}l(t) + 48F(t)^2l(t) + \frac{24}{t}l(t)^2\right\}x^2 \\
& + 4\left\{\frac{2}{t^2}F(t)y^4 + \frac{2}{t^3}[4F(t) + k(t)]y^3 + \frac{2}{t}\left[\frac{6}{t^3}F(t) + \frac{3}{t^3}k(t) + 8F(t)l(t)\right]y^2\right. \\
& \quad \left. + \frac{2}{t}\left[\frac{4}{t^4}F(t) + \frac{3}{t^4}k(t) - 9F(t)k(t)^2 + \frac{16}{t}F(t)l(t) + \frac{18}{t}F(t)l(t)\right]y\right. \\
& \quad \left. + \frac{2}{t^6}F(t) + \frac{2}{t^6}k(t) - \frac{18}{t^2}F(t)k(t)^2 - \frac{27}{t^2}k(t)^3 + \frac{16}{t^3}F(t)l(t)\right. \\
& \quad \left. + \frac{36}{t^3}k(t)l(t) + 24F(t)l(t)^2\right\}x \\
& + \frac{8}{t^2}l(t)y^4 - \frac{4}{t^2}\left[k(t)^2 - \frac{8}{t^2}l(t)\right]y^3 - \frac{4}{t}\left[\frac{3}{t^2}k(t)^2 - \frac{12}{t^3}l(t) - 8l(t)^2\right]y^2 \\
& - \frac{4}{t}\left[\frac{3}{t^3}k(t)^2 - \frac{9}{t^4}l(t) + 18k(t)^2l(t) - \frac{16}{t}l(t)^2\right]y - \frac{4}{t^5}k(t)^2 - \frac{27}{t}k(t)^4 + \frac{8}{t^6}l(t) \\
& - \frac{72}{t^2}k(t)^2l(t) + \frac{32}{t^3}l(t)^2 + 32l(t)^3 = 0, \tag{3.36}
\end{aligned}$$

for the $F(t)$, $k(t)$ and $l(t)$ given in equations (2.46), (2.47) and (2.48).

Figure 3.32 shows that the pre-caustic and pre-wavefront meet at a pair of points in our example. While we cannot exactly calculate these points, we may find their location numerically, which gives them approximately as $(-1.48965, 1.21905)$ and $(1.08254, 0.171904)$.

Again we can numerically calculate the 4 points where the caustic and wavefront meet. They are approximately at the positions $(-6.80559, 2.32857)$, $(-4.08472, 0.0488774)$, $(-3.11051, -0.2)$ and $(-2.23136, 0.757856)$ as shown in Figure 3.33.

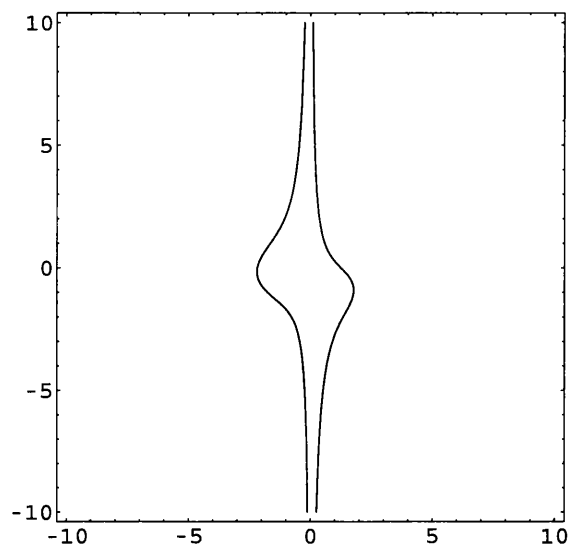


Figure 3.30: Linear potential pre-wavefront for $S_0 = \frac{1}{2}x_0^2y_0$ with $k = 5$ and noise for $\alpha \rightarrow 1$.

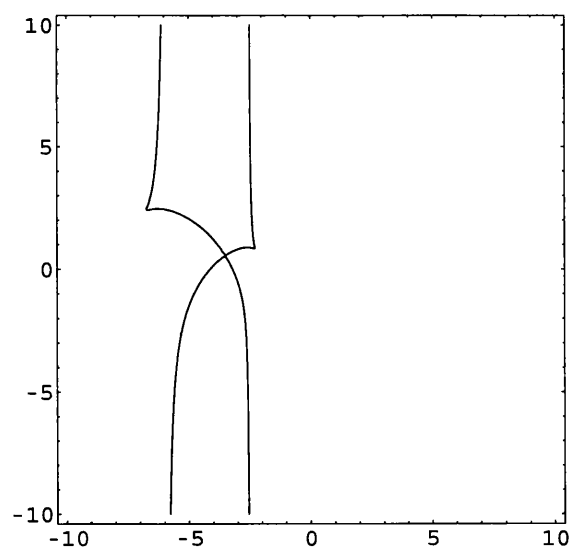


Figure 3.31: Linear potential wavefront for $S_0 = \frac{1}{2}x_0^2y_0$ with $k = 5$ and noise for $\alpha \rightarrow 1$.

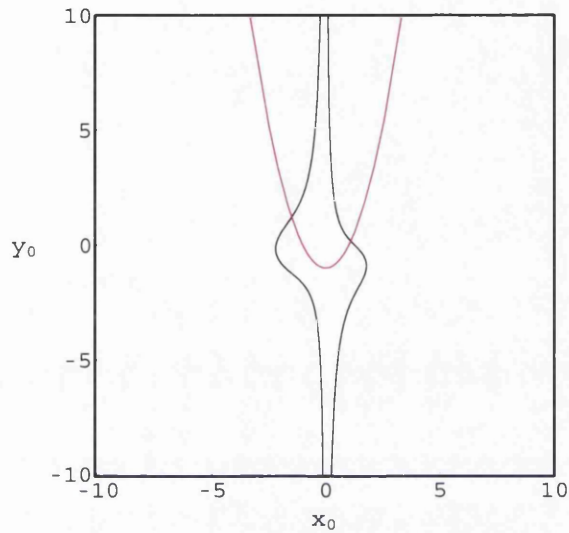


Figure 3.32: Linear potential pre-caustic and pre-wavefront for $S_0 = \frac{1}{2}x_0^2y_0$ with $k = 5$ and noise for $\alpha \rightarrow 1$.

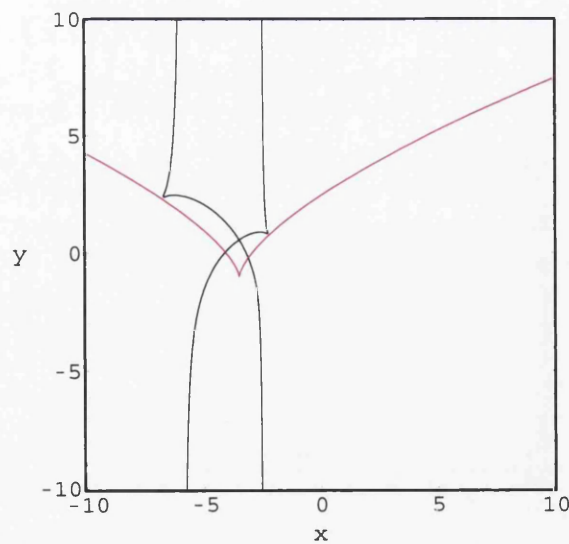


Figure 3.33: Linear potential caustic and wavefront for $S_0 = \frac{1}{2}x_0^2y_0$ with $k = 5$ and noise for $\alpha \rightarrow 1$.

3.2.3 Harmonic Oscillator Potential

In the case of the noisy harmonic oscillator potential with $S_0(\underline{x}_0) = \frac{1}{2}x_0^2y_0$, the phase function is

$$\begin{aligned} \phi(\underline{x}, \underline{x}_0, t) &= \frac{w_1}{2} \left(\frac{(x - x_0)^2 \cos(w_1 t) - 2xx_0}{\sin(w_1 t)} \right) + \frac{w_2}{2} \left(\frac{(y - y_0)^2 \cos(w_2 t) - 2yy_0}{\sin(w_2 t)} \right) \\ &\quad + xW_t - \frac{w_1 x}{\sin(w_1 t)} \int_0^t W_r \cos(w_1 r) dr \\ &\quad + \frac{w_1 x_0}{\sin(w_1 t)} \int_0^t W_r \cos(w_1 r - w_1 t) dr + \eta(t) + \frac{1}{2}x_0^2y_0, \end{aligned} \quad (3.37)$$

which gives the classical mechanical flow as

$$\begin{pmatrix} x \\ y \end{pmatrix} = \begin{pmatrix} x_0 \cos(w_1 t) \\ y_0 \cos(w_2 t) \end{pmatrix} + \begin{pmatrix} \frac{\sin(w_1 t)}{w_1} x_0 y_0 \\ \frac{\sin(w_2 t)}{w_2} x_0^2 \end{pmatrix} + \begin{pmatrix} \int_0^t W_r \cos(w_1 r - w_1 t) dr \\ 0 \end{pmatrix}. \quad (3.38)$$

Here the pre-caustic is exactly the same as in the classical case with a harmonic oscillator potential as calculated in equation (3.20) and depicted by Figure 3.17. Using the simultaneous equations from the classical mechanical flow, we may eliminate the x_0 and y_0 variables from the pre-caustic (3.20) to obtain the equation of the caustic as

$$\begin{aligned} y &= \frac{3}{2} \left(\frac{w_1}{\sin(w_1 t)} \right)^{\frac{2}{3}} \left(\frac{\sin(w_2 t) \cos(w_2 t)}{w_2} \right)^{\frac{1}{3}} \left(\int_0^t W_r \cos(w_1 r - w_1 t) dr - x \right)^{\frac{2}{3}} \\ &\quad - \frac{w_1}{\tan(w_1 t)} \cos(w_2 t). \end{aligned} \quad (3.39)$$

This is shown in Figure 3.34 where we can see the familiar cusp behaviour.

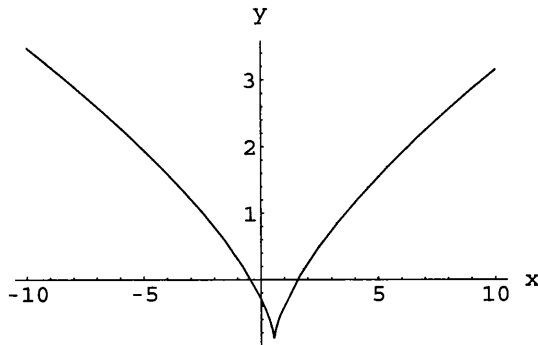


Figure 3.34: Harmonic oscillator caustic for $S_0 = \frac{1}{2}x_0^2y_0$ with $w_1 = 2$, $w_2 = 3$ and noise.

Turning our attention to the solution of the heat equation, we see that after performing the y_0 integration via the Laplace method, we obtain the phase function

$$\begin{aligned}\tilde{\phi}(\underline{x}, x_0, t) = & -\frac{\tan(w_2 t)}{8w_2} x_0^4 + \frac{1}{2} \left(\frac{y}{\cos(w_2 t)} + \frac{w_1}{\tan(w_1 t)} \right) x_0^2 \\ & + \left(\frac{w_1}{\sin(w_1 t)} \int_0^t W_r \cos(w_1 t - w_1 r) dr - \frac{w_1 x}{\sin(w_1 t)} \right) x_0 \\ & + \frac{w_1 x^2}{2 \tan(w_1 t)} + \left(W_t - \frac{w_1}{\sin(w_1 t)} \int_0^t W_r \cos(w_1 r) dr \right) x \\ & + \frac{w_2 y^2}{2 \tan(w_2 t)} - \frac{w_2 y^2}{2 \sin(w_2 t) \cos(w_2 t)} + \eta(t).\end{aligned}$$

Then the integral solution of the heat equation is

$$\begin{aligned}u(\underline{x}, t) & \simeq \frac{1}{2\pi\mu^2} \sqrt{\frac{w_1 w_2}{\sin(w_1 t) \sin(w_2 t)}} \int_0^t T_0(x_0) e^{-\frac{\tilde{\phi}(\underline{x}, x_0, t)}{\mu^2}} dx_0, \\ & \simeq \frac{1}{2\pi\mu^2} \sqrt{\frac{w_1 w_2}{\sin(w_1 t) \sin(w_2 t)}} \int_0^t T_0(x_0) e^{Ax_0^4 + Bx_0^2 + Cx_0 + D} dx_0,\end{aligned}$$

for a convergence factor $T_0(x_0)$ and where A , B , C and D are the obvious coefficients. We see that the addition of a harmonic oscillator potential with a noise term does little to effect the geometry of the cusp catastrophe. Recall that the pre-wavefront in this case is given by equation (2.59), which, for our particular $S_0(\underline{x}_0)$ is simply

$$\begin{aligned}& \frac{w_1}{2\sin(w_1 t)} \left\{ \left[\left(x_0 \cos(w_1 t) + \frac{\sin(w_1 t)}{w_1} x_0 y_0 + \int_0^t W_r \cos(w_1 r - w_1 t) dr \right)^2 + x_0^2 \right] \cos(w_1 t) \right. \\ & \quad \left. - 2 \left(x_0 \cos(w_1 t) + \frac{\sin(w_1 t)}{w_1} x_0 y_0 + \int_0^t W_r \cos(w_1 r - w_1 t) dr \right) x_0 \right\} \\ & + \frac{w_2}{2\sin(w_2 t)} \left\{ \left[\left(y_0 \cos(w_2 t) + \frac{\sin(w_2 t)}{w_2} \frac{x_0^2}{2} \right)^2 + y_0^2 \right] - 2 \left(y_0 \cos(w_2 t) + \frac{\sin(w_2 t)}{w_2} \frac{x_0^2}{2} \right) y_0 \right\} \\ & + \left(x_0 \cos(w_1 t) + \frac{\sin(w_1 t)}{w_1} x_0 y_0 + \int_0^t W_r \cos(w_1 r - w_1 t) dr \right) \\ & \quad \times \left(W_t - \frac{w_1}{\sin(w_1 t)} \int_0^t W_r \cos(wr) dr \right) \\ & + \frac{w_1 x_0}{\sin(w_1 t)} \int_0^t W_r \cos(w_1 r - w_1 t) dr + \eta(t) + \frac{1}{2} x_0^2 y_0 = 0,\end{aligned}\tag{3.40}$$

which is just a quadratic in y_0 and is shown in Figure 3.35. We may eliminate the variables in x_0 and y_0 to find the wavefront, but the result is far too untidy to be worth expressing here, and is shown in Figure 3.36.

Comparing the pre-caustic and the pre-wavefront, we see that they meet in a pair of points, which may be calculated numerically as $(0.955925, 0.871896)$ and $(12.3625, -6.34649)$. The caustic and wavefront meet at 2 points which we can determine numerically to be $(-40.2566, 9.87755)$ and $(0.540013, -0.84164)$.

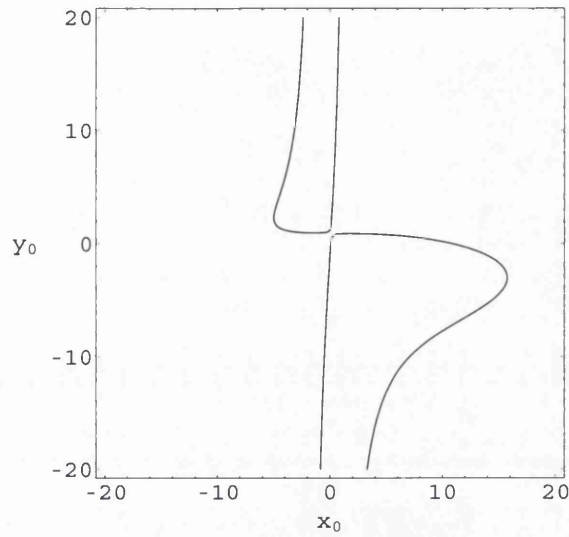


Figure 3.35: Harmonic oscillator pre-wavefront for $S_0 = \frac{1}{2}x_0^2y_0$ with $w_1 = 2$, $w_2 = 3$ and noise.

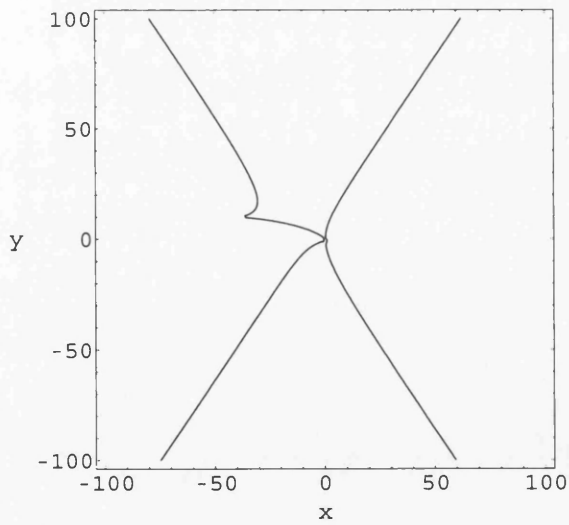


Figure 3.36: Harmonic oscillator wavefront for $S_0 = \frac{1}{2}x_0^2y_0$ with $w_1 = 2$, $w_2 = 3$ and noise.

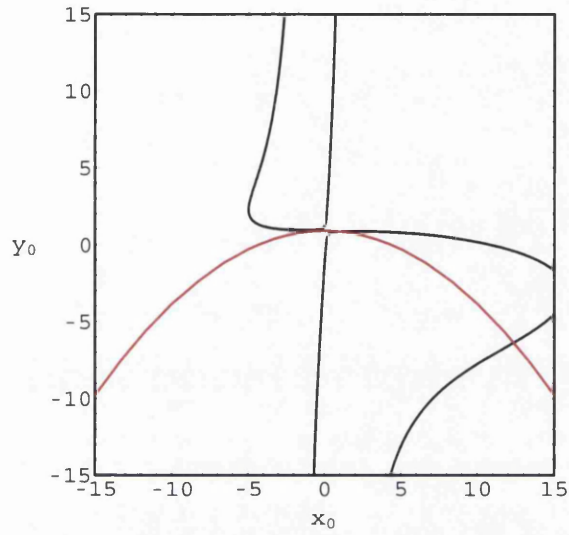


Figure 3.37: Harmonic oscillator pre-caustic and pre-wavefront for $S_0 = \frac{1}{2}x_0^2y_0$ with $w_1 = 2$, $w_2 = 3$ and noise.

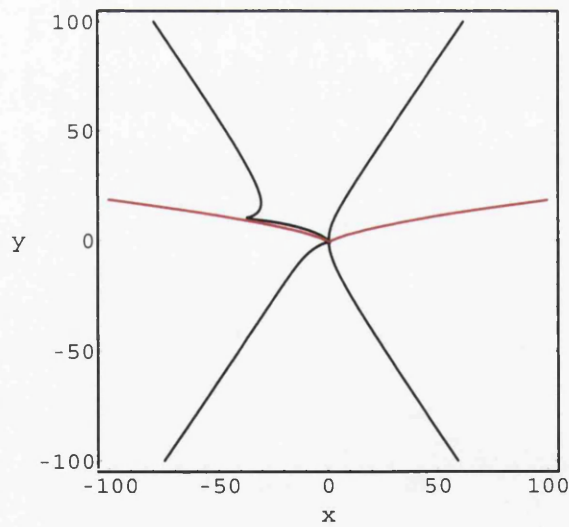


Figure 3.38: Harmonic oscillator caustic and wavefront for $S_0 = \frac{1}{2}x_0^2y_0$ with $w_1 = 2$, $w_2 = 3$ and noise.

Chapter 4

Butterfly and Fish

We give some explicit examples of the singularities of the heat and Burgers' equations for the initial condition $S_0(\underline{x}_0) = x_0^3 y_0 + x_0^2 z_0$, with and without noise terms. We do so for the cases of the zero potential $V(\underline{x}) = 0$, the linear potential $V(\underline{x}) = -kx$ and the harmonic oscillator potential $V(\underline{x}) = -\frac{1}{2}(w_1^2 x^2 + w_2^2 y^2 + w_3^2 z^2)$.

4.1 Classical Case

In this section we discuss the singularities of the classical heat and Burgers' equations for the case's of the above potentials. We shall see that, for this three dimensional example, the generic caustic is that of the butterfly catastrophe as covered in [3]. The introduction of the aforementioned potential terms does little to effect the overall geometry of the butterfly.

4.1.1 Zero Potential

For the case of the butterfly caustic the polynomial phase function is determined by taking $S_0(\underline{x}_0) = x_0^3 y_0 + x_0^2 z_0$. Then the pre-caustic for the Burgers' equation is given by

$$\begin{vmatrix} 1 + 6tx_0 y_0 + 2tz_0 & 3tx_0^2 & 2tx_0 \\ 3tx_0^2 & 1 & 0 \\ 2tx_0 & 0 & 1 \end{vmatrix} = 0,$$

so that we have

$$1 + 6tx_0 y_0 + 2tz_0 - 9t^2 x_0^4 - 4t^2 x_0^2 = 0.$$

By rearranging for $z_0 = z_0(x_0, y_0, t)$ we have the pre-caustic as

$$z_0 = \frac{9}{2}tx_0^4 + 2tx_0^2 - 3x_0 y_0 - \frac{1}{2t}, \quad (4.1)$$

and, for some $t > 0$, this looks like as in Figure 4.1. It is useful, as we shall see later, to look at several slices along the y_0 -axis of the pre-caustic, as in Figure 4.2, where

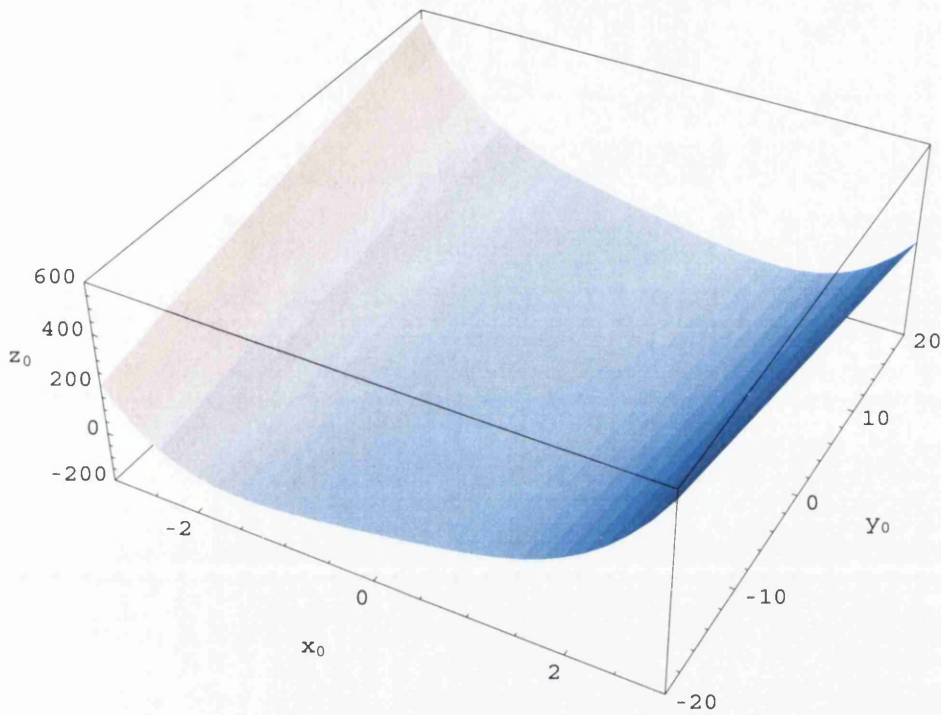


Figure 4.1: Zero potential pre-caustic for $S_0 = x_0^3 y_0 + x_0^2 z_0$.

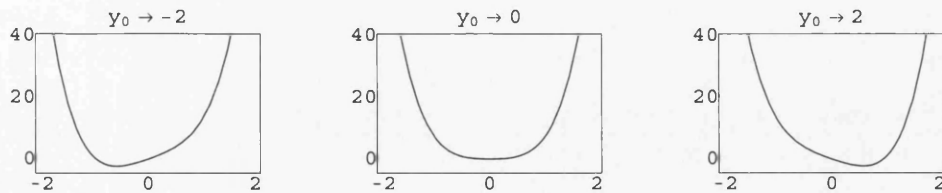


Figure 4.2: Slices of the zero potential pre-caustic for $S_0 = x_0^3 y_0 + x_0^2 z_0$.

we have taken slices through $y_0 = -2, 0, 2$. One question to ask here is ‘What about the big picture?’. Well, we can show that the pre-caustic has only one ‘valley’, i.e. path of points of minima. Simple calculus tells us that the critical points occur when $\frac{\partial z_0}{\partial x_0} = 0$, i.e. when

$$\frac{\partial z_0}{\partial x_0} = 18tx_0^3 + 4tx_0 - 3y_0 = 0.$$

This gives us the path that the critical points lie on

$$y_0 = \frac{2}{3}tx_0(9x_0^2 + 2).$$

We are really interested in the nature of these critical points, so we need to look at how $\frac{\partial z_0}{\partial x_0}$ changes, i.e. we need to look at the second derivative

$$\frac{\partial^2 z_0}{\partial x_0^2} = 54tx_0^2 + 4t.$$

Then clearly, since $t > 0$ and $x_0 \in \mathbb{R}$, we have $\frac{\partial^2 z_0}{\partial x_0^2} > 0$. This shows that the region for which

$$z_0 \geq \frac{9}{2}tx_0^4 + 2tx_0^2 - 3x_0y_0 - \frac{1}{2t},$$

is convex. Hence there can be only one path of critical points, which is our valley. Next we want to find an expression for the caustic. Remember that we have phase function

$$\phi(\underline{x}, \underline{x}_0, t) = \frac{(x - x_0)^2}{2t} + \frac{(y - y_0)^2}{2t} + \frac{(z - z_0)^2}{2t} + x_0^3 y_0 + x_0^2 z_0.$$

Then setting $\nabla_{\underline{x}_0} \phi(\underline{x}, \underline{x}_0, t) = 0$ gives us

$$z_0 = z - tx_0^2, \quad \text{and} \quad y_0 = y - tx_0^3.$$

Using these to do the z_0 and y_0 integrals by Laplace gives us the phase function as

$$\tilde{\phi}(\underline{x}, \underline{x}_0, t) = -\frac{t}{2}x_0^6 - \frac{t}{2}x_0^4 + yx_0^3 + \left(z + \frac{1}{2t}\right)x_0^2 - \frac{x}{t}x_0 + \frac{x^2}{2t},$$

and looking at the solution to the heat equation, we have

$$u(\underline{x}, t) \simeq \frac{1}{(2\pi\mu^2 t)^{\frac{3}{2}}} \int_{\mathbb{R}} T_0(x_0) e^{Ax_0^6 + Bx_0^4 + Cx_0^3 + Dx_0^2 + Ex_0 + F} dx_0,$$

where we have a convergence factor $T_0(x_0)$ and

$$\begin{aligned} A &= \frac{t}{2\mu^2}, & B &= \frac{t}{2\mu^2}, & C &= -\frac{y}{\mu^2}, \\ D &= -\frac{1}{\mu^2} \left(z + \frac{1}{2t}\right), & E &= \frac{x}{\mu^2 t}, & F &= -\frac{x^2}{2\mu^2 t}. \end{aligned}$$

The avid reader will of course notice that this is the canonical form of the butterfly catastrophe, as discussed in [3], a distinctive polynomial of order 6 with no quintic term. Next, recall that we also need $\frac{\partial\phi}{\partial x_0} = 0$, such that

$$\frac{\partial\phi}{\partial x_0} = -3tx_0^5 - 2tx_0^3 + 3yx_0^2 + 2\left(z + \frac{1}{2t}\right)x_0 - \frac{x}{t} = 0,$$

and secondly we need $\frac{\partial^2\phi}{\partial x_0^2} = 0$, i.e.

$$\frac{\partial^2\phi}{\partial x_0^2} = -15tx_0^4 - 6tx_0^2 + 6yx_0 + 2\left(z + \frac{1}{2t}\right) = 0.$$

Solving these simultaneously gives us an implicit equation for the caustic, i.e.

$$\begin{aligned} & \frac{64375}{t^5}x^4 + 202500\frac{y}{t^4}x^3 \\ & + \frac{18}{t}\left[192 + 4900\frac{y^2}{t^2} + \frac{75}{t}\left(16 - 135\frac{y^2}{t^2}\right)\left(\frac{1}{t} + 2z\right) + \frac{2009}{t^2}\left(\frac{1}{t} + 2z\right)^2\right]x^2 \\ & - \frac{36y}{t}\left[16\frac{y^2}{t} + 2187\frac{y^4}{t^3} + 3\left(32 + 965\frac{y^2}{t^2}\right)\left(\frac{1}{t} + 2z\right) \right. \\ & \quad \left. + \frac{560}{t}\left(\frac{1}{t} + 2z\right)^2 + \frac{1200}{t^2}\left(\frac{1}{t} + 2z\right)^3\right]x \\ & - \left(\frac{1}{t} + 2z\right)^2\left[288\frac{y^2}{t} + 6561\frac{y^4}{t^3} + 32\left(8 + 243\frac{y^2}{t^2}\right)\left(\frac{1}{t} + 2z\right) \right. \\ & \quad \left. + \frac{1536}{t}\left(\frac{1}{t} + 2z\right)^2 + \frac{2304}{t^2}\left(\frac{1}{t} + 2z\right)^3\right] = 0. \end{aligned} \quad (4.2)$$

This is the butterfly catastrophe, classified by Thom's catastrophe theory as detailed in [3], and shown in Figure 4.3 at an instance of time $t > 0$. In Figure 4.4 we look at several slices along the y -axis of the caustic, where we have taken slices through $y = -2, 0, 2$. Notice the similarities of the pre-caustic and caustic in this case with the results that we obtained in the earlier chapter when we considered the cusp singularity. Going back to the heat equation, we see that the pre-wavefront is given by equation (2.16) with $S_0(\underline{x}_0) = x_0^3y_0 + x_0^2z_0$ as

$$\frac{t}{2}\left[(3x_0^2y_0 + 2x_0z_0)^2 + (x_0^3)^2 + (x_0^2)^2\right] + x_0^3y_0 + x_0^2z_0 = 0.$$

We can simplify this to get the implicit equation of the pre-wavefront as

$$x_0^2\left(\frac{t}{2}x_0^4 + \frac{t}{2}x_0^2 + \frac{9}{2}tx_0^2y_0^2 + 6tx_0y_0z_0 + x_0y_0 + 2tz_0^2 + z_0\right) = 0, \quad (4.3)$$

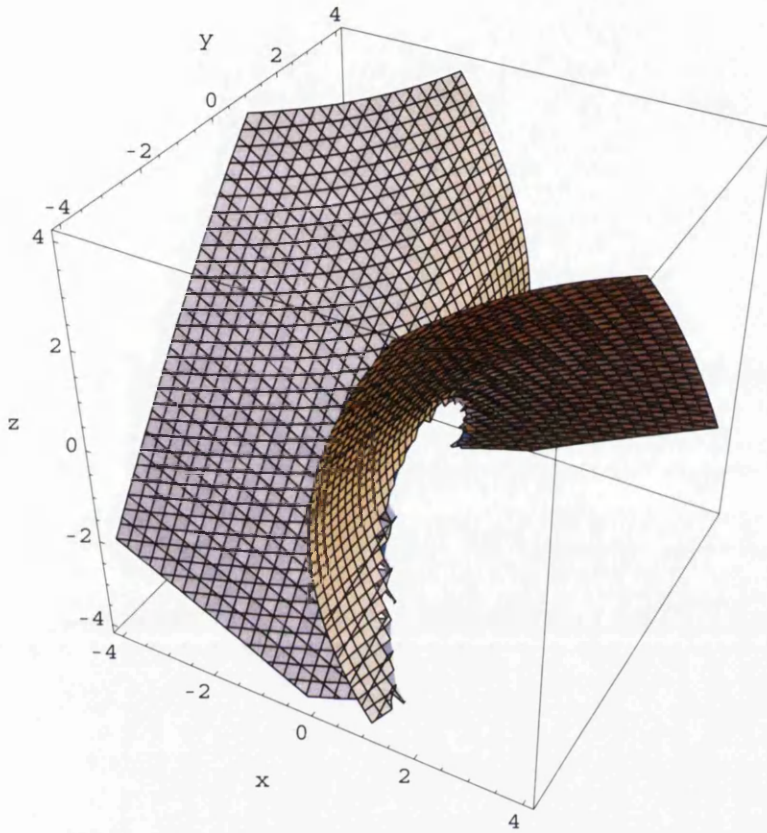


Figure 4.3: Zero potential caustic for $S_0 = x_0^3 y_0 + x_0^2 z_0$.

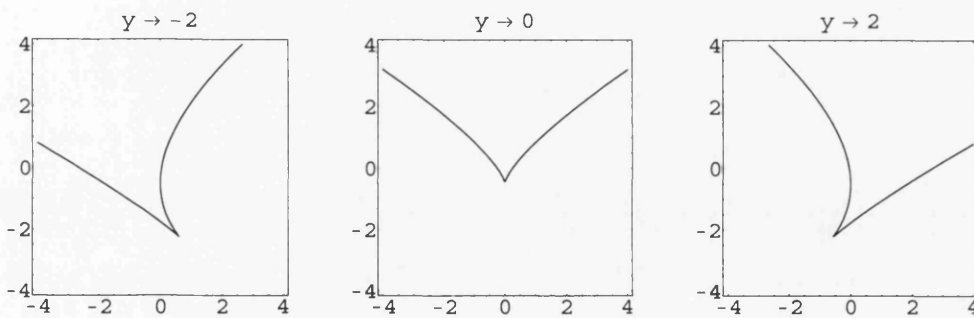


Figure 4.4: Slices of the zero potential caustic for $S_0 = x_0^3 y_0 + x_0^2 z_0$.

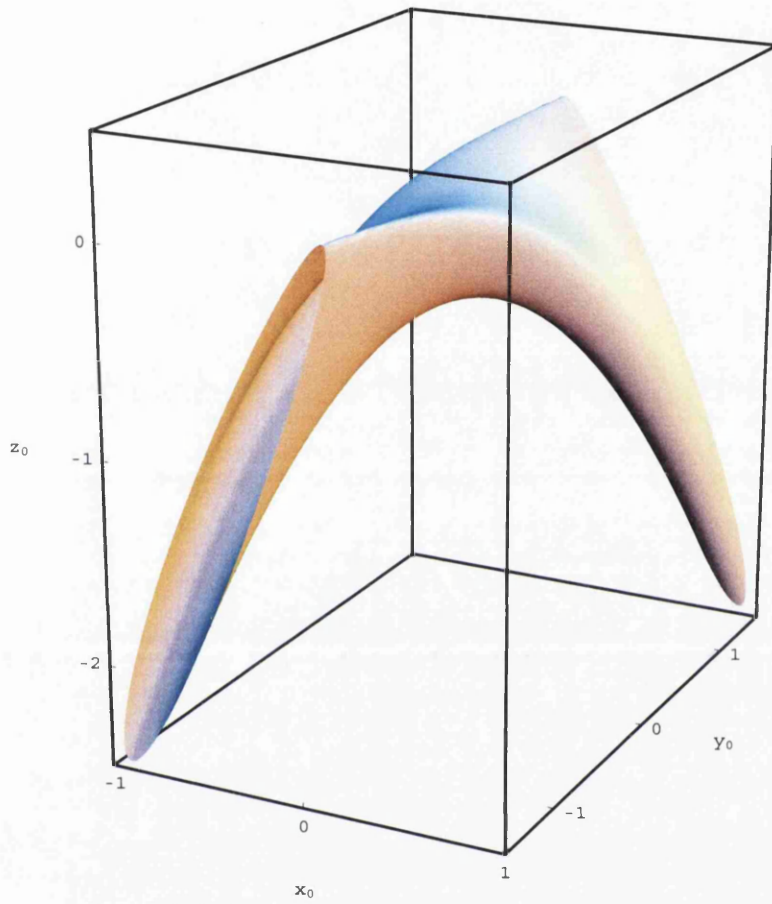


Figure 4.5: Zero potential pre-wavefront for $S_0 = x_0^3 y_0 + x_0^2 z_0$.

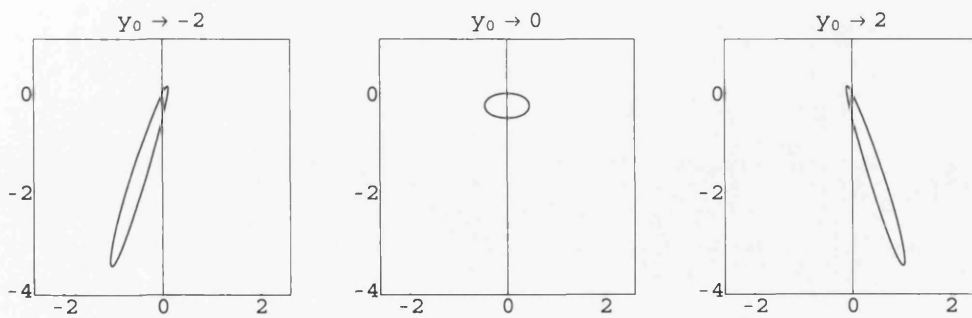


Figure 4.6: Slices of the zero potential pre-wavefront for $S_0 = x_0^3 y_0 + x_0^2 z_0$.

which is the plane $x_0 = 0$ and the surface generated by

$$\frac{t}{2}x_0^4 + \frac{t}{2}x_0^2 + \frac{9}{2}tx_0^2y_0^2 + 6tx_0y_0z_0 + x_0y_0 + 2tz_0^2 + z_0 = 0.$$

For some time $t > 0$, the pre-wavefront is illustrated in Figure 4.5, and Figure 4.6 shows slices of this with respect to the y_0 -axis. It is interesting to see that the slice through $y_0 = 0$ gives us a semi-quadratic ellipse in x_0 and z_0 , i.e.

$$x_0^2 \left(\frac{t}{2}x_0^4 + \frac{t}{2}x_0^2 + 2tz_0^2 + z_0 \right) = 0,$$

or

$$x_0^2 \left[\frac{(x_0^2 + \frac{1}{2})^2}{(\frac{2}{t})} + \frac{(z_0 + \frac{1}{4t})^2}{(\frac{1}{2t})} - \frac{1}{8} \left(t + \frac{1}{t} \right) \right] = 0.$$

The semi-quadratic ellipse has centre at the point $(0, -\frac{1}{4t})$ with semi-major axis $\frac{1}{\sqrt{2}} \left(\sqrt{1 + \frac{1}{t^2}} - 1 \right)^{\frac{1}{2}}$ and semi-minor axis $\frac{1}{4t}$. Also, we see from the above that, for non-zero values of y_0 , we have distorted ellipse-like shapes tending to the left for $y_0 < 0$ and to the right for $y_0 > 0$.

We cannot calculate the wavefront for the heat equation in the usual way, i.e. by solving $\phi(\underline{x}, \underline{x}_0, t) = 0$ and $\nabla_{\underline{x}_0} \phi(\underline{x}, \underline{x}_0, t) = 0$ simultaneously. In order to do so would involve solving a quintic in x_0 and substituting the real solution into a sixth order polynomial in x_0 . Needless to say, this is very difficult to do, but there is another way to plot the wavefront given that we can already plot the pre-wavefront.

We need to look at the points that make up the surface of the pre-wavefront and subject each point to the classical mechanical flow given by the mapping

$$\underline{x} = \underline{x}_0 + t \nabla_{\underline{x}_0} S_0(\underline{x}_0).$$

This comes directly from $\nabla_{\underline{x}_0} \phi(\underline{x}, \underline{x}_0, t) = 0$, so we have the classical mechanical flow as

$$\begin{pmatrix} x \\ y \\ z \end{pmatrix} = \begin{pmatrix} x_0 \\ y_0 \\ z_0 \end{pmatrix} + t \begin{pmatrix} 3x_0^2y_0 + 2x_0z_0 \\ x_0^3 \\ x_0^2 \end{pmatrix}. \quad (4.4)$$

Doing this produces the wavefront of the heat equation for $S_0(\underline{x}_0) = x_0^3y_0 + x_0^2z_0$ as the fish, the twisted tricorn, see [16], or a twisted triple cusped hypo-cycloid, as in Figure 4.7. We can look at slices through the y -axis of this, then at $y = -2, 0, 2$ we have Figure 4.8.

Now compare the pre-caustic to the pre-wavefront. We can calculate the meeting curves of these, as shown in Figure 4.9, by using the pre-caustic (4.1) to eliminate z_0 from the pre-wavefront (4.3). This gives an implicit equation of the meeting curves in x_0 and y_0 . We can then numerically apply the pre-caustic (4.1) to obtain the meeting curves in \mathbb{R}^3 . Essentially we are formulating a vector $(x_0, y_0(x_0), z_0(y_0(x_0), x_0))$

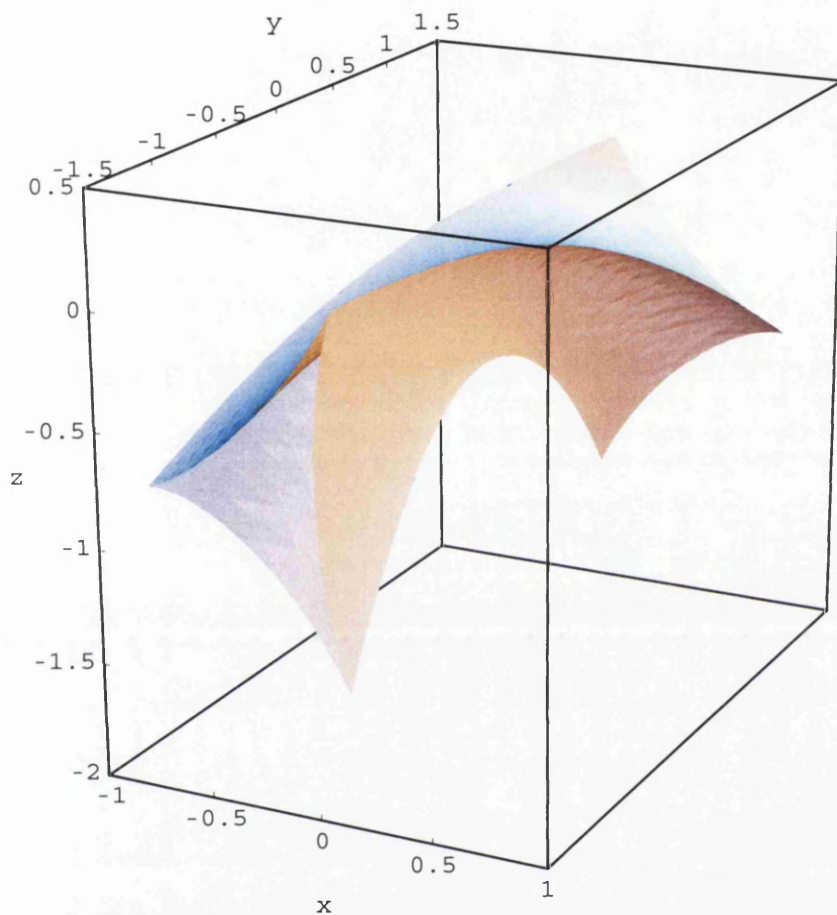


Figure 4.7: Zero potential wavefront for $S_0 = x_0^3 y_0 + x_0^2 z_0$.

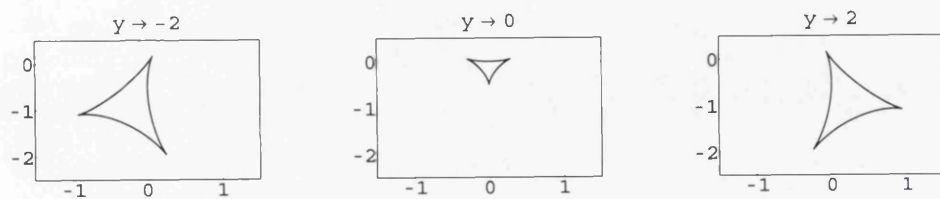


Figure 4.8: Slices of the zero potential wavefront for $S_0 = x_0^3 y_0 + x_0^2 z_0$.

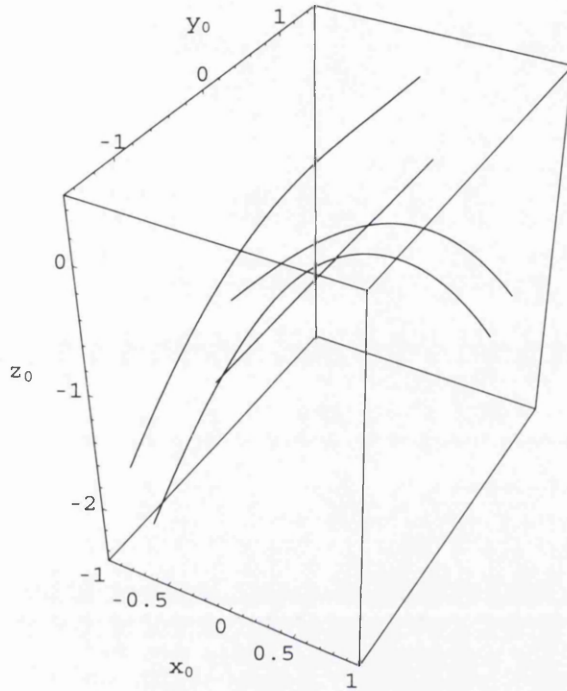


Figure 4.9: Meeting curves of the zero potential pre-caustic and pre-wavefront for $S_0 = x_0^3 y_0 + x_0^2 z_0$.

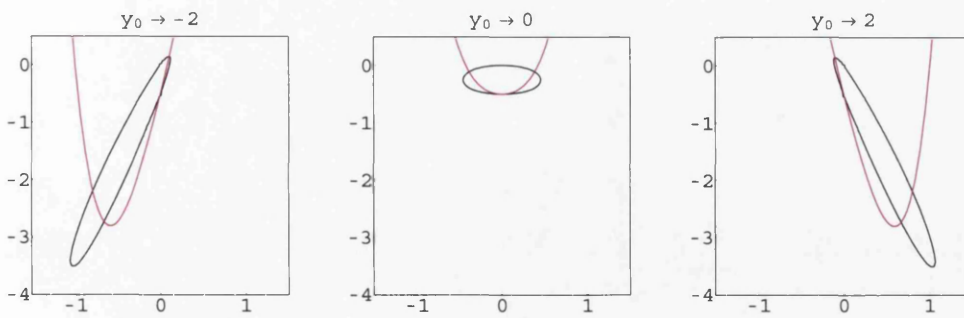


Figure 4.10: Slices of the zero potential pre-caustic and pre-wavefront for $S_0 = x_0^3 y_0 + x_0^2 z_0$.

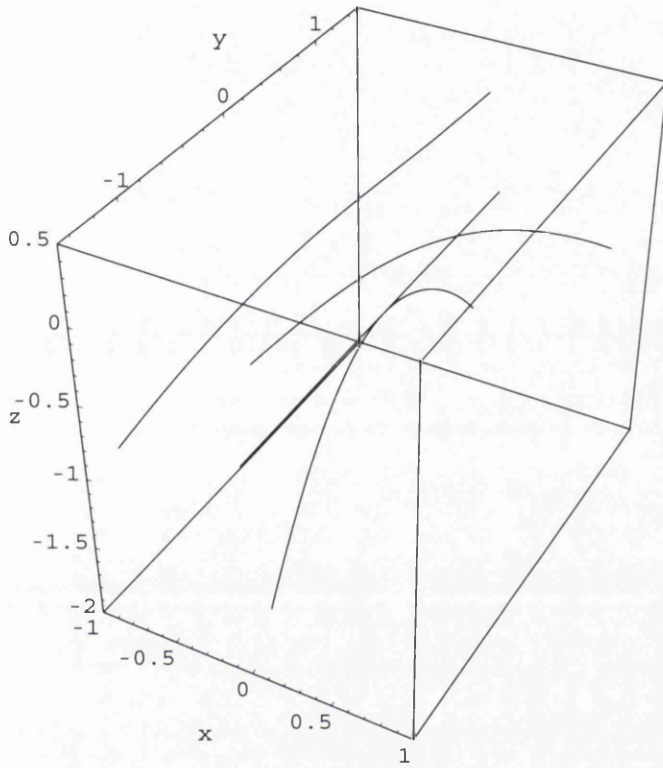


Figure 4.11: Meeting curves of the zero potential caustic and wavefront for $S_0 = x_0^3 y_0 + x_0^2 z_0$.

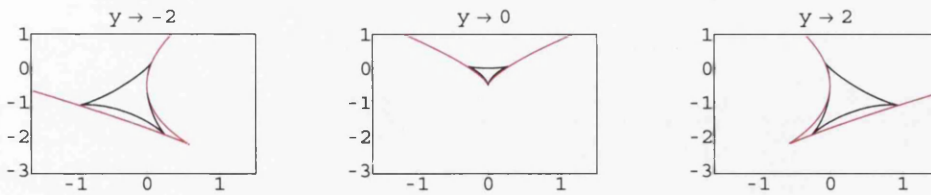


Figure 4.12: Slices of the zero potential caustic and wavefront for $S_0 = x_0^3 y_0 + x_0^2 z_0$.

for the meeting curves, but we are not solving directly for $y_0(x_0)$ which would give the curves explicitly. We can also compare the slices that we took earlier, as in Figure 4.10, which distinctively shows that they meet in four curves. By numerically applying the classical mechanical flow (4.4) to the meeting curves of the pre-caustic and pre-wavefront, Figure 4.9, we can show the meeting curves of the caustic and wavefront, see Figure 4.11. We have used the slices of the caustic and wavefront to further illustrate these meeting curves, as in Figure 4.12. Notice the similarities of this case to that of the Cusp and Tricorn case, especially in the case where $y_0 = y = 0$.

4.1.2 Linear Potential

We now look at the three dimensional heat equation with a linear potential in one direction only, i.e.

$$\frac{\partial u_t}{\partial t} = \frac{\mu^2}{2} \Delta u_t - \frac{Kx}{\mu^2} u_t, \quad (4.5)$$

where we have phase function given by

$$\phi(\underline{x}, \underline{x}_0, t) = \frac{(\underline{x} - \underline{x}_0)^2}{2t} + \frac{kt}{2}(x - x_0) - \frac{t^3 k^2}{24} + x_0^3 y_0 + x_0^2 z_0. \quad (4.6)$$

We can easily calculate the pre-caustic in this case as it is given by equation (2.23) as

$$z_0 = \frac{9}{2} t x_0^4 + 2t x_0^2 - 3x_0 y_0 - \frac{1}{2t}, \quad (4.7)$$

which is exactly the same as the zero potential pre-caustic, equation (4.1), as illustrated in Figures 4.1 and 4.2. The classical mechanical flow in this case is given by equation (2.22) as

$$\begin{pmatrix} x \\ y \\ z \end{pmatrix} = \begin{pmatrix} x_0 \\ y_0 \\ z_0 \end{pmatrix} + \frac{t^2}{2} \begin{pmatrix} k \\ 0 \\ 0 \end{pmatrix} + t \begin{pmatrix} 3x_0^2 y_0 2x_0 z_0 \\ x_0^3 \\ x_0^2 \\ 0 \end{pmatrix} \quad (4.8)$$

which gives the y_0 and z_0 minimas as

$$y_0 = y - t x_0^3 \quad \text{and} \quad z_0 = z - t x_0^2.$$

We can now use these to calculate the solution after doing the z_0 and y_0 integrals by the Laplace method. This gives our phase function as

$$\tilde{\phi}(\underline{x}, \underline{x}_0, t) = -\frac{t}{2} x_0^6 - \frac{t}{2} x_0^4 + y x_0^3 + \left(z + \frac{1}{2t}\right) x_0^2 + \left(\frac{t}{2} k - \frac{x}{t}\right) x_0 + \frac{x^2}{2t} + \frac{tk}{2} x - \frac{k^2 t^3}{24}, \quad (4.9)$$

which gives the solution of the heat equation as

$$u(\underline{x}, t) \simeq \frac{1}{(2\pi\mu^2 t)^{\frac{3}{2}}} \int_{\mathbb{R}} T_0(x_0) e^{Ax_0^6 + Bx_0^4 + Cx_0^3 + Dx_0^2 + Ex_0 + F} dx_0, \quad (4.10)$$



where we have a convergence factor $T_0(x_0)$ and

$$\begin{aligned} A &= \frac{t}{2\mu^2}, & B &= \frac{t}{2\mu^2}, & C &= -\frac{y}{\mu^2}, & D &= -\frac{1}{\mu^2} \left(z + \frac{1}{2t} \right), \\ E &= -\frac{1}{\mu^2} \left(\frac{t}{2}k - \frac{x}{t} \right), & F &= -\frac{1}{\mu^2} \left(\frac{x^2}{2t} + \frac{tk}{2}x - \frac{k^2 t^3}{24} \right). \end{aligned}$$

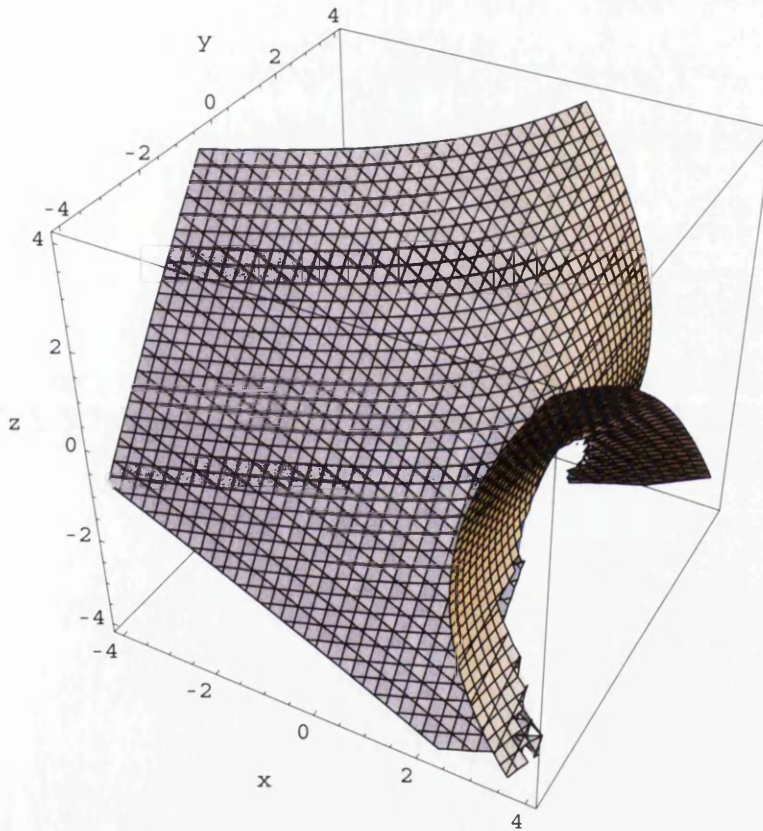


Figure 4.13: Linear potential caustic for $S_0 = x_0^3 y_0 + x_0^2 z_0$ with $k = 5$.

Notice that we still have the canonical form of the butterfly catastrophe. By eliminating x_0 from the phase function (4.8) and its first derivative with respect to x_0 we

can obtain the equation of the caustic as

$$\begin{aligned}
& \frac{1350000}{t^8} x^4 + \frac{540000}{t^6} \left(\frac{6y}{t} - 5k \right) x^3 \\
& + \frac{72}{t^4} \left\{ \frac{900}{t^2} \left[22 - \frac{45}{t} \left(2z - \frac{1}{t} \right) \right] y^2 - \frac{67500}{t} k y \right. \\
& \quad \left. + \left[28125k^2 + 768 + \frac{4800}{t} \left(2z - \frac{1}{t} \right) + \frac{8000}{t^2} \left(2z - \frac{1}{t} \right)^2 \right] \right\} x^2 \\
& - \frac{72}{t^2} \left\{ \frac{17496}{t^5} y^5 + \frac{24}{t^3} \left[32 + \frac{945}{t} \left(2z - \frac{1}{t} \right) \right] y^3 + 900 \frac{k}{t^2} \left[22 - \frac{45}{t} \left(2z - \frac{1}{t} \right) \right] y^2 \right. \\
& \quad - \frac{2}{t} \left[16875k^2 - \frac{384}{t} \left(2z - \frac{1}{t} \right) - \frac{2240}{t^2} \left(2z - \frac{1}{t} \right)^2 - \frac{4800}{t^3} \left(2z - \frac{1}{t} \right)^3 \right] y \\
& \quad \left. + k \left[9375k^2 + 768 + \frac{4800}{t} \left(2z - \frac{1}{t} \right) + \frac{8000}{t^2} \left(2z - \frac{1}{t} \right)^2 \right] \right\} x \\
& + 629856 \frac{k}{t^5} y^5 - \frac{104976}{t^6} \left(2z - \frac{1}{t} \right)^2 y^4 + 864 \frac{k}{t} \left[32 + \frac{945}{t} \left(2z - \frac{1}{t} \right) \right] y^3 \\
& + \frac{72}{t^2} \left[4950k^2 - 10125 \frac{k^2}{t} \left(2z - \frac{1}{t} \right) - \frac{64}{t^2} \left(2z - \frac{1}{t} \right)^2 - \frac{1728}{t^3} \left(2z - \frac{1}{t} \right)^3 \right] y^2 \\
& + 84375k^4 + 13824k^2 + 86400 \frac{k^2}{t} \left(2z - \frac{1}{t} \right) + 144000 \frac{k^2}{t^2} \left(2z - \frac{1}{t} \right)^2 - \frac{4096}{t^3} \left(2z - \frac{1}{t} \right)^3 \\
& \quad - \frac{24576}{t^4} \left(2z - \frac{1}{t} \right)^4 - \frac{36864}{t^5} \left(2z - \frac{1}{t} \right)^5 = 0 \quad (4.11)
\end{aligned}$$

which is just the zero potential caustic being displaced in the x direction by the linear potential, as depicted in Figure 4.13.

Simplifying equation (2.24) for our linear potential $\underline{K} = (k, 0, 0)$ with initial condition $S_0(\underline{x}_0) = x_0^3 y_0 + x_0^2 z_0$, we have the equation of the pre-wavefront as

$$\begin{aligned}
& + \frac{t}{2} x_0^6 + \frac{t}{2} (1 + 9y_0^2) x_0^4 + y_0 (1 + 6tz_0) x_0^3 \\
& + (3kt^2 y_0 + 2tz_0^2 + z_0) x_0^2 + kt^2 \left(z_0 + \frac{1}{t} \right) x_0 + \frac{k^2 t^3}{3} = 0 \quad (4.12)
\end{aligned}$$

The pre-wavefront in this case is shown in Figure 4.14 with slices of the pre-wavefront illustrated in Figure 4.15. In order to calculate the wavefront in this case we must use the same numerical method as in the zero potential case, with classical mechanical flow given by equation (4.8). This numerically produces the wavefront as in Figure 4.16 with slices taken in Figure 4.17.

Comparing the pre-caustic to the pre-wavefront, we compute their meeting curves as shown in Figure 4.18. This is done by using the pre-caustic (4.7) to eliminate z_0 from the pre-wavefront (4.12), which gives an implicit equation of the meeting curves in x_0 and y_0 that we can then numerically apply the pre-caustic (4.7) to, yielding curves of intersection in \mathbb{R}^3 . By numerically applying the classical mechanical flow for the linear potential case (4.8), we show the meeting curves of the caustic and wavefront, see Figure 4.19. We can also compare the slices that we took earlier. For the pre-caustic and pre-wavefront, we have Figure 4.20, and for the caustic and wavefront we have Figure 4.21.

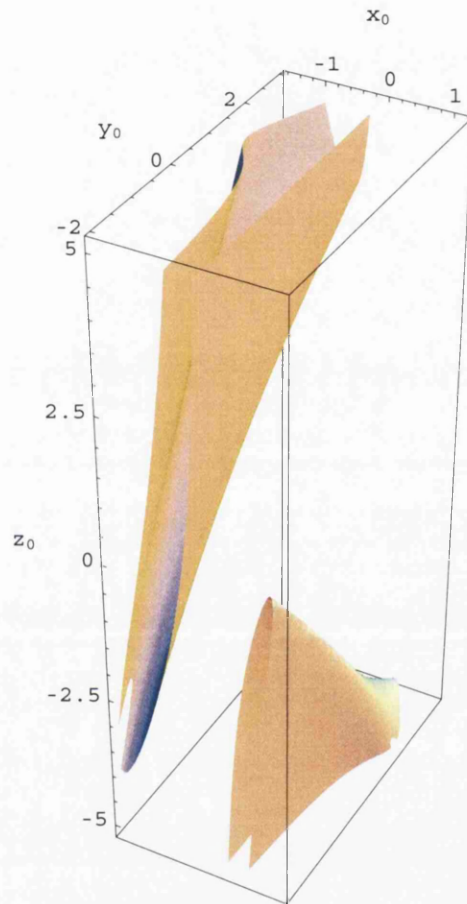


Figure 4.14: Linear potential pre-wavefront for $S_0 = x_0^3 y_0 + x_0^2 z_0$ with $k = 5$.

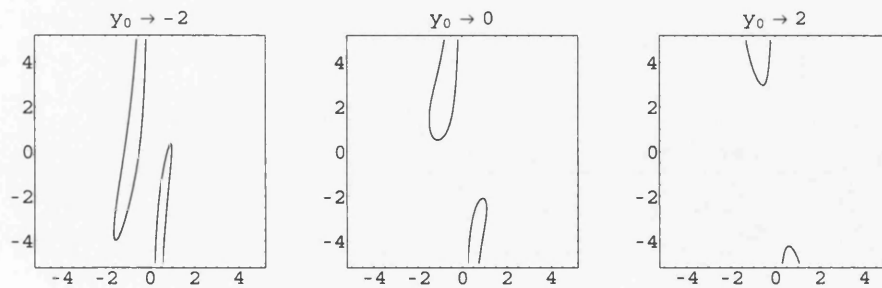


Figure 4.15: Slices of the linear potential pre-wavefront for $S_0 = x_0^3 y_0 + x_0^2 z_0$ with $k = 5$.

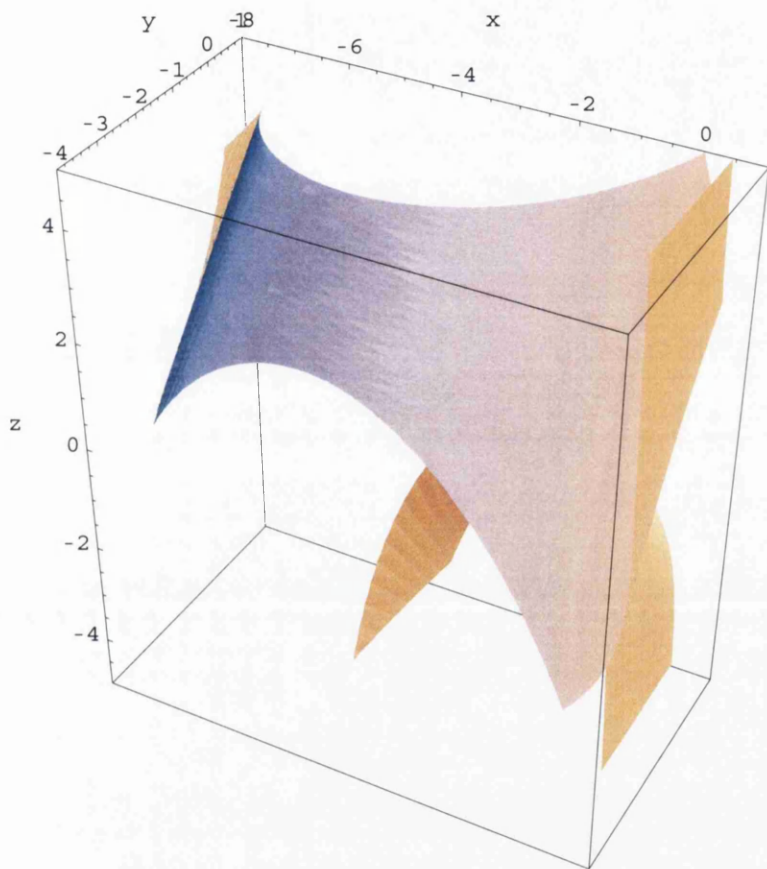


Figure 4.16: Linear potential wavefront for $S_0 = x_0^3 y_0 + x_0^2 z_0$ with $k = 5$.

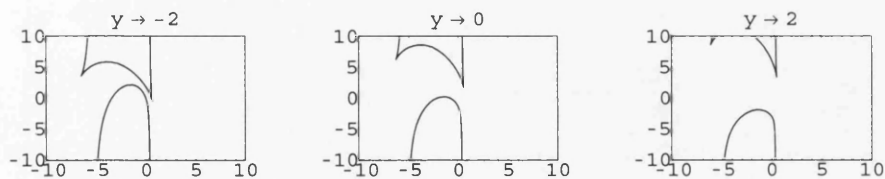


Figure 4.17: Slices of the linear potential wavefront for $S_0 = x_0^3 y_0 + x_0^2 z_0$ with $k = 5$.

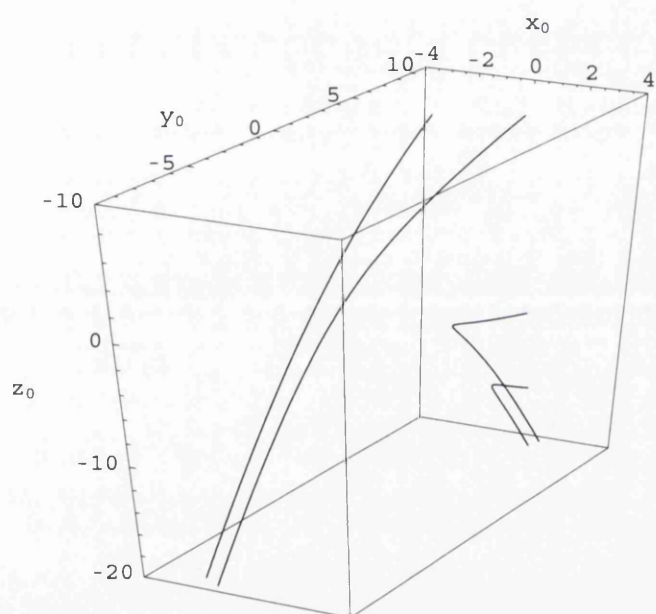


Figure 4.18: Meeting curves of the linear potential pre-caustic and pre-wavefront for $S_0 = x_0^3 y_0 + x_0^2 z_0$ with $k = 5$.

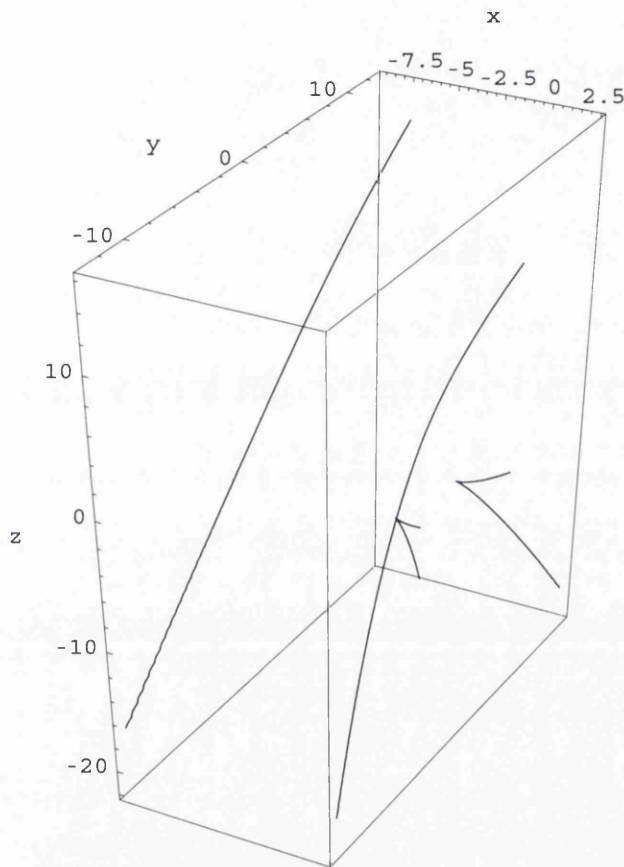


Figure 4.19: Meeting curves of the linear potential caustic and wavefront for $S_0 = x_0^3 y_0 + x_0^2 z_0$ with $k = 5$.

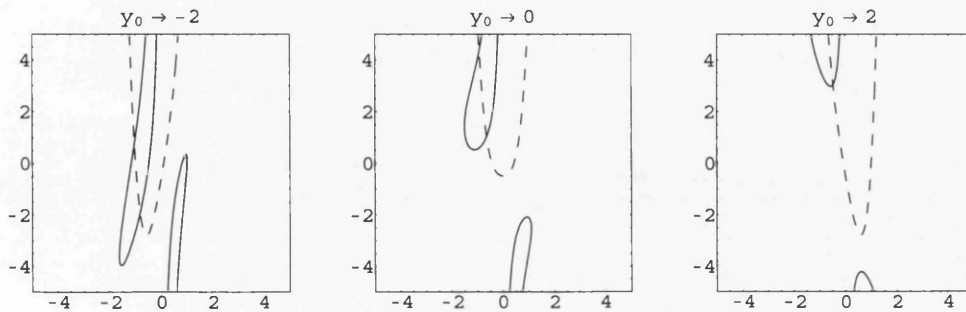


Figure 4.20: Slices of the linear potential pre-caustic and pre-wavefront for $S_0 = x_0^3 y_0 + x_0^2 z_0$ with $k = 5$.

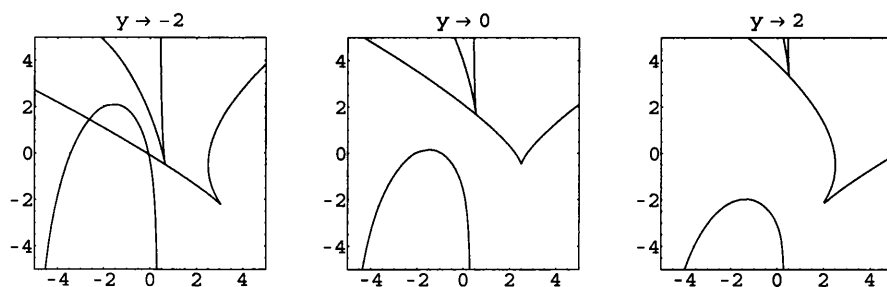


Figure 4.21: Slices of the linear potential caustic and wavefront for $S_0 = x_0^3 y_0 + x_0^2 z_0$ with $k = 5$.

4.1.3 Harmonic Oscillator Potential

In this case we are looking at the three dimensional heat equation with a harmonic oscillator potential, equation (2.27), where we have a phase function $\phi(\underline{x}, \underline{x}_0, t)$ given by equation (2.26) as

$$\begin{aligned} \phi(\underline{x}, \underline{x}_0, t) = & \frac{w_1}{2} \left(\frac{(x^2 + x_0^2) \cos(w_1 t) - 2xx_0}{\sin(w_1 t)} \right) + \frac{w_2}{2} \left(\frac{(y^2 + y_0^2) \cos(w_2 t) - 2yy_0}{\sin(w_2 t)} \right) \\ & + \frac{w_3}{2} \left(\frac{(z^2 + z_0^2) \cos(w_3 t) - 2zz_0}{\sin(w_3 t)} \right) + x_0^3 y_0 + x_0^2 z_0. \end{aligned}$$

We may calculate the pre-caustic as by using equation (2.30) to obtain an explicit form as

$$z_0 = \frac{9}{2} \frac{x_0^4}{w_2} \tan(w_2 t) + \frac{2x_0^2}{w_3} \tan(w_3 t) - \frac{w_1}{2 \tan(w_1 t)} - 3x_0 y_0. \quad (4.13)$$

However it is not possible to obtain an explicit form of the caustic and the wavefront. If we look at the phase function in this case, equation (2.28) with $S_0(\underline{x}_0) = x_0^3 y_0 + x_0^2 z_0$, then using the classical mechanical flow, equation (2.29) $\nabla_{\underline{x}_0} \phi = 0$, we see that

$$y_0 = \frac{y}{\cos(w_2 t)} - \frac{\tan(w_2 t)}{w_2} x_0^3, \quad \text{and} \quad z_0 = \frac{z}{\cos(w_3 t)} - \frac{\tan(w_3 t)}{w_3} x_0^2.$$

Now, by the Laplace method, see Section 1.4, we see that the phase function becomes

$$\begin{aligned} \tilde{\phi}(\underline{x}, \underline{x}_0, t) = & -\frac{\tan(w_2 t)}{2w_2} x_0^6 - \frac{\tan(w_3 t)}{2w_3} x_0^4 + \frac{y}{\cos(w_2 t)} x_0^3 \\ & + \left(\frac{z}{\cos(w_3 t)} + \frac{w_1}{2 \tan(w_1 t)} \right) x_0^2 - \frac{w_1 x}{\sin(w_1 t)} x_0 + \frac{w_1 x^2}{2 \tan(w_1 t)} \\ & - \frac{w_2 y^2 \tan(w_2 t)}{2} - \frac{w_3 z^2 \tan(w_3 t)}{2}. \end{aligned}$$

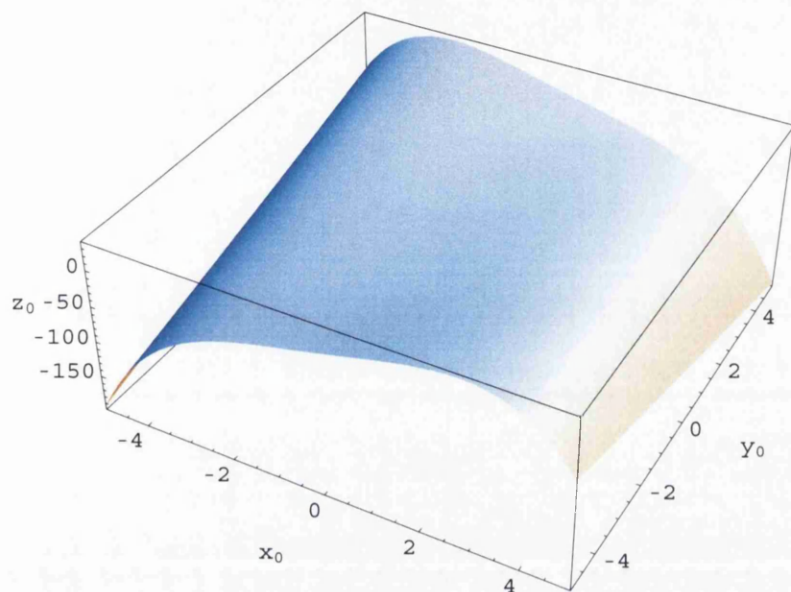


Figure 4.22: Harmonic oscillator potential pre-caustic for $S_0 = x_0^3 y_0 + x_0^2 z_0$ with $w_1 = 2$, $w_2 = 3$ and $w_3 = 4$.

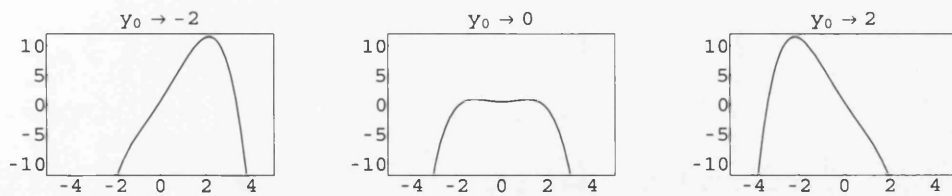


Figure 4.23: Slices of the harmonic oscillator potential pre-caustic for $S_0 = x_0^3 y_0 + x_0^2 z_0$ with $w_1 = 2$, $w_2 = 3$ and $w_3 = 4$.

This gives the solution of the heat equation as

$$u(\underline{x}, t) \simeq \frac{1}{(2\pi\mu^2)^{\frac{3}{2}}} \sqrt{\frac{w_1 w_2 w_3}{\sin(w_1 t) \sin(w_2 t) \sin(w_3 t)}} \int_{\mathbb{R}} T_0(x_0) e^{Ax_0^2 + Bx_0^4 + Cx_0^3 + Dx_0^2 + Ex_0 + F} dx_0, \quad (4.14)$$

where we have a convergence factor $T_0(x_0)$ and

$$\begin{aligned} A &= \frac{\tan(w_2 t)}{2w_2 \mu^2}, & B &= \frac{\tan(w_3 t)}{2w_3 \mu^2}, & C &= -\frac{y}{\mu^2 \cos(w_2 t)}, \\ D &= -\frac{1}{\mu^2} \left(\frac{z}{\cos(w_3 t)} + \frac{w_1}{2 \tan(w_1 t)} \right), & E &= \frac{w_1 x}{\mu^2 \sin(w_1 t)}, \\ F &= -\frac{w_1 x^2}{2\mu^2 \tan(w_1 t)} + \frac{w_2 y^2 \tan(w_2 t)}{2\mu^2} + \frac{w_3 z^2 \tan(w_3 t)}{2\mu^2}. \end{aligned}$$

Notice that the overall geometry of the butterfly catastrophe is still intact, i.e. we still have a polynomial of degree 6 with no quintic term. We can further eliminate the x_0 variable to obtain the implicit equation of the caustic as

$$\begin{aligned} 0 &= \frac{84375w_1^4 w_2^3}{\sin^4(w_1 t) \tan^3(w_2 t)} x^4 + \frac{202500w_1^3 w_2^4 \tan(w_3 t)}{w_3 \sin^3(w_1 t) \sin(w_2 t) \tan^3(w_2 t)} y x^3 \\ &+ \frac{18w_1^2 w_2^2}{\sin^2(w_1 t) \tan^2(w_2 t)} \left\{ -\frac{225w_2^2}{\sin^2(w_2 t)} \left[45 \left(\frac{2z}{\cos(w_1 t)} + \frac{w_1}{\tan(w_1 t)} \right) - \frac{22w_2 \tan^2(w_3 t)}{w_3^2 \tan(w_2 t)} \right] y^2 \right. \\ &\quad + \frac{16w_2^2 \tan(w_3 t)}{w_3 \tan^2(w_2 t)} \left[125 \left(\frac{2z}{\cos(w_1 t)} + \frac{w_1}{\tan(w_1 t)} \right)^2 \right. \\ &\quad \quad \left. \left. + \frac{75w_2 \tan^2(w_3 t)}{w_3^2 \tan(w_2 t)} \left(\frac{2z}{\cos(w_1 t)} + \frac{w_1}{\tan(w_1 t)} \right) + \frac{12w_2^2 \tan^4(w_3 t)}{w_3^2 \tan^2(w_2 t)} \right] \right\} x^2 \\ &- \frac{36w_1 w_2}{\sin(w_1 t) \sin(w_2 t)} \left\{ \frac{2187w_2^4}{\sin^4(w_2 t)} y^4 \right. \\ &\quad + \frac{3w_2^4 \tan(w_3 t)}{w_3 \sin^2(w_2 t) \tan^2(w_2 t)} \left[945 \left(\frac{2z}{\cos(w_1 t)} + \frac{w_1}{\tan(w_1 t)} \right) + \frac{32w_2 \tan^2(w_3 t)}{w_3^2 \tan(w_2 t)} \right] y^2 \\ &\quad + \frac{16w_2^3}{\tan^3(w_2 t)} \left(\frac{2z}{\cos(w_1 t)} + \frac{w_1}{\tan(w_1 t)} \right) \left[75 \left(\frac{2z}{\cos(w_1 t)} + \frac{w_1}{\tan(w_1 t)} \right)^2 \right. \\ &\quad \quad \left. \left. + \frac{35w_2 \tan^2(w_3 t)}{w_3^2 \tan(w_2 t)} \left(\frac{2z}{\cos(w_1 t)} + \frac{w_1}{\tan(w_1 t)} \right) + \frac{6w_2^2 \tan^4(w_3 t)}{w_3^4 \tan^2(w_2 t)} \right] \right\} y x \\ &- \frac{w_2}{\tan(w_2 t)} \left(\frac{2z}{\cos(w_1 t)} + \frac{w_1}{\tan(w_1 t)} \right)^2 \left\{ \frac{6561w_2^4}{\sin^4(w_2 t)} y^4 \right. \\ &\quad + \frac{288w_2^4}{\sin^2(w_2 t) \tan^2(w_2 t)} \left[27 \left(\frac{2z}{\cos(w_1 t)} + \frac{w_1}{\tan(w_1 t)} \right) + \frac{w_2 \tan^2(w_3 t)}{w_3^2 \tan(w_2 t)} \right] y^2 \\ &\quad \left. \left. + \frac{256w_2^3}{\tan^3(w_2 t)} \left(\frac{2z}{\cos(w_1 t)} + \frac{w_1}{\tan(w_1 t)} \right) \left[3 \left(\frac{2z}{\cos(w_1 t)} + \frac{w_1}{\tan(w_1 t)} \right) + \frac{w_2 \tan^2(w_3 t)}{w_3^2 \tan(w_2 t)} \right]^2 \right\}. \quad (4.15) \end{aligned}$$

This is illustrated in Figure 4.24 and slices are also taken in Figure 4.25. Again, care has been taken in choosing $t < \frac{\pi}{\max(w_i)}$. Recall that equation (2.31) gives the equation

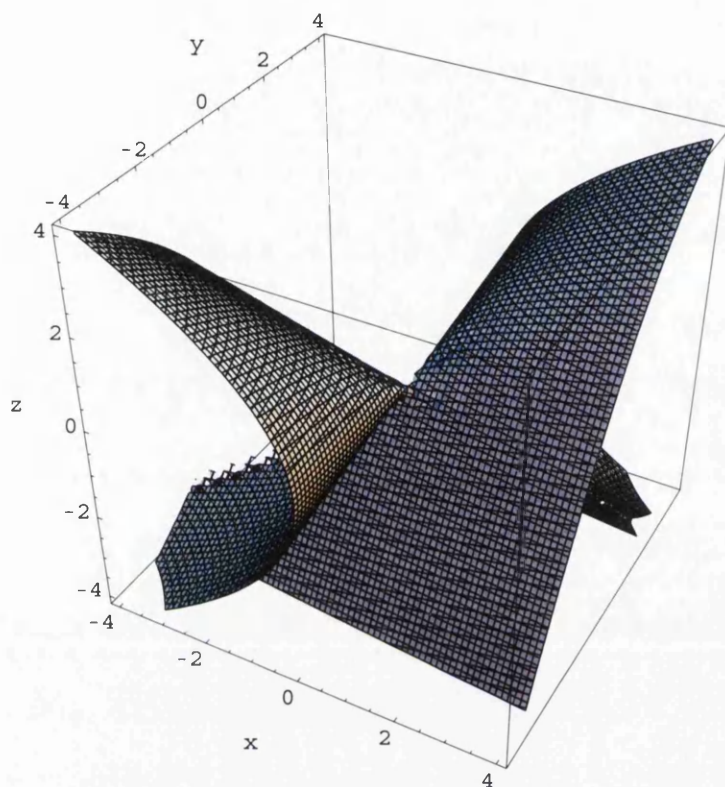


Figure 4.24: Harmonic oscillator potential caustic for $S_0 = x_0^3 y_0 + x_0^2 z_0$ with $w_1 = 2$, $w_2 = 3$ and $w_3 = 4$.

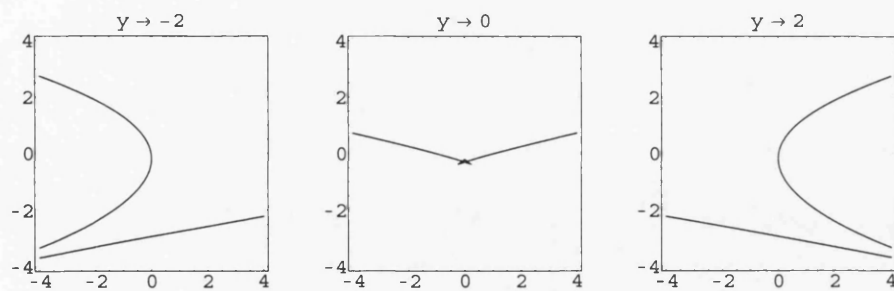


Figure 4.25: Slices of the harmonic oscillator potential caustic for $S_0 = x_0^3 y_0 + x_0^2 z_0$ with $w_1 = 2$, $w_2 = 3$ and $w_3 = 4$.

of the pre-wavefront, which for our $S_0(\underline{x}) = x_0^3 y_0 + x_0^2 z_0$ just turns out to be

$$\begin{aligned}
& \frac{w_1}{2 \sin(w_1 t)} \left\{ \left[\left(x_0 \cos(w_1 t) + \frac{\sin(w_1 t)}{w_1} (3x_0^2 y_0 + 2x_0 z_0) \right)^2 + x_0^2 \right] \cos(w_1 t) \right. \\
& \quad \left. - 2 \left(x_0 \cos(w_1 t) + \frac{\sin(w_1 t)}{w_1} (3x_0^2 y_0 + 2x_0 z_0) \right) x_0 \right\} \\
& + \frac{w_2}{2 \sin(w_2 t)} \left\{ \left[\left(y_0 \cos(w_2 t) + \frac{\sin(w_2 t)}{w_2} x_0^3 \right)^2 + y_0^2 \right] \cos(w_2 t) \right. \\
& \quad \left. - 2 \left(y_0 \cos(w_2 t) + \frac{\sin(w_2 t)}{w_2} x_0^3 \right) y_0 \right\} \\
& + \frac{w_3}{2 \sin(w_3 t)} \left\{ \left[\left(z_0 \cos(w_3 t) + \frac{\sin(w_3 t)}{w_3} x_0^2 \right)^2 + z_0^2 \right] \cos(w_3 t) \right. \\
& \quad \left. - 2 \left(z_0 \cos(w_3 t) + \frac{\sin(w_3 t)}{w_3} x_0^2 \right) z_0 \right\} + x_0^3 y_0 + x_0^2 z_0 = 0.
\end{aligned} \tag{4.16}$$

The pre-wavefront is depicted in Figure 4.26 with slices through the y_0 -axis shown in Figure 4.27. Recall that in the zero potential case, Section 4.1.1, we could not calculate the wavefront directly. We have the same problem here, so we must numerically apply the classical mechanical flow

$$\begin{pmatrix} x \\ y \\ z \end{pmatrix} = \begin{pmatrix} x_0 \cos(w_1 t) \\ y_0 \cos(w_2 t) \\ z_0 \cos(w_3 t) \end{pmatrix} + \begin{pmatrix} \frac{\sin(w_1 t)}{w_1} (x_0^3 y_0 + x_0^2 z_0) \\ \frac{\sin(w_2 t)}{w_2} x_0^3 \\ \frac{\sin(w_3 t)}{w_3} x_0^2 \end{pmatrix}, \tag{4.17}$$

to the pre-wavefront. Then the wavefront is depicted in Figure 4.28 with slices through the y -axis shown in Figure 4.29.

Once again, we can calculate the meeting curves of the pre-caustic 4.22 and pre-wavefront 4.26 by eliminating the z_0 variable from equation (4.16) using (4.13). This gives an implicit equation for the meeting curves in x_0 and y_0 which we can numerically map into \mathbb{R}^3 by using the equation of the pre-caustic (4.13). The meeting curves are shown in Figure 4.30 and we have taken slices through these meeting curves, in Figure 4.31, to better illustrate their meeting points. Furthermore, to show the meeting curves of the caustic and wavefront we have numerically applied the classical mechanical flow, equation (4.17), to obtain Figure 4.32. We also compare the meeting points of the slices of the caustic and wavefront in Figure 4.33.

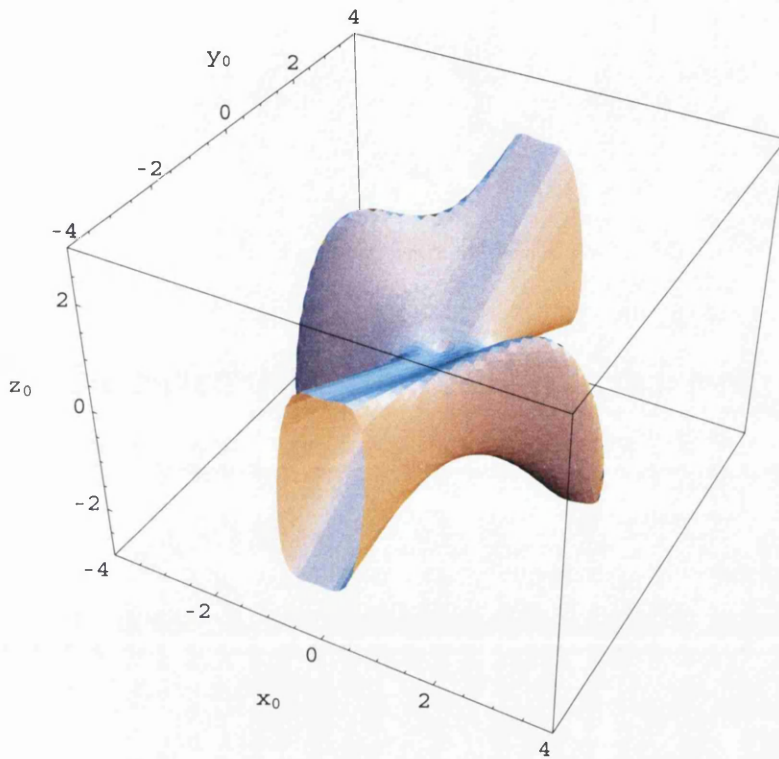


Figure 4.26: Harmonic oscillator pre-wavefront for $S_0 = x_0^3 y_0 + x_0^2 z_0$ with $w_1 = 2$, $w_2 = 3$ and $w_3 = 4$.

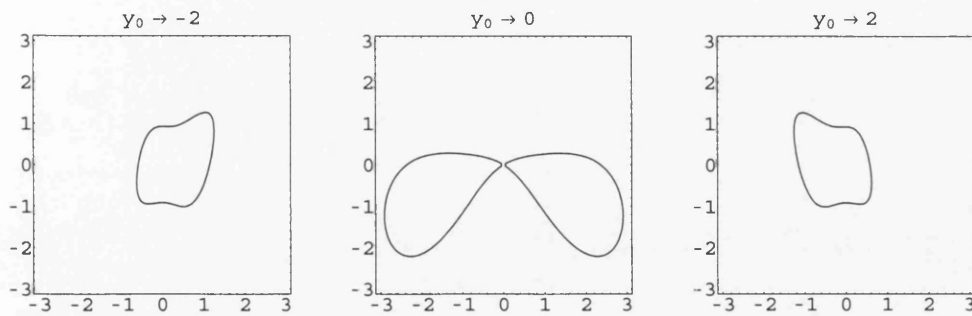


Figure 4.27: Slices of the harmonic oscillator pre-wavefront for $S_0 = x_0^3 y_0 + x_0^2 z_0$ with $w_1 = 2$, $w_2 = 3$ and $w_3 = 4$.

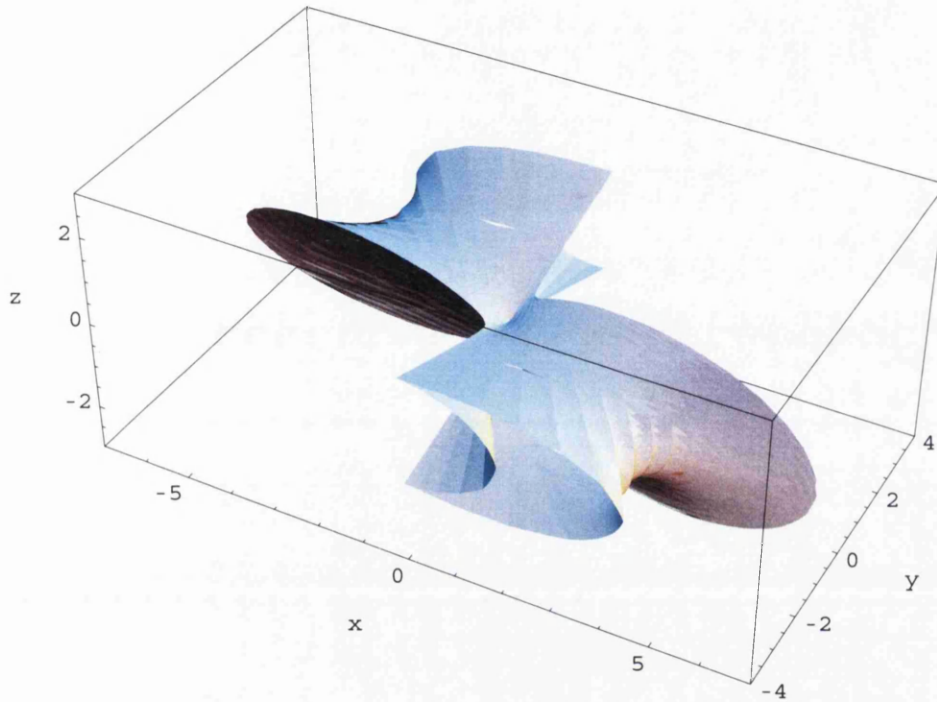


Figure 4.28: Harmonic oscillator potential wavefront for $S_0 = x_0^3 y_0 + x_0^2 z_0$ with $w_1 = 2$, $w_2 = 3$ and $w_3 = 4$.

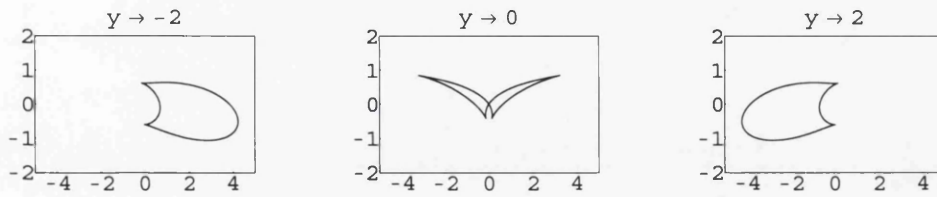


Figure 4.29: Slices of the harmonic oscillator potential wavefront for $S_0 = x_0^3 y_0 + x_0^2 z_0$ with $w_1 = 2$, $w_2 = 3$ and $w_3 = 4$.

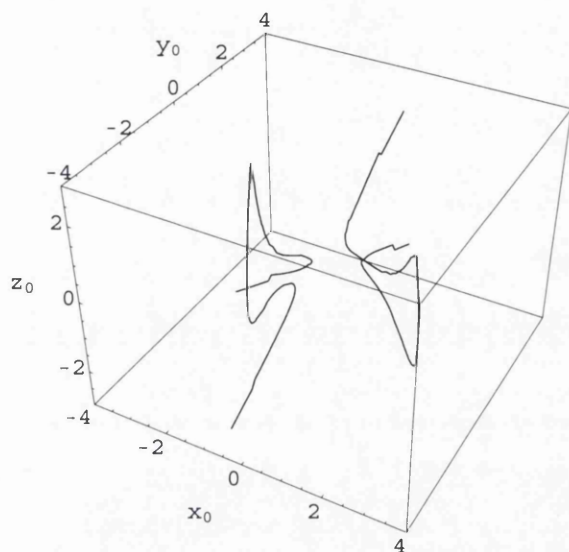


Figure 4.30: Meeting curves of the harmonic oscillator potential pre-caustic and pre-wavefront for $S_0 = x_0^3 y_0 + x_0^2 z_0$ with $w_1 = 2$, $w_2 = 3$ and $w_3 = 4$.

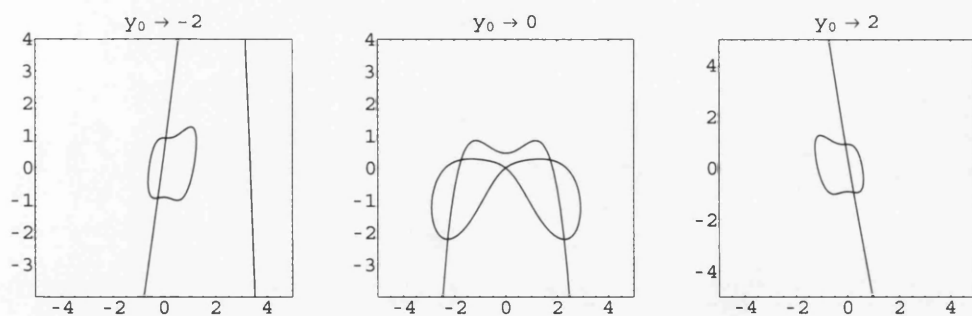


Figure 4.31: Slices of the harmonic oscillator potential pre-caustic and pre-wavefront for $S_0 = x_0^3 y_0 + x_0^2 z_0$ with $w_1 = 2$, $w_2 = 3$ and $w_3 = 4$.

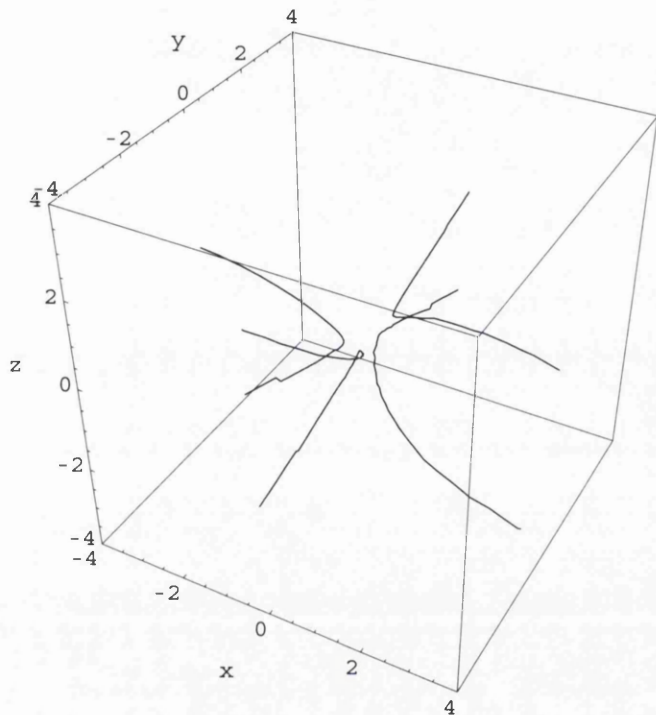


Figure 4.32: Meeting curves of the harmonic oscillator potential caustic and wavefront for $S_0 = x_0^3 y_0 + x_0^2 z_0$ with $w_1 = 2$, $w_2 = 3$ and $w_3 = 4$.

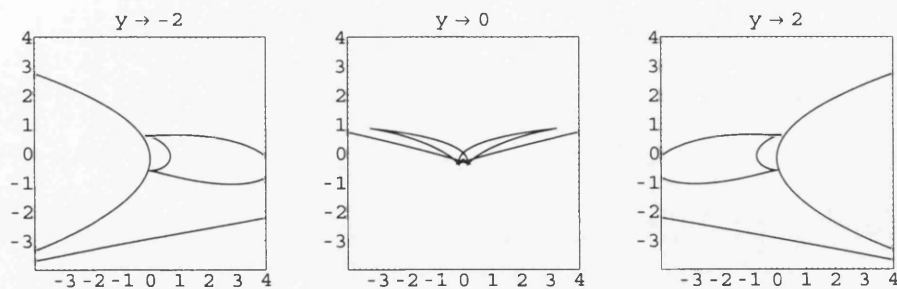


Figure 4.33: Slices of the harmonic oscillator potential caustic and wavefront for $S_0 = x_0^3 y_0 + x_0^2 z_0$ with $w_1 = 2$, $w_2 = 3$ and $w_3 = 4$.

4.2 Noisy Case

In similar fashion to Chapter 3, we now study the effects of a linear noise term $-\frac{x}{\mu^2}u \circ \partial W_t$ upon the Butterfly and Fish type singularities in the previous section. We provide an analysis and exact formulae for the singularities of the stochastic heat and Burgers' equations. We shall see that the addition of a noisy term doesn't effect the overall geometry of the Butterfly, and as expected, there is still no effect upon the pre-caustic curves.

4.2.1 Zero Potential

Looking at the case of $S_0(\underline{x}_0) = x_0^3 y_0 + x_0^2 z_0$, and this time adding the terms that arise from the addition of a linear noise term $-\frac{x}{\mu^2}u \circ \partial W_t$, as discussed in Section 2.3.1, gives us the phase function,

$$\begin{aligned} \phi(\underline{x}, \underline{x}_0, t) = & \frac{(x - x_0)^2}{2t} + \frac{(y - y_0)^2}{2t} + \frac{(z - z_0)^2}{2t} + xW_t \\ & - \frac{(x - x_0)}{t} \int_0^t W_s ds + \frac{\zeta(t)}{t} + x_0^3 y_0 + x_0^2 z_0. \end{aligned}$$

The pre-caustic in this case is exactly the same as that calculated in the case without noise, namely equation (4.1)

$$z_0 = \frac{9}{2}tx_0^4 + 2tx_0^2 - 3x_0y_0 - \frac{1}{2t}.$$

Naturally, its appearance is exactly as in Figure 4.1. By means of the previously discussed Laplace method, we can eliminate the y_0 and z_0 terms from the phase function, to obtain,

$$\begin{aligned} \phi(x, x_0, t) = & -\frac{t}{2}x_0^6 - \frac{t}{2}x_0^4 + yx_0^3 + \left(\frac{1}{2t} + z\right)x_0^2 + \frac{1}{t} \left(\int_0^t W_s ds - x\right)x_0 \\ & + \left(\frac{x^2}{2t} + xW_t - \frac{x}{t} \int_0^t W_s ds + \frac{\zeta(t)}{t}\right). \end{aligned}$$

Looking at the solution to the heat equation, we have

$$u(\underline{x}, t) \simeq \frac{1}{(2\pi\mu^2 t)^{\frac{3}{2}}} \int_{\mathbb{R}} T_0(x_0) e^{Ax_0^6 + Bx_0^4 + Cx_0^3 + Dx_0^2 + Ex_0 + F} dx_0,$$

where we have a convergence factor $T_0(x_0)$ and the obvious coefficients

$$\begin{aligned} A &= \frac{t}{2\mu^2}, & B &= \frac{t}{2\mu^2}, & C &= -\frac{y}{\mu^2}, \\ D &= -\frac{1}{\mu^2} \left(z + \frac{1}{2t}\right), & E &= -\frac{1}{\mu^2 t} \left(\int_0^t W_s ds - x\right), \\ F &= -\frac{1}{\mu^2} \left(\frac{x^2}{2t} + xW_t - \frac{x}{t} \int_0^t W_s ds + \frac{\zeta(t)}{t}\right). \end{aligned}$$

Of course, this is just the generic form of the cusp catastrophe, with a random displacement in the x direction. Eliminating the x_0 term gives us the equation of the caustic as

$$\begin{aligned}
& 84375 \left(x - \int_0^t W_s ds \right)^4 + 202500ty \left(x - \int_0^t W_s ds \right)^3 \\
& \quad + 18 \left\{ 225y^2 [22t^2 - 45(1 + 2tz)] + 192t^4 \right. \\
& \quad \quad \left. + 1200t^2(1 + 2tz) + 2000(1 + 2tz)^2 \right\} \left(x - \int_0^t W_s ds \right)^2 \\
& - 36 \frac{y}{t} \left\{ 2187t^2y^4 + 3t^2y^2 [32t^2 + 945(1 + 2tz)] \right. \\
& \quad \left. + 16(1 + 2tz) [6t^4 + 35t^2(1 + 2tz) + 75(1 + 2tz)^2] \right\} \left(x - \int_0^t W_s ds \right) \\
& \quad - \frac{(1 + 2tz)^2}{t^2} \left\{ 6561t^2y^4 + 288t^2y^2 [t^2 + 27(1 + 2tz)] \right. \\
& \quad \quad \left. + 256(1 + 2tz) [t^2 + 3(1 + 2tz)]^2 \right\} = 0,
\end{aligned}$$

and depicted in Figure 4.34. This is just the classical case of the butterfly displaced in the x -axis by the same random displacement as what we obtained in the previous section for the noisy cusp and tricorn. The random displacement is more evident when we look at the slices of this through the y -axis at $y = -2, 0, 2$, as shown in Figure 4.35.

Next recall that equation (2.37) gives us the form of the pre-wavefront for a general $S_0(x_0)$ such that for $S_0 = x_0^3y_0 + x_0^2z_0$ we have the pre-wavefront given by

$$\begin{aligned}
& \frac{t}{2} \left[(3x_0^2y_0 + 2x_0z_0)^2 + x_0^6 + x_0^4 \right] + x_0^3y_0 + x_0^2z_0 - \frac{1}{2t} \left(\int_0^t W_s ds \right)^2 \\
& \quad + \left(x_0 + t(3x_0^2y_0 + 2x_0z_0) + \int_0^t W_s ds \right) W_t + \frac{\zeta(t)}{t} = 0. \quad (4.18)
\end{aligned}$$

This pre-wavefront is shown in Figure 4.36 and we look at slices of the pre-wavefront through $y_0 = -2, 0, 2$ in Figure 4.37. In this case, as in that covered earlier for the classical case, we cannot determine an exact equation for the wavefront. We have to apply the following classical mechanical flow $\nabla_{x_0}\phi = 0$ upon the pre-wavefront,

$$\begin{pmatrix} x \\ y \\ z \end{pmatrix} = \begin{pmatrix} x_0 \\ y_0 \\ z_0 \end{pmatrix} + t \begin{pmatrix} 3x_0^2y_0 + 2x_0z_0 \\ x_0^3 \\ x_0^2 \end{pmatrix} + \begin{pmatrix} \int_0^t W_s ds \\ 0 \\ 0 \end{pmatrix}. \quad (4.19)$$

Doing so yields the wavefront as in Figure 4.38, with slices through $y = -2, 0, 2$ shown in Figure 4.39. Notice the similarities of this with the Noisy Cusp and Tricorn case, especially the slices through $y_0 = 0$ and $y = 0$.

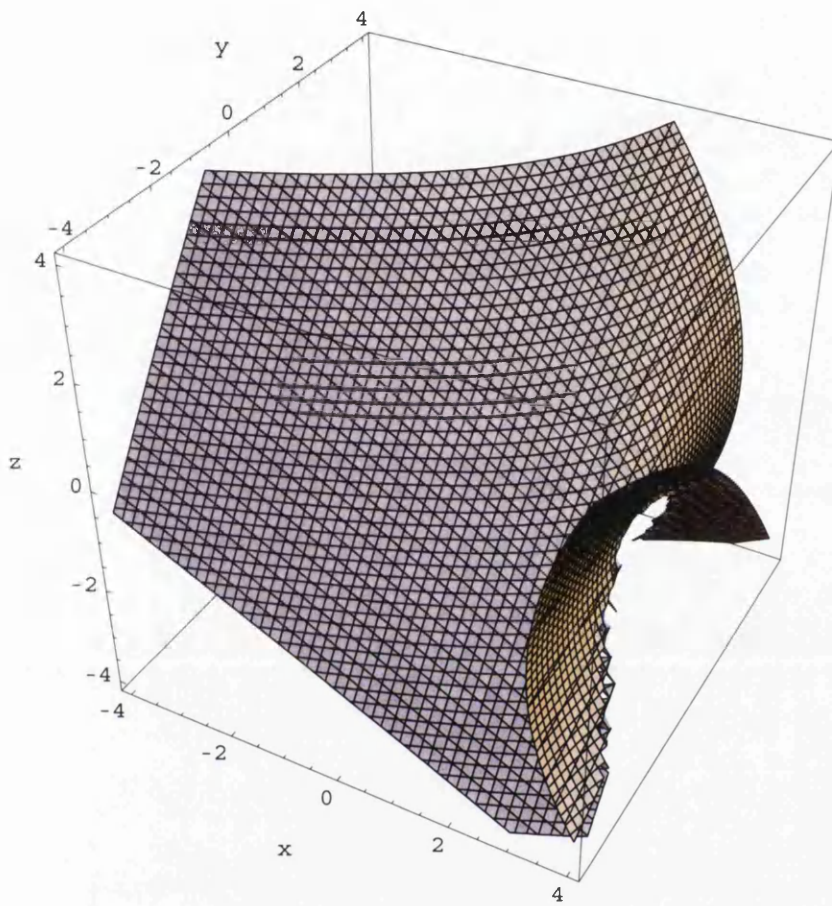


Figure 4.34: Zero potential caustic for $S_0 = x_0^3 y_0 + x_0^2 z_0$ with noise.

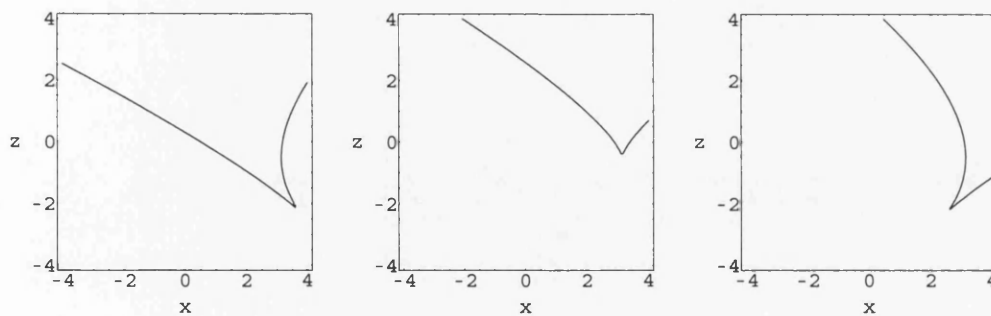


Figure 4.35: Slices of the zero potential caustic for $S_0 = x_0^3 y_0 + x_0^2 z_0$ with noise.

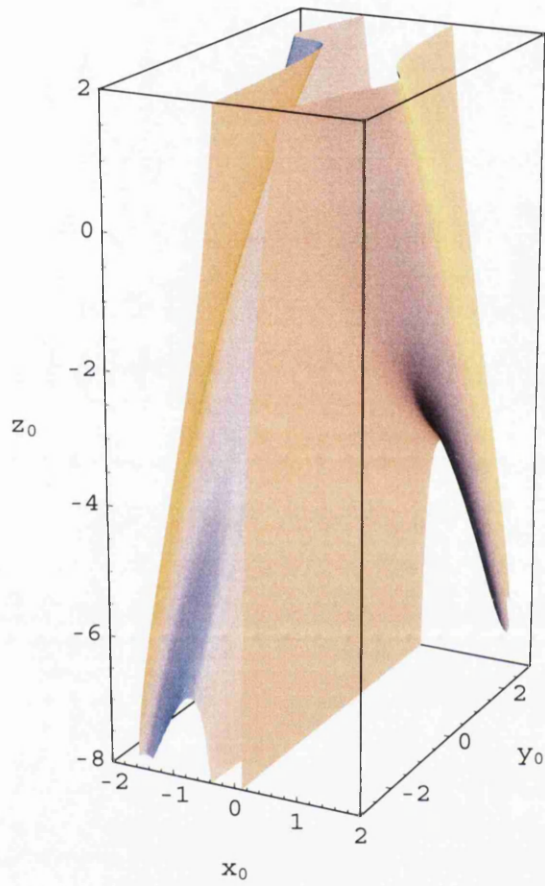


Figure 4.36: Zero potential pre-wavefront for $S_0 = x_0^3 y_0 + x_0^2 z_0$ with noise.

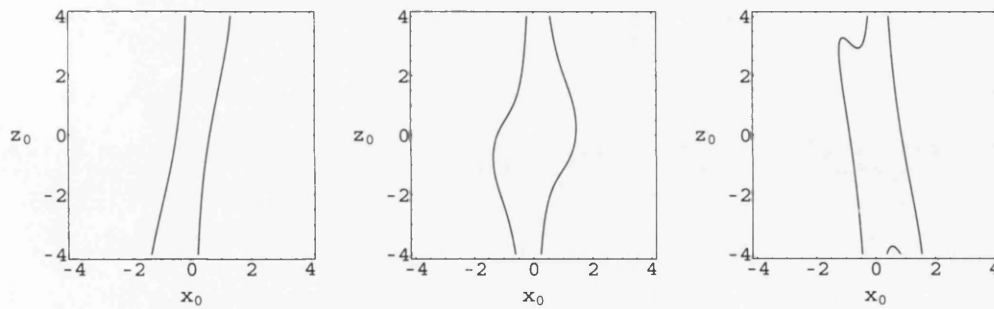


Figure 4.37: Slices of the zero potential pre-wavefront for $S_0 = x_0^3 y_0 + x_0^2 z_0$ with noise.

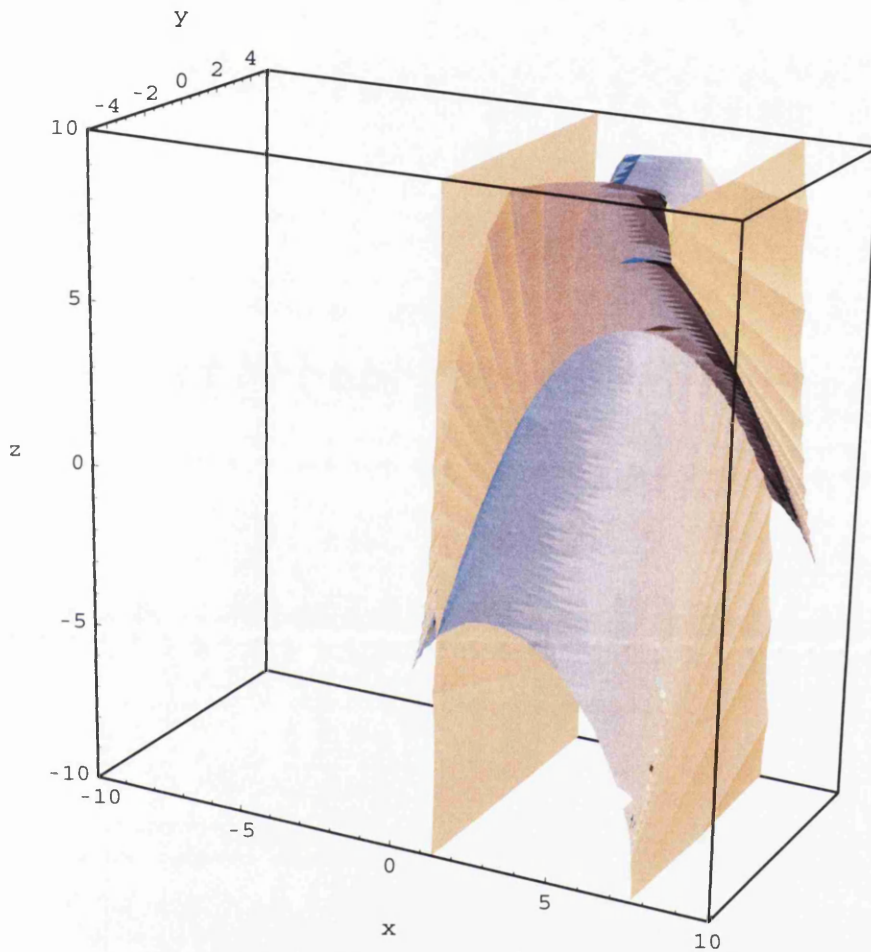


Figure 4.38: Zero potential wavefront for $S_0 = x_0^3 y_0 + x_0^2 z_0$ with noise.

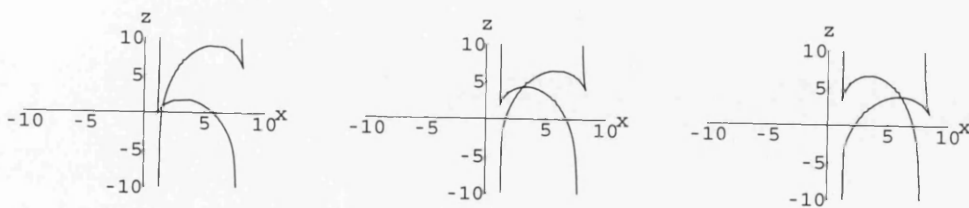


Figure 4.39: Slices of the zero potential wavefront for $S_0 = x_0^3 y_0 + x_0^2 z_0$ with noise.

In Figure 4.40 we illustrate the pair of meeting curves of the pre-caustic and pre-wavefront and, for an alternate view, we have shown the previous series of slices in Figure 4.41. Furthermore, we have shown the meeting curves of the caustic and wavefront, Figure 4.42. However, we discover a problem with using the usual method of applying the classical mechanical flow, equation (4.19), to the pre-curves, thus numerically calculating the meeting curves of the caustic and wavefront. Observe that in Figure 4.42 we only obtain a pair of curves, but Figure 4.43 clearly shows that the caustic and wavefront meet in four positions. It has been shown that the numerically calculated meeting curves meet in a cusp formation due to the pair of meeting curves of the pre-curves, see [16], but the additional curves are coincidental.

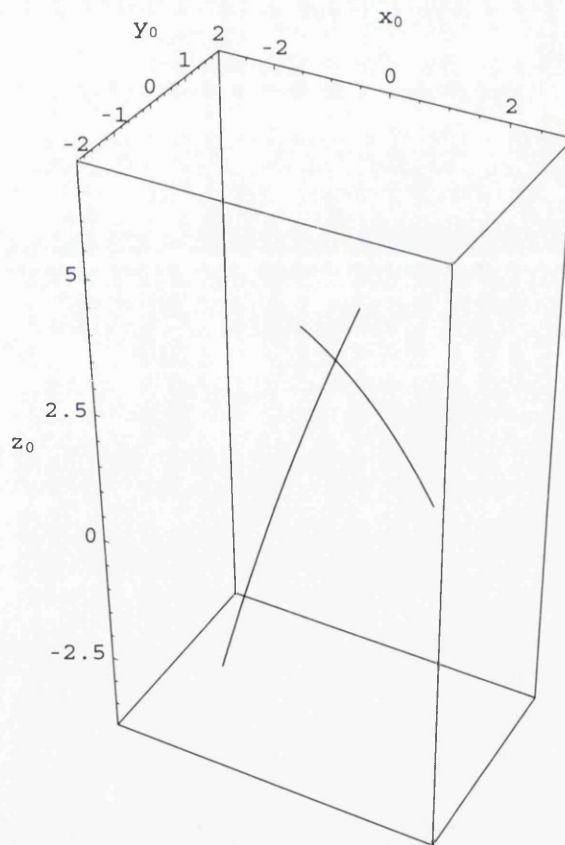


Figure 4.40: Meeting curves of the zero potential pre-caustic and pre-wavefront for $S_0 = x_0^3 y_0 + x_0^2 z_0$ with noise.

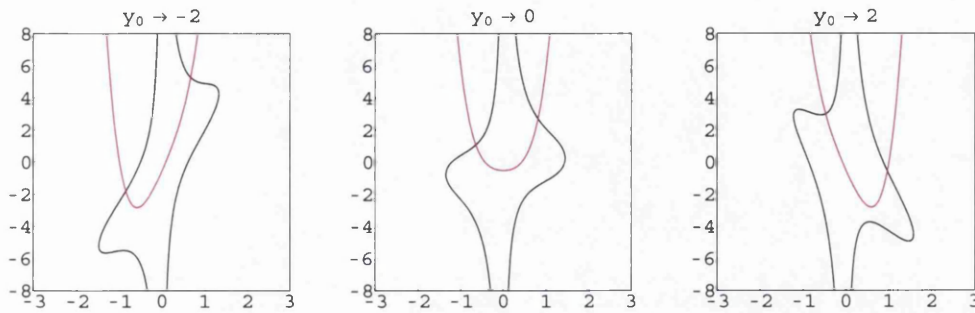


Figure 4.41: Slices of the zero potential pre-caustic and pre-wavefront for $S_0 = x_0^3 y_0 + x_0^2 z_0$ with noise.

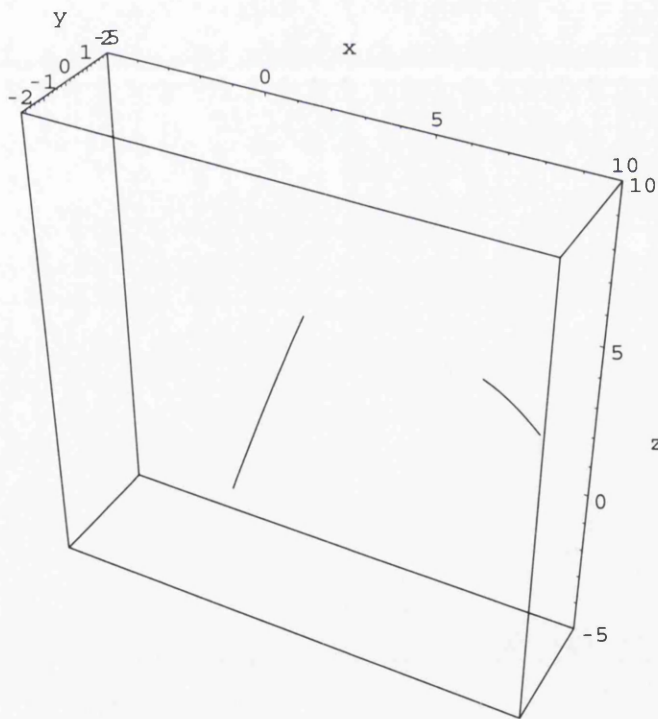


Figure 4.42: Meeting curves of the zero potential caustic and wavefront for $S_0 = x_0^3 y_0 + x_0^2 z_0$ with noise.

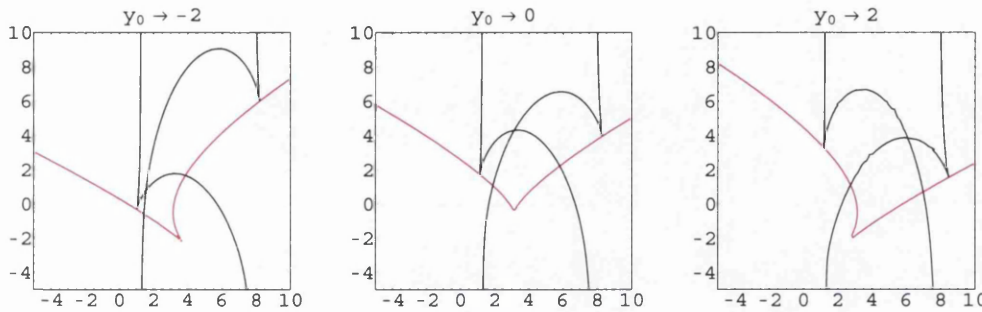


Figure 4.43: Slices of the zero potential caustic and wavefront for $S_0 = x_0^3 y_0 + x_0^2 z_0$ with noise.

4.2.2 Linear Potential

The mathematics for this case has already been set out in Chapter 2, and the computational techniques illustrated in the previous sections of this, and the last, Chapter. With this in mind, we simply present the mathematical formulae and illustrate the associated surfaces.

To begin with, we have a classical mechanical flow, given by equation (2.51), and calculated for our specific $S_0(\underline{x}_0) = x_0^3 y_0 + x_0^2 z_0$ as

$$\underline{x} = \underline{x}_0 + t \begin{pmatrix} k(t) \\ 0 \\ 0 \end{pmatrix} + t \begin{pmatrix} 3x_0^2 y_0 + 2x_0 z_0 \\ x_0^3 \\ x_0^2 \end{pmatrix}, \tag{4.20}$$

where our random functions $k(t)$, $l(t)$ and $F(t)$ given in equations (2.47), (2.48) and (2.47). With the pre-caustic, we simply obtain the exact pre-caustic as in the classical case with a zero potential, namely

$$z_0 = \frac{9}{2} t x_0^4 + 2 t x_0^2 - 3 x_0 y_0 - \frac{1}{2t},$$

which is illustrated in Figures 4.1 and 4.2.

The equation of the caustic, taking out a factor of $\frac{16}{t^8}$, is

$$\begin{aligned}
& \frac{84375}{t^2} x^4 + \frac{67500}{t} (3y - 5k(t)) x^3 \\
& + 18 \left\{ \frac{225}{t^2} (22t^2 - 90tz - 45) y^2 - 33750k(t) y \right. \\
& \quad \left. + \frac{16}{t^2} [12t^4 + 150t^3z + 25t^2(3 + 20z^2) + 500tz + 125] + 28125k^2(t) \right\} x^2 \\
& - \frac{36}{t} \left\{ 2187y^5 + 3(32t^2 + 1890tz + 945) y^3 + 225k(t)(22t^2 - 90tz - 45) y^2 \right. \\
& \quad \left. + \left[\frac{16}{t^2} (12t^5z + 2t^4(3 + 70z^2) + 20t^3z(7 + 30z^2) + 5t^2(7 + 180z^2) + 450tz + 75) \right. \right. \\
& \quad \left. \left. - 16875t^2k(t)^2 \right] y \right. \\
& \quad \left. + 16k(t) [12t^4 + 150t^3z + 25t^2(3 + 20z^2) + 500tz + 125] + 9375t^2k(t)^3 \right\} x \\
& + 78732k(t) y^5 - \frac{6561}{t^2} (2tz + 1)^2 y^4 + 108(32t^2 + 1890tz + 945) k(t) y^3 \\
& - \frac{18}{t^2} [16(2tz + 1)^2 (t^2 + 54tz + 27) - 225t^2(22t^2 - 90tz - 45) k(t)^2] y^2 \\
& + \frac{36}{t^2} k(t) \left\{ 16 [12t^5z + 2t^4(3 + 70z^2) + 20t^3z(7 + 30z^2) + 5t^2(7 + 180z^2) + 450tz + 75] \right. \\
& \quad \left. - 5625t^4k(t)^2 \right\} y - \frac{256}{t^4} (1 + 2tz)^3 (t^2 + 6tz + 3)^2 \\
& + 288 [12t^4 + 150t^3z + 25t^2(3 + 20z^2) + 500tz + 125] k(t)^2 + 84375t^2k(t)^4 = 0,
\end{aligned} \tag{4.21}$$

and is illustrated in Figures 4.44 and 4.45.

The pre-wavefront is depicted in Figures 4.46 and 4.47 and, by using equation (2.52), we obtain the formula for the pre-wavefront as the following

$$\begin{aligned}
& \frac{t}{2} x_0^6 + \frac{t}{2} (1 + 9y_0^2) x_0^4 + y_0 (1 + 6tz_0) x_0^3 + \{3t[F(t) + k(t)] y_0 + z_0 + 2tz_0^2\} x_0^2 \\
& + [F(t) + k(t)] (1 + 2tz_0) x_0 + \frac{t}{2} k(t)^2 + l(t) + tF(t)k(t) = 0. \tag{4.22}
\end{aligned}$$

The wavefront in this case is depicted as in Figures 4.48 and 4.49. We have used the classical mechanical flow (4.20) to calculate the wavefront numerically, using pre-described techniques.

Lastly, Figures 4.50 and 4.51 illustrate the meeting curves of the pre-caustic and pre-wavefront, while Figures 4.52 and 4.53 show the same for the caustic and wavefront.

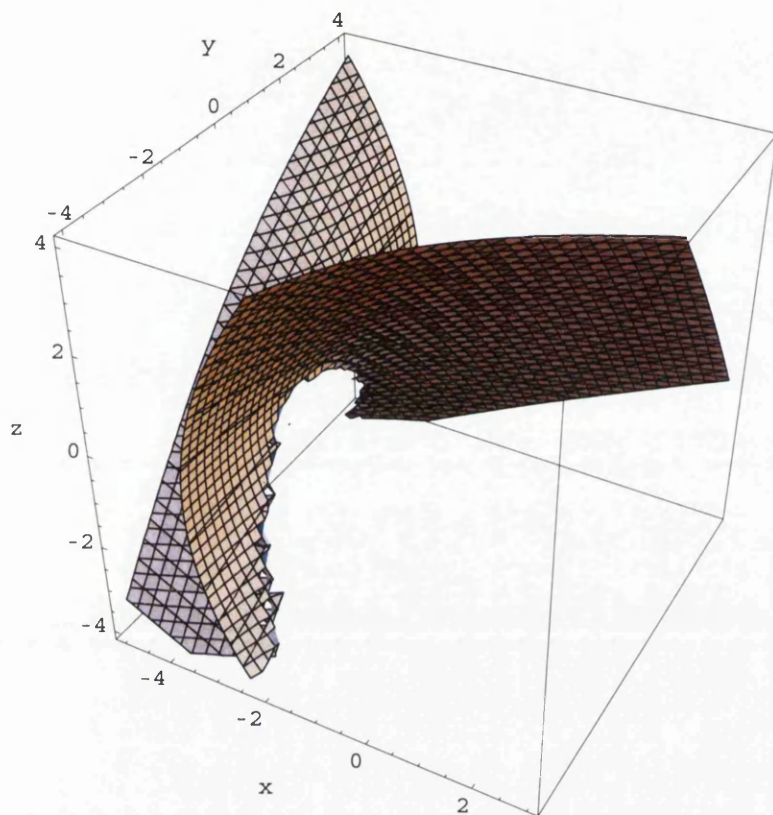


Figure 4.44: Linear potential caustic for $S_0 = x_0^3 y_0 + x_0^2 z_0$ with $k = 5$ and noise.

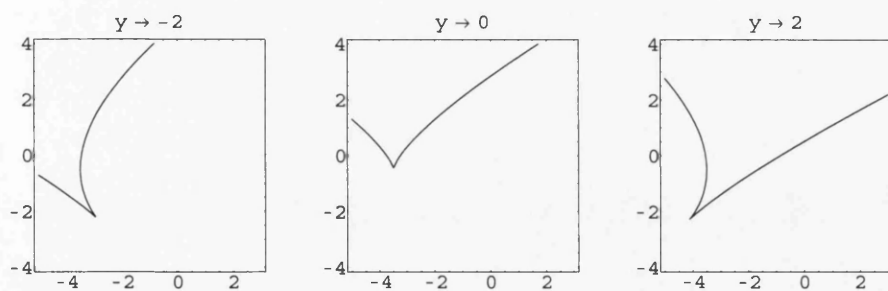


Figure 4.45: Slices of the linear potential caustic for $S_0 = x_0^3 y_0 + x_0^2 z_0$ with $k = 5$ and noise.

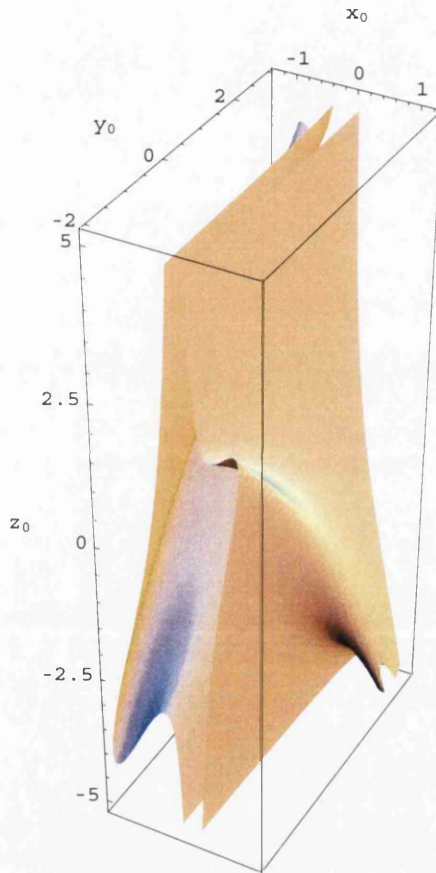


Figure 4.46: Linear potential pre-wavefront for $S_0 = x_0^3 y_0 + x_0^2 z_0$ with $k = 5$ and noise.

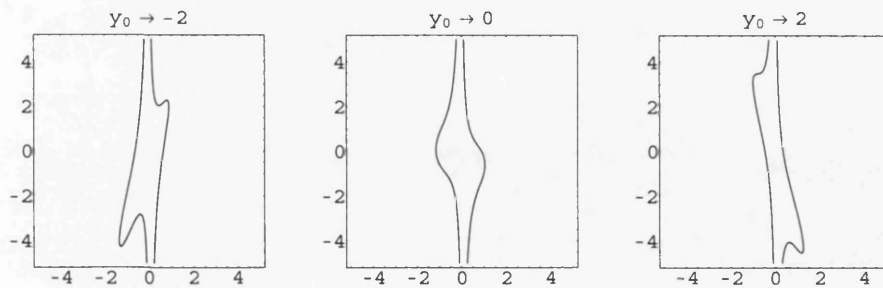


Figure 4.47: Slices of the linear potential pre-wavefront for $S_0 = x_0^3 y_0 + x_0^2 z_0$ with $k = 5$ and noise.

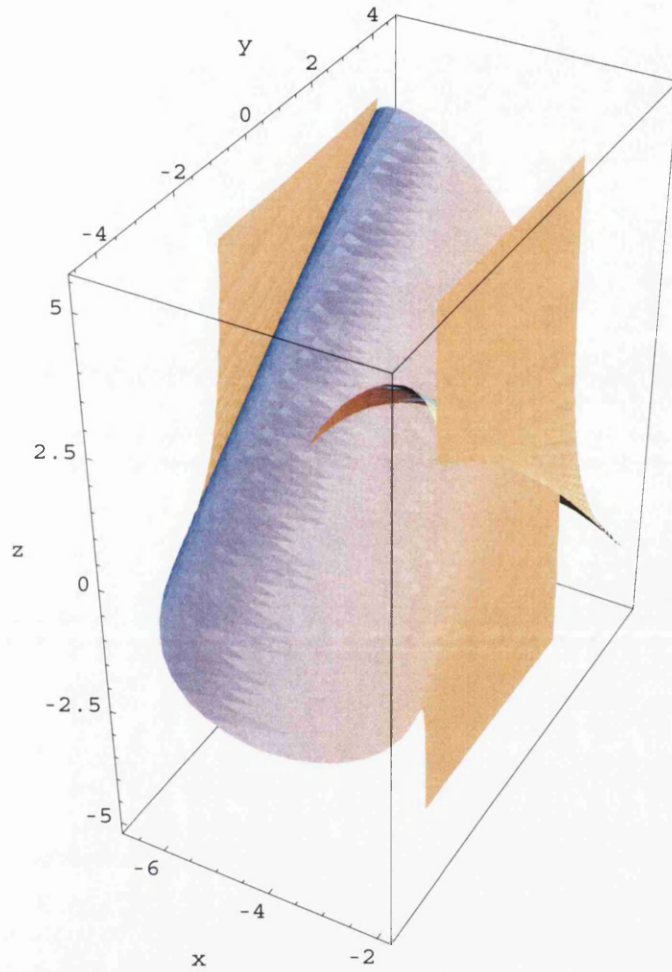


Figure 4.48: Linear potential wavefront for $S_0 = x_0^3 y_0 + x_0^2 z_0$ with $k = 5$ and noise.

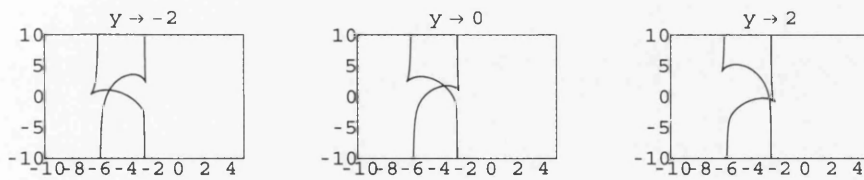


Figure 4.49: Slices of the linear potential wavefront for $S_0 = x_0^3 y_0 + x_0^2 z_0$ with $k = 5$ and noise.

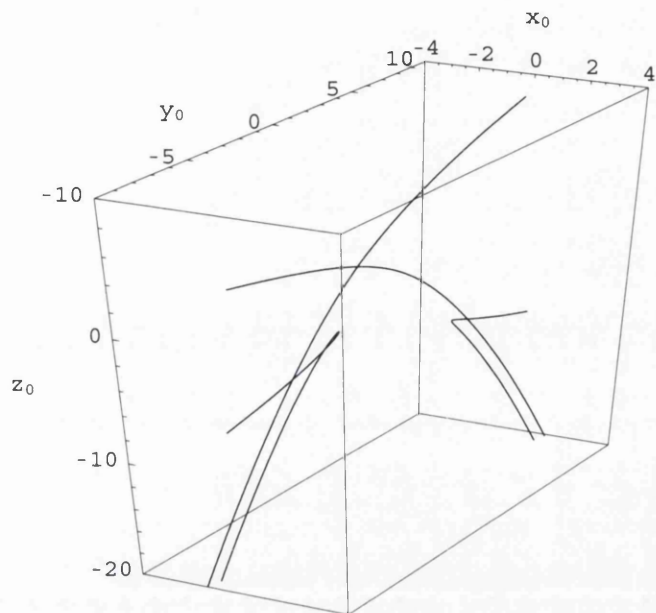


Figure 4.50: Meeting curves of the linear potential pre-caustic and pre-wavefront for $S_0 = x_0^3 y_0 + x_0^2 z_0$ with $k = 5$ and noise.

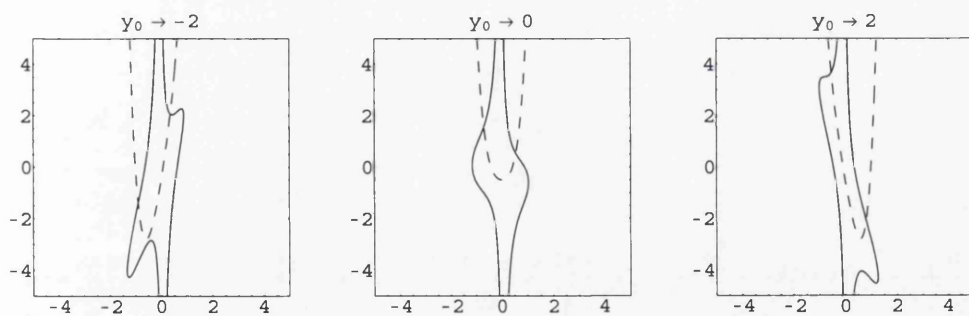


Figure 4.51: Slices of the linear potential pre-caustic and pre-wavefront for $S_0 = x_0^3 y_0 + x_0^2 z_0$ with $k = 5$ and noise.

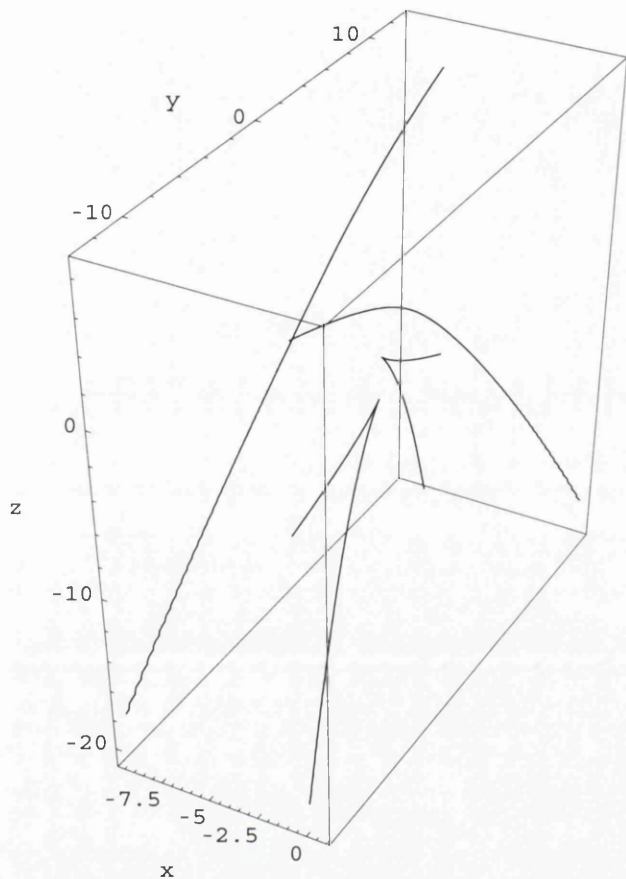


Figure 4.52: Meeting curves of the linear potential caustic and wavefront for $S_0 = x_0^3 y_0 + x_0^2 z_0$ with $k = 5$ and noise.

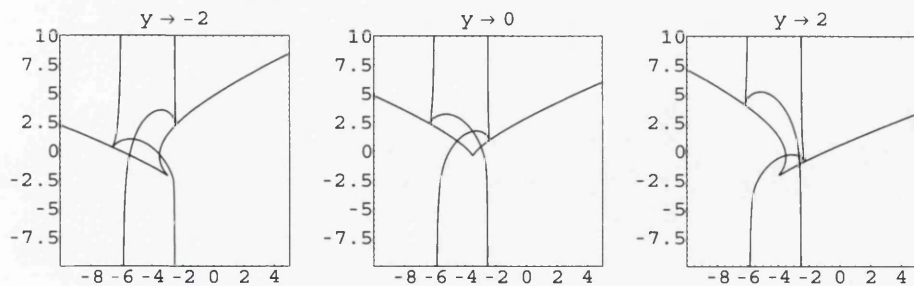


Figure 4.53: Slices of the linear potential caustic and wavefront for $S_0 = x_0^3 y_0 + x_0^2 z_0$ with $k = 5$ and noise.

4.2.3 Harmonic Oscillator Potential

In this last section we merely present the illustrations for the caustics and wavefronts for a Harmonic Oscillator Potential with a noise term, as in Section 2.3.3, and the initial condition $S_0(\underline{x}_0) = x_0^3 y_0 + x_0^2 z_0$. Recall that in this case we have a phase function given by

$$\begin{aligned} \phi(\underline{x}, \underline{x}_0, t) &= \frac{w_1}{2} \left[\frac{(x^2 + x_0^2) \cos(w_1 t) - 2xx_0}{\sin(w_1 t)} \right] + \frac{w_2}{2} \left[\frac{(y^2 + y_0^2) \cos(w_2 t) - 2yy_0}{\sin(w_2 t)} \right] \\ &+ \frac{w_3}{2} \left[\frac{(z^2 + z_0^2) \cos(w_3 t) - 2zz_0}{\sin(w_3 t)} \right] + xW_t + \eta(t) \\ &- \frac{w_1}{\sin(w_1 t)} \int_0^t W_r [x \cos(w_1 r) - x_0 \cos(w_1 r - w_1 t)] dr + x_0^3 y_0 + x_0^2 z_0, \end{aligned} \quad (4.23)$$

and a classical mechanical flow

$$\begin{aligned} \begin{pmatrix} x \\ y \\ z \end{pmatrix} &= \begin{pmatrix} x_0 \cos(w_1 t) \\ y_0 \cos(w_2 t) \\ z_0 \cos(w_3 t) \end{pmatrix} + \begin{pmatrix} \frac{\sin(w_1 t)}{w_1} (3x_0^2 y_0 + 2x_0 z_0) \\ \frac{\sin(w_2 t)}{w_2} x_0^3 \\ \frac{\sin(w_3 t)}{w_3} x_0^2 \end{pmatrix} \\ &+ \begin{pmatrix} \int_0^t W_r \cos(w_1 r - w_1 t) dr \\ 0 \\ 0 \end{pmatrix}. \end{aligned} \quad (4.24)$$

The pre-caustic is exactly the same as in the classical mechanical case, see Figures 4.22 and 4.23. The rest of the Figures follow.

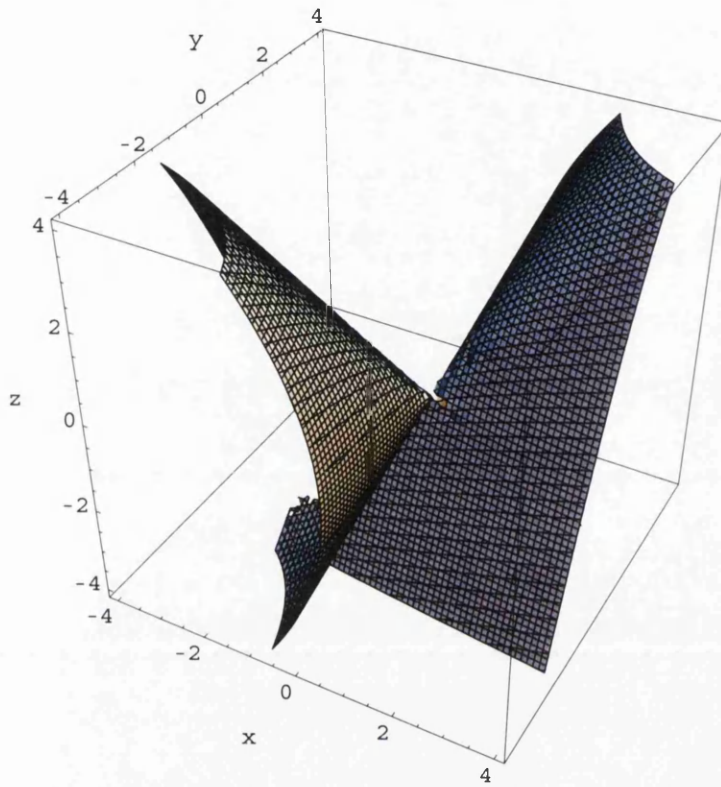


Figure 4.54: Harmonic oscillator potential caustic for $S_0 = x_0^3 y_0 + x_0^2 z_0$ with $w_1 = 2$, $w_2 = 3$, $w_3 = 4$ and noise.

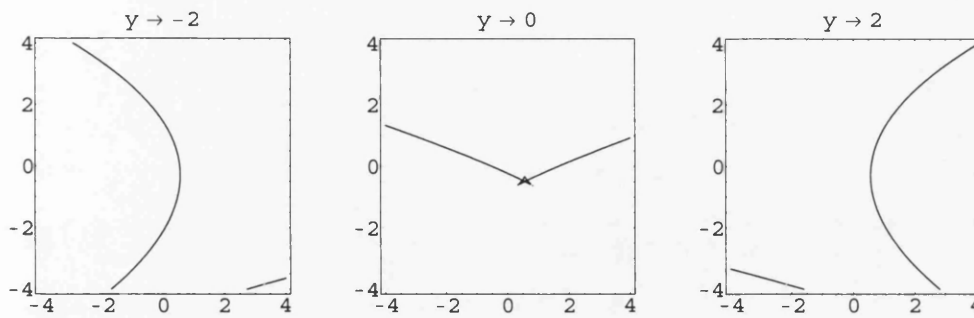


Figure 4.55: Slices of the harmonic oscillator potential caustic for $S_0 = x_0^3 y_0 + x_0^2 z_0$ with $w_1 = 2$, $w_2 = 3$, $w_3 = 4$ and noise.

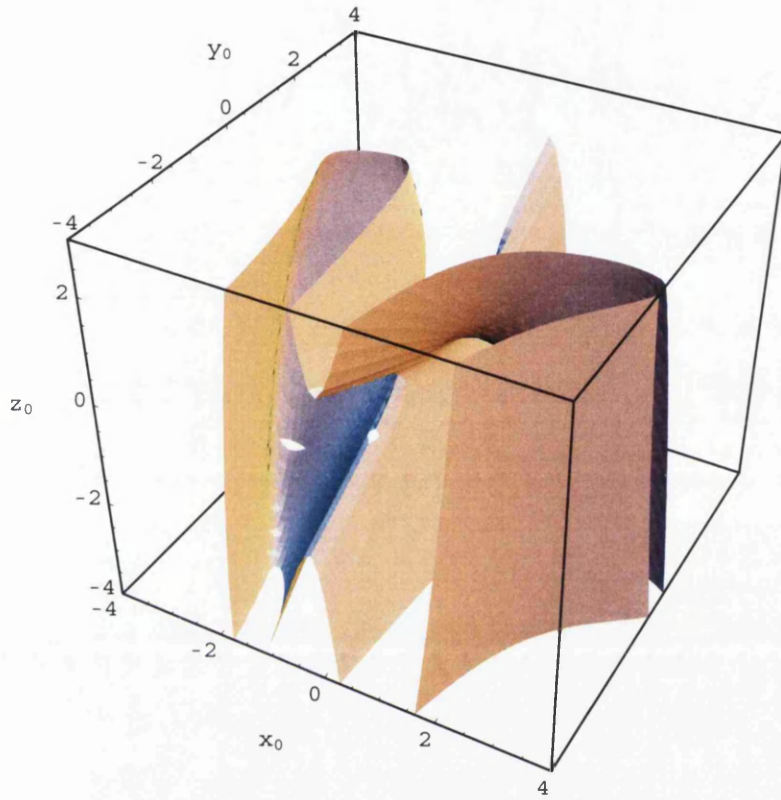


Figure 4.56: Harmonic oscillator pre-wavefront for $S_0 = x_0^3 y_0 + x_0^2 z_0$ with $w_1 = 2$, $w_2 = 3$, $w_3 = 4$ and noise.

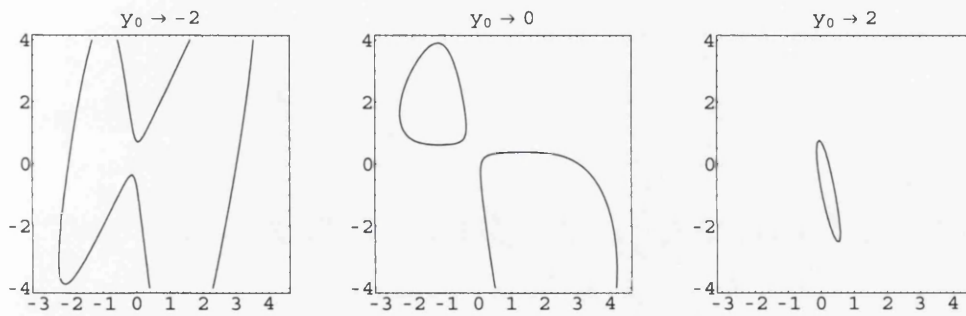


Figure 4.57: Slices of the harmonic oscillator pre-wavefront for $S_0 = x_0^3 y_0 + x_0^2 z_0$ with $w_1 = 2$, $w_2 = 3$, $w_3 = 4$ and noise.

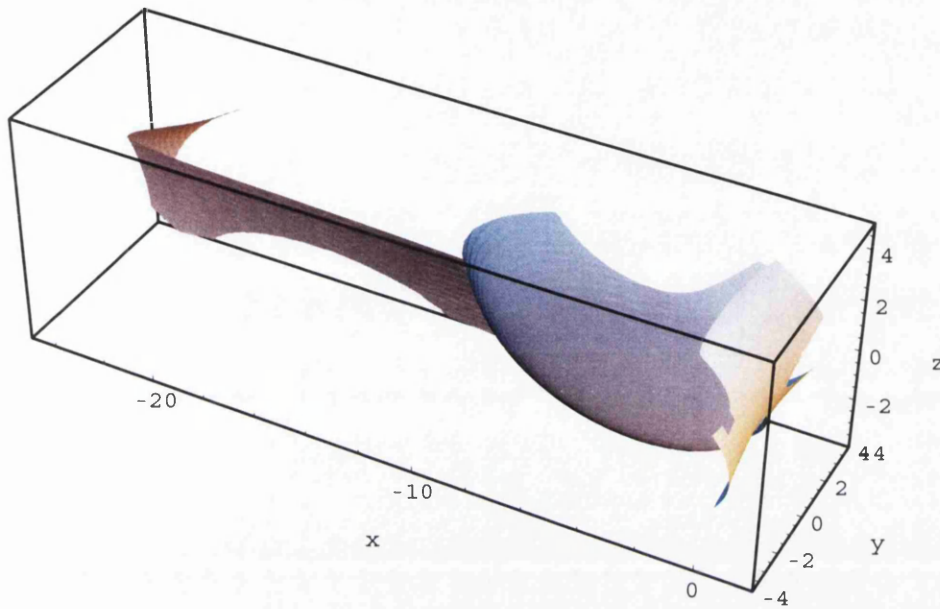


Figure 4.58: Harmonic oscillator potential wavefront for $S_0 = x_0^3 y_0 + x_0^2 z_0$ with $w_1 = 2$, $w_2 = 3$, $w_3 = 4$ and noise.

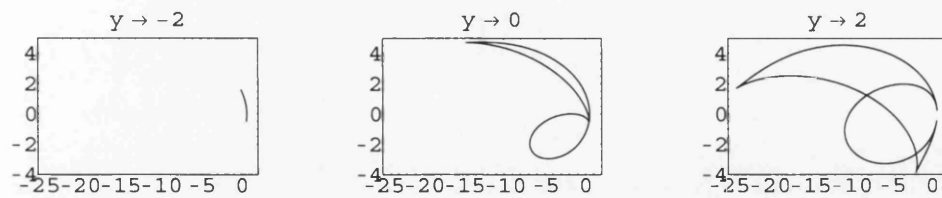


Figure 4.59: Slices of the harmonic oscillator potential wavefront for $S_0 = x_0^3 y_0 + x_0^2 z_0$ with $w_1 = 2$, $w_2 = 3$, $w_3 = 4$ and noise.

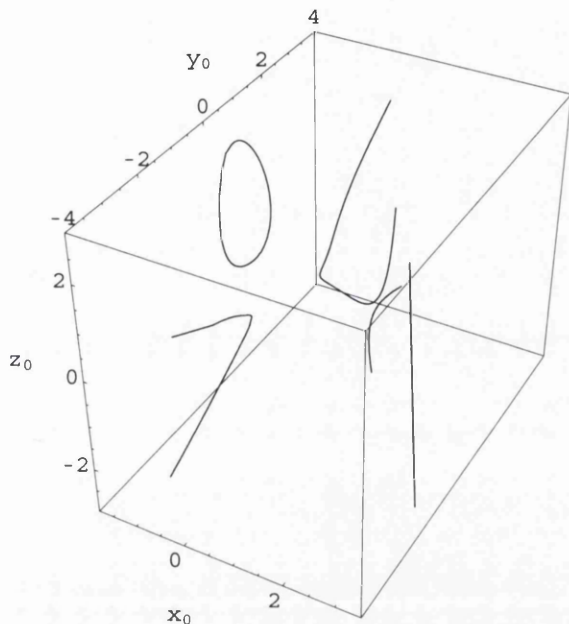


Figure 4.60: Meeting curves of the harmonic oscillator potential pre-caustic and pre-wavefront for $S_0 = x_0^3 y_0 + x_0^2 z_0$ with $w_1 = 2$, $w_2 = 3$, $w_3 = 4$ and noise.

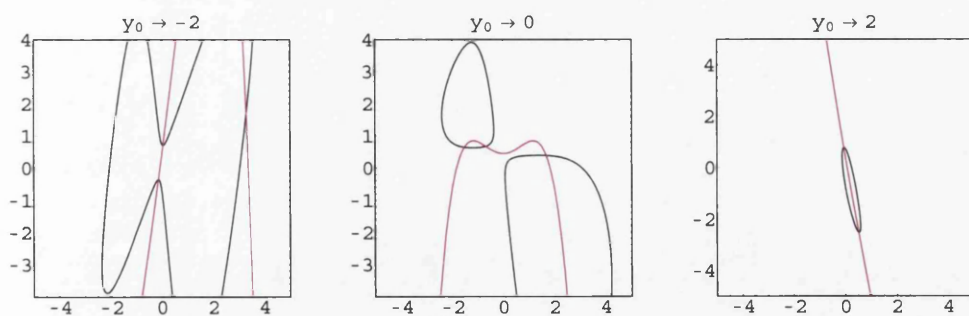


Figure 4.61: Slices of the harmonic oscillator potential pre-caustic and pre-wavefront for $S_0 = x_0^3 y_0 + x_0^2 z_0$ with $w_1 = 2$, $w_2 = 3$, $w_3 = 4$ and noise.

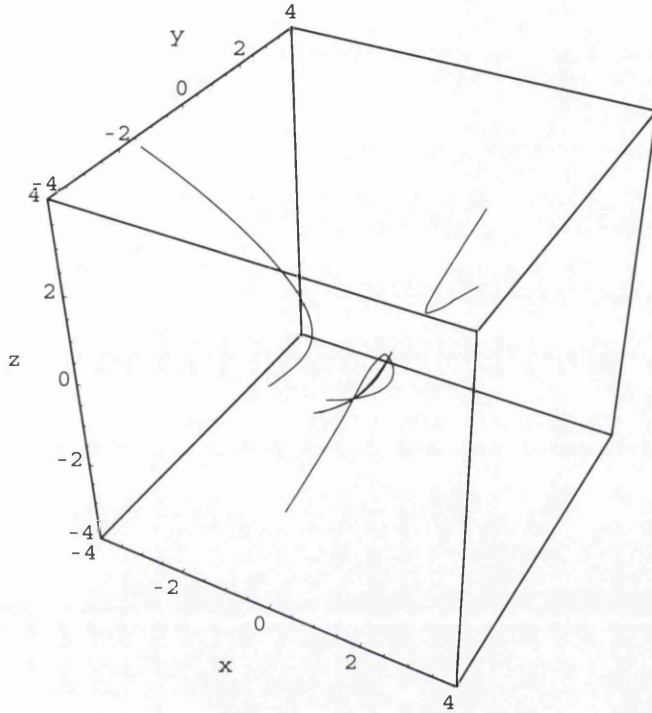


Figure 4.62: Meeting curves of the harmonic oscillator potential caustic and wavefront for $S_0 = x_0^3 y_0 + x_0^2 z_0$ with $w_1 = 2, w_2 = 3, w_3 = 4$ and noise.

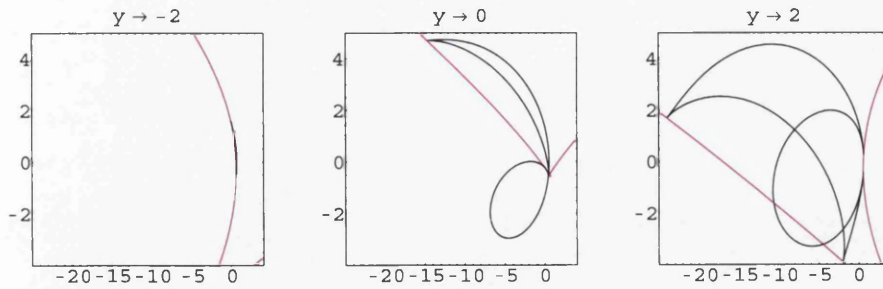


Figure 4.63: Slices of the harmonic oscillator potential caustic and wavefront for $S_0 = x_0^3 y_0 + x_0^2 z_0$ with $w_1 = 2, w_2 = 3, w_3 = 4$ and noise.

Part III
Appendix

Appendix A

On Mechanics

A.1 Hopf-Cole Transformation in \mathbb{R}^n

Consider the n dimensional heat equation with a potential term $V(\underline{x})$, namely equation (1.1),

$$\frac{\partial u}{\partial t} = \frac{\mu^2}{2} \Delta u + \frac{V(\underline{x})}{\mu^2} u, \quad (\text{A.1})$$

for $u = u(\underline{x}, t)$ and $\underline{x} = (x_1, x_2, \dots, x_n)$ with $x_i = x_i(t)$. We may use the Hopf-Cole transformation $\underline{v} = -\mu^2 \nabla \ln u$ to transform the heat equation into a Burgers equation with viscosity μ^2 , i.e.

$$\frac{\partial \underline{v}}{\partial t} + (\underline{v} \cdot \nabla) \underline{v} = \frac{\mu^2}{2} \Delta \underline{v} - \nabla V(\underline{x}). \quad (\text{A.2})$$

First let us look at the Hopf-Cole transformation in more detail, we have

$$\underline{v} = -\mu^2 \nabla \ln u = -\frac{\mu^2}{u} \nabla u. \quad (\text{A.3})$$

Then the first time derivative of \underline{v} is just

$$\frac{\partial \underline{v}}{\partial t} = \frac{\mu^2}{u^2} \frac{\partial u}{\partial t} \nabla u - \frac{\mu^2}{u} \frac{\partial}{\partial t} (\nabla u). \quad (\text{A.4})$$

It is all important that before proceeding we consider the product $(\underline{v} \cdot \nabla) \underline{v}$ for the \underline{v} given by the Hopf-Cole transformation, hence this gives

$$\begin{aligned} (\underline{v} \cdot \nabla) \underline{v} &= -\frac{\mu^2}{u} (\nabla u \cdot \nabla) \left(-\frac{\mu^2}{u} \nabla u \right) \\ &= \frac{\mu^4}{u} (\nabla u \cdot \nabla) \left(\frac{\nabla u}{u} \right). \end{aligned}$$

Giving

$$\begin{aligned}
(\underline{v} \cdot \nabla) \underline{v} &= \frac{\mu^4}{u} \left(\sum_{i=1}^n \frac{\partial u}{\partial x_1} \frac{\partial}{\partial x_i} \right) \left(\frac{\nabla u}{u} \right) \\
&= \frac{\mu^4}{u} \left[\sum_{i=1}^n \frac{\partial u}{\partial x_i} \left(-\frac{1}{u^2} \frac{\partial u}{\partial x_i} \right) \nabla u + \frac{1}{u} \begin{pmatrix} \sum_{i=1}^n u'_i u''_{i,1} \\ \sum_{i=1}^n u'_i u''_{i,2} \\ \vdots \\ \sum_{i=1}^n u'_i u''_{i,n} \end{pmatrix} \right] \\
&= \frac{\mu^4}{u} \left[-\frac{(\nabla u)^2}{u^2} \nabla u + \frac{1}{u} \begin{pmatrix} \sum_{i=1}^n u'_i u''_{i,1} \\ \sum_{i=1}^n u'_i u''_{i,2} \\ \vdots \\ \sum_{i=1}^n u'_i u''_{i,n} \end{pmatrix} \right].
\end{aligned}$$

Now recall from equation (A.3) that we have

$$\underline{v}^2 = \underline{v} \cdot \underline{v} = \frac{\mu^4}{u^2} (\nabla u)^2, \quad (\text{A.5})$$

such that we obtain

$$(\underline{v} \cdot \nabla) \underline{v} = \frac{\underline{v}^2}{\mu^2} \underline{v} + \frac{\mu^4}{u^2} \begin{pmatrix} \sum_{i=1}^n u'_i u''_{i,1} \\ \sum_{i=1}^n u'_i u''_{i,2} \\ \vdots \\ \sum_{i=1}^n u'_i u''_{i,n} \end{pmatrix}. \quad (\text{A.6})$$

This is important for when we calculate $\Delta \underline{v}$ we shall obtain terms of this form. Next we need to compute the Laplacian of \underline{v} ,

$$\Delta \underline{v} = \Delta \left(-\frac{\mu^2}{u} \nabla u \right),$$

where we need the following identity for a scalar α and vector \underline{r} ,

$$\Delta (\alpha \underline{r}) = (\Delta \alpha) \underline{r} + \alpha \Delta \underline{r} + 2 \nabla \alpha \cdot \nabla \underline{r}.$$

Then this gives

$$\Delta \underline{v} = -\mu^2 \left\{ \Delta \left(\frac{1}{u} \right) \nabla u + \frac{1}{u} \Delta (\nabla u) + 2 \nabla \left(\frac{1}{u} \right) \cdot \nabla \left(\frac{1}{u} \right) \right\}, \quad (\text{A.7})$$

which we shall split this into three parts to make it easier to work with.

First we need to consider $-\mu^2 \Delta \left(\frac{1}{u}\right) \nabla u$, then we have

$$\begin{aligned}
-\mu^2 \Delta \left(\frac{1}{u}\right) \nabla u &= -\mu^2 \left[\sum_{i=1}^n \frac{\partial^2}{\partial x_i^2} \left(\frac{1}{u}\right) \right] \nabla u \\
&= -\mu^2 \left[\sum_{i=1}^n \frac{\partial}{\partial x_i} \left(-\frac{1}{u^2} \frac{\partial u}{\partial x_i} \right) \right] \nabla u \\
&= -\mu^2 \left\{ \sum_{i=1}^n \left[\frac{2}{u^3} \left(\frac{\partial u}{\partial x_i} \right)^2 - \frac{1}{u^2} \frac{\partial^2 u}{\partial x_i^2} \right] \right\} \nabla u \\
&= -2 \frac{\mu^2}{u^3} (\nabla u)^2 \nabla u + \frac{\mu^2}{u^2} \Delta u \nabla u.
\end{aligned}$$

Now, from the heat equation (A.1), we see that

$$\mu^2 \Delta u = 2 \frac{\partial u}{\partial t} - \frac{2}{\mu^2} V(\underline{x}) u,$$

and from equation (A.5), we also have

$$(\nabla u)^2 = \frac{u^2}{\mu^4} v^2,$$

so then this gives

$$\begin{aligned}
-\mu^2 \Delta \left(\frac{1}{u}\right) \nabla u &= -\frac{2}{\mu^2} \left(\frac{v^2}{u}\right) \nabla u + \frac{2}{u^2} \left[\frac{\partial u}{\partial t} - \frac{V(\underline{x})}{\mu^2} u \right] \nabla u \\
&= \frac{2}{\mu^4} v^2 v + \frac{2}{u^2} \left[\frac{\partial u}{\partial t} - \frac{V(\underline{x})}{\mu^2} u \right] \nabla u.
\end{aligned} \tag{A.8}$$

Next we calculate $-\frac{\mu^2}{u} \Delta (\nabla u)$ so we have

$$-\frac{\mu^2}{u} \Delta (\nabla u) = -\frac{\mu^2}{u} \nabla [\nabla \cdot (\nabla u)] + \frac{\mu^2}{u} \nabla \wedge [\nabla \wedge (\nabla u)],$$

but since we are assuming that $u(\underline{x}, t)$ is continuous on \mathbb{R}^n we must have

$$\frac{\partial^2 u}{\partial x_i \partial x_j} = \frac{\partial^2 u}{\partial x_j \partial x_i}.$$

Hence we see that $\nabla \wedge (\nabla u) = 0$, and thus we have

$$-\frac{\mu^2}{u} \Delta (\nabla u) = -\frac{\mu^2}{u} \nabla (\Delta u),$$

but by the heat equation (A.1), we have

$$-\frac{\mu^2}{u}\Delta(\nabla u) = -\frac{2}{u}\nabla\left[\frac{\partial u}{\partial t} - \frac{V(\underline{x})}{\mu^2}u\right]. \quad (\text{A.9})$$

Later, we shall see that it is essential that $u(\underline{x}, t)$ is always continuous on $\mathbb{R}^n \times [0, \infty)$, such that we have

$$\nabla \dot{u} = \frac{\partial}{\partial t}(\nabla u).$$

Thirdly, we need to calculate $-2\mu^2\nabla(\nabla u)\nabla\left(\frac{1}{u}\right)$, then we have

$$\begin{aligned} -2\mu^2\nabla(\nabla u)\nabla\left(\frac{1}{u}\right) &= 2\mu^2\begin{pmatrix} \nabla u'_1 \\ \nabla u'_2 \\ \vdots \\ \nabla u'_n \end{pmatrix} \left[\frac{1}{u^2}\nabla u\right] \\ &= 2\frac{\mu^2}{u^2}\begin{pmatrix} u''_{1,1} & u''_{2,1} & \cdots & u''_{n,1} \\ u''_{1,2} & u''_{2,2} & \cdots & u''_{n,2} \\ \vdots & \vdots & \ddots & \vdots \\ u''_{1,n} & u''_{2,n} & \cdots & u''_{n,n} \end{pmatrix} \begin{pmatrix} u'_1 \\ u'_2 \\ \vdots \\ u'_n \end{pmatrix} \\ \text{i.e. } -2\mu^2\nabla(\nabla u)\nabla\left(\frac{1}{u}\right) &= 2\frac{\mu^2}{u^2}\begin{pmatrix} \sum_{i=1}^n u''_{i,1}u'_i \\ \sum_{i=1}^n u''_{i,2}u'_i \\ \vdots \\ \sum_{i=1}^n u''_{i,n}u'_i \end{pmatrix}. \end{aligned} \quad (\text{A.10})$$

Now that we have all of the available information, we can piece together $\Delta \underline{v}$ from equations (A.8), (A.9) and (A.10), giving

$$\Delta \underline{v} = \frac{2}{\mu^4}\underline{v}^2\underline{v} + \frac{2}{u^2}\left[\frac{\partial u}{\partial t} - \frac{V(\underline{x})}{\mu^2}u\right]\nabla u - \frac{2}{u}\nabla\left(\frac{\partial u}{\partial t} - \frac{V(\underline{x})}{\mu^2}u\right) + 2\frac{\mu^2}{u^2}\begin{pmatrix} \sum_{i=1}^n u''_{i,1}u'_i \\ \sum_{i=1}^n u''_{i,2}u'_i \\ \vdots \\ \sum_{i=1}^n u''_{i,n}u'_i \end{pmatrix}.$$

Observe that the terms combine to give

$$\begin{aligned} \Delta \underline{v} &= \frac{2}{\mu^2}\left[\frac{\underline{v}^2}{\mu^2}\underline{v} + \frac{\mu^4}{u^2}\begin{pmatrix} \sum_{i=1}^n u''_{i,1}u'_i \\ \sum_{i=1}^n u''_{i,2}u'_i \\ \vdots \\ \sum_{i=1}^n u''_{i,n}u'_i \end{pmatrix}\right] \\ &\quad + \frac{2}{\mu^2}\left\{\frac{\mu^2}{u^2}\left[\frac{\partial u}{\partial t} - \frac{V(\underline{x})}{\mu^2}u\right]\nabla u + \frac{\mu^2}{u}\nabla\left(\frac{\partial u}{\partial t} - \frac{V(\underline{x})}{\mu^2}u\right)\right\}, \end{aligned}$$

where the terms in the first square bracket are just $(\underline{v} \cdot \nabla) \underline{v}$

$$\Delta \underline{v} = \frac{2}{\mu^2} (\underline{v} \cdot \nabla) \underline{v} + \frac{2}{\mu^2} \left[\frac{\mu^2}{u^2} \frac{\partial u}{\partial t} \nabla u - \frac{\mu^2}{u} \nabla \left(\frac{\partial u}{\partial t} \right) + \nabla V(\underline{x}) \right].$$

Observe that we can use the first time derivative of \underline{v} , equation (A.4), to give

$$\Delta \underline{v} = \frac{2}{\mu^2} (\underline{v} \cdot \nabla) \underline{v} + \frac{2}{\mu^2} \left(\frac{\partial \underline{v}}{\partial t} + \nabla V(\underline{x}) \right),$$

such that we have the viscous Burgers' equation in n dimensions, namely

$$\frac{\partial \underline{v}}{\partial t} + (\underline{v} \cdot \nabla) \underline{v} = \frac{\mu^2}{2} \Delta \underline{v} - \nabla V(\underline{x}),$$

as required.

Appendix B

On Stochastics

B.1 Itô and Stratonovich Integrals

We assume that the reader already has a sufficient knowledge of stochastic processes so we can show here the relationships between the Itô and Stratonovich integrals. For a reference on stochastic processes one could try [17, 18]. Recall that if $f(x, t) \in C^2$ and W_t is a Wiener process, then $F_t = f(W_t, t)$ is an Itô process and we have the well known Itô's formula as

$$dF_t = \frac{\partial f}{\partial x} \Big|_{(W_t, t)} dW_t + \left(\frac{\partial f}{\partial t} \Big|_{(W_t, t)} + \frac{1}{2} \frac{\partial^2 f}{\partial x^2} \Big|_{(W_t, t)} \right) dt. \quad (\text{B.1})$$

Now, [19] tells us that the Itô and Stratonovich calculi are connected by the relationship

$$f(W_t, t) \circ dW_t = f(W_t, t) dW_t + \frac{1}{2} df(W_t, t) dW_t. \quad (\text{B.2})$$

The Stratonovich integral has several interesting properties, which we shall now illustrate by means of examples.

B.1.1 Examples

Example 1

If we take $f(x, t) = t$ then we see that we have the Stratonovich integral

$$\int_0^t s \circ dW_s = \int_0^t s dW_s + \frac{1}{2} \int_0^t ds dW_s,$$

but $ds dW_s = 0$ by the McKean rule, so we have the following integral that can be evaluated by integration by parts to give

$$\begin{aligned}\int_0^t s \circ dW_s &= \int_0^t s dW_s \\ &= tW_t - \int_0^t W_s ds.\end{aligned}$$

This is an example of the property that the Stratonovich and Itô integrals are the same when considering smooth functions of t only, i.e. when we look at $f(x, t) = f(t)$ we have

$$\begin{aligned}\int_0^t f(s) \circ dW_s &= \int_0^t f(s) dW_s \\ &= f(t)W_t - \int_0^t W_s df(s).\end{aligned}$$

Example 2

If we now set $f(x, t) = x$ then we see that

$$\begin{aligned}\int_0^t W_s \circ dW_s &= \int_0^t W_s dW_s + \frac{1}{2} \int_0^t dW_s dW_s \\ &= \int_0^t W_s dW_s + \frac{1}{2} \int_0^t ds,\end{aligned}$$

but from Itô's formula we have

$$\begin{aligned}\int_0^t W_s \circ dW_s &= \int_0^t d\left(\frac{W_s^2}{2}\right) - \frac{1}{2} \int_0^t ds + \frac{1}{2} \int_0^t ds \\ &= \frac{W_s^2}{2}.\end{aligned}$$

This shows an important property of the Stratonovich integral, that is, if we take a $f(x, t) = g'(x)$ then we have

$$\begin{aligned}\int_0^t g'(W_s) \circ dW_s &= \int_0^t g'(W_s) dW_s + \frac{1}{2} \int_0^t dg'(W_s) dW_s \\ &= \int_0^t g'(W_s) dW_s + \frac{1}{2} \int_0^t g''(W_s) ds,\end{aligned}$$

but from Itô's formula we have

$$dg(W_s) = g'(W_s) dW_s + \frac{1}{2} g''(W_s) dt.$$

such that

$$\int_0^t g'(W_s) \circ dW_s = g(W_t) - g(0) + \frac{1}{2} \int_0^t g'' ds - \frac{1}{2} \int_0^t g'' ds.$$

The important concept to remember here is that Stratonovich integrals obey normal calculus, i.e. there is no correction term,

$$\int_a^b g'(W_s) \circ dW_s = g(W_s) \Big|_a^b.$$

B.2 Evaluating the $\zeta(t)$ Integral in the Zero Potential Case

Recall that in the zero potential noisy case, Section 2.3.1, we encountered a term of the form

$$\zeta(t) = \int_0^t \int_0^r s(r-t) \circ dW_s \circ dW_r.$$

We shall evaluate this using the formula for a Stratonovich integral. We first have to integrate

$$\int_0^r s \circ dW_s = \int_0^r s dW_s + \frac{1}{2} \int_0^r ds dW_s,$$

which, by the McKean multiplication rule, is just the stochastic integral which we can evaluate by Itô's formula. We have

$$\int_0^r s \circ dW_s = rW_r - \int_0^r W_s ds.$$

Then putting this back into our function $\zeta(t)$ yields

$$\zeta(t) = \int_0^t (r-t) \left(rW_r - \int_0^r W_s ds \right) \circ dW_r.$$

This is simpler to evaluate as four integrals, i.e.

$$\zeta(t) = \int_0^t r^2 W_r \circ dW_r - t \int_0^t r W_r \circ dW_r - \int_0^t r \int_0^r W_s ds \circ dW_r + t \int_0^t \int_0^r W_s ds \circ dW_r. \quad (\text{B.3})$$

Looking at the first integral we have, by the Stratonovich formula,

$$\int_0^t r^2 W_r \circ dW_r = \int_0^t r^2 W_r dW_r + \frac{1}{2} \int_0^t d(r^2 W_r) dW_r.$$

Also, by the Itô formula we have $d(r^2W_r) = r^2dW_r + 2rW_rdr$, and by the McKean multiplication rule this gives us

$$\begin{aligned}\int_0^t r^2W_r \circ dW_r &= \int_0^t r^2W_r dW_r + \frac{1}{2} \int_0^t r^2 dr \\ &= \frac{t^2}{2}W_t^2 - \int_0^t rW_r^2 dr\end{aligned}$$

Now, move onto the second integral, the Stratonovich formula gives us

$$\int_0^t rW_r \circ dW_r = \int_0^t rW_r dW_r + \frac{1}{2} \int_0^t d(rW_r) dW_r.$$

Then by the Itô formula we have $d(rW_r) = r dW_r + W_r dr$ and the McKean multiplication rule gives us

$$\begin{aligned}\int_0^t rW_r \circ dW_r &= \int_0^t rW_r dW_r + \frac{1}{2} \int_0^t r dr \\ &= \frac{t}{2}W_t^2 - \frac{1}{2} \int_0^t W_r^2 dr\end{aligned}$$

The third and fourth terms are a bit more cumbersome, but evaluate to

$$\int_0^t \int_0^r rW_s ds \circ dW_r = \int_0^t \int_0^r rW_s ds dW_r,$$

and

$$\int_0^t \int_0^r W_s ds \circ dW_r = \int_0^t \int_0^r W_s ds dW_r.$$

Then putting these back into equation (B.3) gives us

$$\zeta(t) = \frac{1}{2} \int_0^t W_r^2 dr - \frac{1}{t} \int_0^t rW_r^2 dr + \int_0^t \int_0^t W_s ds dW_r - \frac{1}{t} \int_0^t r \int_0^t W_s ds dW_r.$$

B.3 Approximating Randomness

We detail here the approach that we used to approximate the random variables that we encountered in Chapter 2. To approximate the random variables we simply chose a time $t \rightarrow 1$ and allocated a real value to the random variable, as shown in the following table.

We began by choosing $W_0 = 0$, $W_1 = -\sqrt{2}$, and $\int_0^1 W_s ds = \pi$. We then used a simple trapezium approximation for $W_{0.5}$ and this was used to estimate values for the remaining integrals.

Table B.1: Approximations of Random Variables

Random Variable	Chosen Value
W_t	$-\sqrt{2}$
$\int_0^t W_s ds$	π
$\int_0^t \frac{W_r}{r} dr$	10
$\int_0^t r W_r dr$	1
$\int_0^t W_r^2 dr$	34
$\int_0^t W_r \cos(2r) dr$	2.7523
$\int_0^t W_r \cos(2r - 2t) dr$	0.5589
$\int_0^t \int_0^r W_s ds dr$	3
$\int_0^t \frac{1}{r^2} \int_0^r W_s ds dr$	16
$\int_0^t \frac{W_r}{r} \int_0^r W_s ds dr$	23
$\zeta(t)$	5
$\eta(t)$	4

List of Figures

1.1	Phase Space Diagram	18
3.1	Zero potential pre-caustic for $S_0 = \frac{1}{2}x_0^2y_0$	52
3.2	Evolving zero potential pre-caustics for $S_0 = \frac{1}{2}x_0^2y_0$	52
3.3	Zero potential caustic for $S_0 = \frac{1}{2}x_0^2y_0$	54
3.4	Evolving zero potential caustics for $S_0 = \frac{1}{2}x_0^2y_0$	55
3.5	Zero potential pre-wavefront for $S_0 = \frac{1}{2}x_0^2y_0$	56
3.6	Evolving zero potential pre-wavefronts for $S_0 = \frac{1}{2}x_0^2y_0$	57
3.7	Zero potential wavefront for $S_0 = \frac{1}{2}x_0^2y_0$	57
3.8	Evolving zero potential wavefronts for $S_0 = \frac{1}{2}x_0^2y_0$	58
3.9	Zero potential pre-caustic and pre-wavefront for $S_0 = \frac{1}{2}x_0^2y_0$	59
3.10	Zero potential caustic and wavefront for $S_0 = \frac{1}{2}x_0^2y_0$	59
3.11	Evolving linear potential caustics for $S_0 = \frac{1}{2}x_0^2y_0$ with $k = 5$	62
3.12	Evolving linear potential pre-wavefronts for $S_0 = \frac{1}{2}x_0^2y_0$ with $k = 5$	62
3.13	Linear potential pre-wavefront generator for $S_0 = \frac{1}{2}x_0^2y_0$ with $k = 5$	63
3.14	Evolving linear potential wavefronts for $S_0 = \frac{1}{2}x_0^2y_0$ with $k = 5$	64
3.15	Linear potential pre-caustic and pre-wavefront for $S_0 = \frac{1}{2}x_0^2y_0$ with $k = 5$	65
3.16	Linear potential caustic and wavefront for $S_0 = \frac{1}{2}x_0^2y_0$ with $k = 5$	65
3.17	Periodic harmonic oscillator pre-caustics for $S_0 = \frac{1}{2}x_0^2y_0$ with $w_1 = 2$ and $w_2 = 3$	67
3.18	Periodic harmonic oscillator caustics for $S_0 = \frac{1}{2}x_0^2y_0$ with $w_1 = 2$ and $w_2 = 3$	69
3.19	Periodic harmonic oscillator pre-wavefronts for $S_0 = \frac{1}{2}x_0^2y_0$ with $w_1 = 2$ and $w_2 = 3$	72
3.20	73
3.21	Periodic harmonic oscillator wavefronts for $S_0 = \frac{1}{2}x_0^2y_0$ with $w_1 = 2$ and $w_2 = 3$	74
3.22	Harmonic oscillator pre-caustic and pre-wavefront for $S_0 = \frac{1}{2}x_0^2y_0$ with $w_1 = 2$ and $w_2 = 3$	75
3.23	Harmonic oscillator caustic and wavefront for $S_0 = \frac{1}{2}x_0^2y_0$ with $w_1 = 2$ and $w_2 = 3$	75

3.24	Zero potential caustic for $S_0 = \frac{1}{2}x_0^2y_0$ with noise.	77
3.25	Zero potential pre-wavefront for $S_0 = \frac{1}{2}x_0^2y_0$ with noise.	80
3.26	Zero potential wavefront for $S_0 = \frac{1}{2}x_0^2y_0$ with noise.	80
3.27	Zero potential pre-caustic and pre-wavefront for $S_0 = \frac{1}{2}x_0^2y_0$ with noise.	81
3.28	Zero potential caustic and wavefront for $S_0 = \frac{1}{2}x_0^2y_0$ with noise.	81
3.29	Linear potential caustic for $S_0 = \frac{1}{2}x_0^2y_0$ with $k = 5$ and noise for $\alpha \rightarrow 1$	82
3.30	Linear potential pre-wavefront for $S_0 = \frac{1}{2}x_0^2y_0$ with $k = 5$ and noise for $\alpha \rightarrow 1$	85
3.31	Linear potential wavefront for $S_0 = \frac{1}{2}x_0^2y_0$ with $k = 5$ and noise for $\alpha \rightarrow 1$	85
3.32	Linear potential pre-caustic and pre-wavefront for $S_0 = \frac{1}{2}x_0^2y_0$ with $k = 5$ and noise for $\alpha \rightarrow 1$	86
3.33	Linear potential caustic and wavefront for $S_0 = \frac{1}{2}x_0^2y_0$ with $k = 5$ and noise for $\alpha \rightarrow 1$	86
3.34	Harmonic oscillator caustic for $S_0 = \frac{1}{2}x_0^2y_0$ with $w_1 = 2$, $w_2 = 3$ and noise.	87
3.35	Harmonic oscillator pre-wavefront for $S_0 = \frac{1}{2}x_0^2y_0$ with $w_1 = 2$, $w_2 = 3$ and noise.	89
3.36	Harmonic oscillator wavefront for $S_0 = \frac{1}{2}x_0^2y_0$ with $w_1 = 2$, $w_2 = 3$ and noise.	89
3.37	Harmonic oscillator pre-caustic and pre-wavefront for $S_0 = \frac{1}{2}x_0^2y_0$ with $w_1 = 2$, $w_2 = 3$ and noise.	90
3.38	Harmonic oscillator caustic and wavefront for $S_0 = \frac{1}{2}x_0^2y_0$ with $w_1 = 2$, $w_2 = 3$ and noise.	90
4.1	Zero potential pre-caustic for $S_0 = x_0^3y_0 + x_0^2z_0$	92
4.2	Slices of the zero potential pre-caustic for $S_0 = x_0^3y_0 + x_0^2z_0$	92
4.3	Zero potential caustic for $S_0 = x_0^3y_0 + x_0^2z_0$	95
4.4	Slices of the zero potential caustic for $S_0 = x_0^3y_0 + x_0^2z_0$	95
4.5	Zero potential pre-wavefront for $S_0 = x_0^3y_0 + x_0^2z_0$	96
4.6	Slices of the zero potential pre-wavefront for $S_0 = x_0^3y_0 + x_0^2z_0$	96
4.7	Zero potential wavefront for $S_0 = x_0^3y_0 + x_0^2z_0$	98
4.8	Slices of the zero potential wavefront for $S_0 = x_0^3y_0 + x_0^2z_0$	98
4.9	Meeting curves of the zero potential pre-caustic and pre-wavefront for $S_0 = x_0^3y_0 + x_0^2z_0$	99
4.10	Slices of the zero potential pre-caustic and pre-wavefront for $S_0 = x_0^3y_0 + x_0^2z_0$	99
4.11	Meeting curves of the zero potential caustic and wavefront for $S_0 = x_0^3y_0 + x_0^2z_0$	100
4.12	Slices of the zero potential caustic and wavefront for $S_0 = x_0^3y_0 + x_0^2z_0$	100
4.13	Linear potential caustic for $S_0 = x_0^3y_0 + x_0^2z_0$ with $k = 5$	102
4.14	Linear potential pre-wavefront for $S_0 = x_0^3y_0 + x_0^2z_0$ with $k = 5$	104

4.15 Slices of the linear potential pre-wavefront for $S_0 = x_0^3 y_0 + x_0^2 z_0$ with $k = 5$	104
4.16 Linear potential wavefront for $S_0 = x_0^3 y_0 + x_0^2 z_0$ with $k = 5$	105
4.17 Slices of the linear potential wavefront for $S_0 = x_0^3 y_0 + x_0^2 z_0$ with $k = 5$	105
4.18 Meeting curves of the linear potential pre-caustic and pre-wavefront for $S_0 = x_0^3 y_0 + x_0^2 z_0$ with $k = 5$	106
4.19 Meeting curves of the linear potential caustic and wavefront for $S_0 = x_0^3 y_0 + x_0^2 z_0$ with $k = 5$	107
4.20 Slices of the linear potential pre-caustic and pre-wavefront for $S_0 = x_0^3 y_0 + x_0^2 z_0$ with $k = 5$	107
4.21 Slices of the linear potential caustic and wavefront for $S_0 = x_0^3 y_0 + x_0^2 z_0$ with $k = 5$	108
4.22 Harmonic oscillator potential pre-caustic for $S_0 = x_0^3 y_0 + x_0^2 z_0$ with $w_1 = 2, w_2 = 3$ and $w_3 = 4$	109
4.23 Slices of the harmonic oscillator potential pre-caustic for $S_0 = x_0^3 y_0 + x_0^2 z_0$ with $w_1 = 2, w_2 = 3$ and $w_3 = 4$	109
4.24 Harmonic oscillator potential caustic for $S_0 = x_0^3 y_0 + x_0^2 z_0$ with $w_1 = 2, w_2 = 3$ and $w_3 = 4$	111
4.25 Slices of the harmonic oscillator potential caustic for $S_0 = x_0^3 y_0 + x_0^2 z_0$ with $w_1 = 2, w_2 = 3$ and $w_3 = 4$	111
4.26 Harmonic oscillator pre-wavefront for $S_0 = x_0^3 y_0 + x_0^2 z_0$ with $w_1 = 2, w_2 = 3$ and $w_3 = 4$	113
4.27 Slices of the harmonic oscillator pre-wavefront for $S_0 = x_0^3 y_0 + x_0^2 z_0$ with $w_1 = 2, w_2 = 3$ and $w_3 = 4$	113
4.28 Harmonic oscillator potential wavefront for $S_0 = x_0^3 y_0 + x_0^2 z_0$ with $w_1 = 2, w_2 = 3$ and $w_3 = 4$	114
4.29 Slices of the harmonic oscillator potential wavefront for $S_0 = x_0^3 y_0 + x_0^2 z_0$ with $w_1 = 2, w_2 = 3$ and $w_3 = 4$	114
4.30 Meeting curves of the harmonic oscillator potential pre-caustic and pre-wavefront for $S_0 = x_0^3 y_0 + x_0^2 z_0$ with $w_1 = 2, w_2 = 3$ and $w_3 = 4$	115
4.31 Slices of the harmonic oscillator potential pre-caustic and pre-wavefront for $S_0 = x_0^3 y_0 + x_0^2 z_0$ with $w_1 = 2, w_2 = 3$ and $w_3 = 4$	115
4.32 Meeting curves of the harmonic oscillator potential caustic and wavefront for $S_0 = x_0^3 y_0 + x_0^2 z_0$ with $w_1 = 2, w_2 = 3$ and $w_3 = 4$	116
4.33 Slices of the harmonic oscillator potential caustic and wavefront for $S_0 = x_0^3 y_0 + x_0^2 z_0$ with $w_1 = 2, w_2 = 3$ and $w_3 = 4$	116
4.34 Zero potential caustic for $S_0 = x_0^3 y_0 + x_0^2 z_0$ with noise.	119
4.35 Slices of the zero potential caustic for $S_0 = x_0^3 y_0 + x_0^2 z_0$ with noise.	119
4.36 Zero potential pre-wavefront for $S_0 = x_0^3 y_0 + x_0^2 z_0$ with noise.	120
4.37 Slices of the zero potential pre-wavefront for $S_0 = x_0^3 y_0 + x_0^2 z_0$ with noise.	120
4.38 Zero potential wavefront for $S_0 = x_0^3 y_0 + x_0^2 z_0$ with noise.	121
4.39 Slices of the zero potential wavefront for $S_0 = x_0^3 y_0 + x_0^2 z_0$ with noise.	121

4.40 Meeting curves of the zero potential pre-caustic and pre-wavefront for $S_0 = x_0^3 y_0 + x_0^2 z_0$ with noise.	122
4.41 Slices of the zero potential pre-caustic and pre-wavefront for $S_0 = x_0^3 y_0 + x_0^2 z_0$ with noise.	123
4.42 Meeting curves of the zero potential caustic and wavefront for $S_0 = x_0^3 y_0 + x_0^2 z_0$ with noise.	123
4.43 Slices of the zero potential caustic and wavefront for $S_0 = x_0^3 y_0 + x_0^2 z_0$ with noise.	124
4.44 Linear potential caustic for $S_0 = x_0^3 y_0 + x_0^2 z_0$ with $k = 5$ and noise.	126
4.45 Slices of the linear potential caustic for $S_0 = x_0^3 y_0 + x_0^2 z_0$ with $k = 5$ and noise.	126
4.46 Linear potential pre-wavefront for $S_0 = x_0^3 y_0 + x_0^2 z_0$ with $k = 5$ and noise.	127
4.47 Slices of the linear potential pre-wavefront for $S_0 = x_0^3 y_0 + x_0^2 z_0$ with $k = 5$ and noise.	127
4.48 Linear potential wavefront for $S_0 = x_0^3 y_0 + x_0^2 z_0$ with $k = 5$ and noise.	128
4.49 Slices of the linear potential wavefront for $S_0 = x_0^3 y_0 + x_0^2 z_0$ with $k = 5$ and noise.	128
4.50 Meeting curves of the linear potential pre-caustic and pre-wavefront for $S_0 = x_0^3 y_0 + x_0^2 z_0$ with $k = 5$ and noise.	129
4.51 Slices of the linear potential pre-caustic and pre-wavefront for $S_0 = x_0^3 y_0 + x_0^2 z_0$ with $k = 5$ and noise.	129
4.52 Meeting curves of the linear potential caustic and wavefront for $S_0 = x_0^3 y_0 + x_0^2 z_0$ with $k = 5$ and noise.	130
4.53 Slices of the linear potential caustic and wavefront for $S_0 = x_0^3 y_0 + x_0^2 z_0$ with $k = 5$ and noise.	130
4.54 Harmonic oscillator potential caustic for $S_0 = x_0^3 y_0 + x_0^2 z_0$ with $w_1 = 2$, $w_2 = 3$, $w_3 = 4$ and noise.	132
4.55 Slices of the harmonic oscillator potential caustic for $S_0 = x_0^3 y_0 + x_0^2 z_0$ with $w_1 = 2$, $w_2 = 3$, $w_3 = 4$ and noise.	132
4.56 Harmonic oscillator pre-wavefront for $S_0 = x_0^3 y_0 + x_0^2 z_0$ with $w_1 = 2$, $w_2 = 3$, $w_3 = 4$ and noise.	133
4.57 Slices of the harmonic oscillator pre-wavefront for $S_0 = x_0^3 y_0 + x_0^2 z_0$ with $w_1 = 2$, $w_2 = 3$, $w_3 = 4$ and noise.	133
4.58 Harmonic oscillator potential wavefront for $S_0 = x_0^3 y_0 + x_0^2 z_0$ with $w_1 = 2$, $w_2 = 3$, $w_3 = 4$ and noise.	134
4.59 Slices of the harmonic oscillator potential wavefront for $S_0 = x_0^3 y_0 + x_0^2 z_0$ with $w_1 = 2$, $w_2 = 3$, $w_3 = 4$ and noise.	134
4.60 Meeting curves of the harmonic oscillator potential pre-caustic and pre-wavefront for $S_0 = x_0^3 y_0 + x_0^2 z_0$ with $w_1 = 2$, $w_2 = 3$, $w_3 = 4$ and noise.	135
4.61 Slices of the harmonic oscillator potential pre-caustic and pre-wavefront for $S_0 = x_0^3 y_0 + x_0^2 z_0$ with $w_1 = 2$, $w_2 = 3$, $w_3 = 4$ and noise.	135

- 4.62 Meeting curves of the harmonic oscillator potential caustic and wavefront for $S_0 = x_0^3 y_0 + x_0^2 z_0$ with $w_1 = 2$, $w_2 = 3$, $w_3 = 4$ and noise. . . 136
- 4.63 Slices of the harmonic oscillator potential caustic and wavefront for $S_0 = x_0^3 y_0 + x_0^2 z_0$ with $w_1 = 2$, $w_2 = 3$, $w_3 = 4$ and noise. 136

Bibliography

- [1] A. Truman and T. Zastawniak.
Stochastic Mehler Kernels via Oscillatory Path Integrals.
Journal of the Korean Mathematical Society, Volume 38, 2001.
- [2] L. A. Rincón Solís.
Topics on Stochastic Schrödinger Equations and Estimates for the Derivatives of Diffusion Semigroups.
PhD thesis, University of Wales Swansea, 1999.
- [3] P.T. Saunders.
An Introduction to Catastrophe Theory.
Cambridge University Press, 1980.
- [4] J. R. Canon.
One Dimensional Heat Equation, volume 23 of *Encyclopedia of Mathematics and its Applications*.
Addison-Wesley Publishing Company Inc., 1984.
- [5] A. Truman and T. Zastawniak.
Stochastic PDE's of Schrödinger Type and Stochastic Mehler Kernels - a Path Integral Approach.
Progress in Probability, Volume 45, 1999.
- [6] D. H. Wilson.
Hydrodynamics.
Edward Arnold, 1959.
- [7] E. Hopf.
The Partial Differential Equation $u_t + uu_x = \mu u_{xx}$.
Communications of Pure and Applied Mathematics, 1950.
- [8] J. D. Cole.
On a Quasi-Linear Parabolic Equation Occurring in Aerodynamics.
Quarterly of Applied Mathematics, Volume 9, 1951.
- [9] V. I. Arnol'd.
Mathematical Methods of Classical Mechanics.
Springer, second edition, 1997.

- [10] A. Truman and H.Z. Zhao.
Stochastic Burgers' Equations and their Semi-Classical Expansions.
Communications in Mathematical Physics, Volume 194, 1998.
- [11] C. Humphreys.
Stochastic analysis, semiclassical methods and poisson-lèvy excursion measures.
Master's thesis, University of Wales Swansea, 2000.
- [12] A. Truman, I. M. Davies and H. Z. Zhao.
Stochastic Heat and Burgers Equations and their Singularities I - Geometrical Properties (Dedicated to V. I. Arnol'd).
Journal of Mathematical Physics, Volume 48, 2002.
- [13] S.A. Albeverio and R.J. Høegh-Krohn.
Mathematical Theory of Feynman Path Integrals.
Lecture Notes in Mathematics, Volume 523, 1976.
- [14] K. Itô.
Generalised Uniform Complex Measures in the Hilbertian Metric Space with their Application to the Feynman Path Integral.
Proceedings of the Fifth Berkeley Symposium on Mathematical Statistics and Probability, 1967.
- [15] C. N. Reynolds.
On the Swallowtail Singularity of the Burgers Equation, work in progress.
PhD thesis, University of Wales Swansea, 2002.
- [16] A. Truman, I. M. Davies and H. Z. Zhao.
Stochastic Heat and Burgers Equations and their Singularities - Geometrical and Analytical Properties (The Fish and the Butterfly, and Why).
Texas Mathematical Physics Preprint Archive, 2001.
http://www.ma.utexas.edu/mp_arc-bin/mpa?yn=01-45.
- [17] Z. Brzeźniak and T. Zastawniak.
Basic Stochastic Processes.
Springer, 1998.
- [18] B. Øksendal.
Stochastic Differential Equations: An Introduction with Applications.
Springer, fifth edition, 1998.
- [19] L.C.G. Rogers and D. Williams.
Diffusions, Markov Processes and Martingales, volume 2: Itô Calculus.
John Wiley and Sons, 1987.